EVALUATION OF MODEL UNCERTAINTIES IN LRFD CALIBRATION PROCESS OF DRILLED SHAFT AXIAL DESIGN

by

Mohammad Rakib Hasan

Presented to the Faculty of the Graduate School of

The University of Texas at Arlington in Partial Fulfillment

of the Requirements

for the Degree of

DOCTOR OF PHILOSOPHY

THE UNIVERSITY OF TEXAS AT ARLINGTON

August 2019

This dissertation is dedicated to my parents for their constant support and motivation throughout my life.

ACKNOWLEDGEMENTS

At first, I would like to express my deepest gratitude and acknowledgement to my advisor Dr. Xinbao Yu for his endless guidance and encouragement during my doctoral research. I am thankful to him for providing me the opportunity of working under his supervision. This research would not come to fruition without his counseling.

I also would like to thank my committee members Dr. Shahadat Hossain, Dr. Laureno Hoyos and Dr. Samantha Sabatino for their valuable comments, help and time. I am thankful to Dr. Xinbao Yu, Dr. Laureano Hoyos, Dr. Sahadat Hossain, Dr. Aera LeBoulluec, Dr. Dong-Jun Seo and Dr. Chein-Pai Han for fulfilling my experience at University of Texas at Arlington by sharing their knowledge during my course works required for the doctoral program.

Finally, I would like to thank my parents, my siblings and my beloved wife for their endless love and encouragement which kept me motivated. None of these would happen without them.

July 29, 2019

ABSTRACT

OPTIMIZATION OF LRFD CALIBRATION OF DRILLED SHAFTS

by

Mohammad Rakib Hasan

The University of Texas at Arlington, 2019

Supervising Professor: Xinbao Yu

The Federal Highway Administration (FHWA) released a policy in 2000 that required all new federally funded bridges to be designed using the AASHTO LRFD specifications by October 2007. The transition from ASD to LRFD posed a challenge due to the lack of area specific resistance factors. Though several studies were performed to calibrate area specific resistance factors, they did not improve from the resistance factors suggested in AASHTO 2012. The objective of this study is to analyze the uncertainties in LRFD calibration and to calibrate more accurate and improved resistance factors. A drilled shaft load test database from Mississippi and Louisiana has been selected to carry on the research. Osterberg Cell load test was a majority among the load tests in the database. Extrapolation is required in most Osterberg cell load test which may cause errors in the calibration. An analysis of the error due to the extrapolation can result in more accurate LRFD calibration of resistance factors. The analysis was performed on 8 drilled shaft cases from Louisiana and Mississippi. 4 of the 8 drilled shafts reached 5% of the shaft diameter (D) failure criterion and 4 of the drilled shafts were close to 5%D. For each of the cases, extrapolation was performed on tip and side resistance curves to get the equivalent top-down curve.

Data points were removed systematically from the end of top and bottom movement curves and extrapolation was performed for each trial to get an equivalent top-down curve. Bias and error values was measured for each of the trial top down scurves for both 5% of the drilled shaft diameter (D). 80 extrapolation cases were achieved from this analysis. Finally, multiple linear regression analysis was performed on the extrapolated data set in order to reduce the effect of the extrapolation error on the resistance factor. Applying bounded bias distribution may also result in more accurate resistance factors, since the bias values have significant role in the calibration process. As the probability of failure significantly depends on the lower tail of the distribution of the resistance values and there is a physical presence of a lower limit of the resistance of a drilled shaft, introducing a lower bound to the resistance distribution will ensure more realistic calibration of the resistance factors. An analysis by simulation of load tests to failure on will also help to understand the reasons for low resistance factor values. The objective of this study is also to minimize effect of extrapolation by means of finite element modelling of the bidirectional load tests included in a database collected from Louisiana and Mississippi. The finite element modelling was performed in PLAXIS 2D until the top and the bottom movement curves reach the measured loads corresponding to the failure criteria. LRFD calibration of resistance factors was performed based on the simulated bidirectional load test database and the results were compared to the results from conventional approach.

Table of Contents

LIST OF ILLUSTRATIONS

LIST OF TABLES

Chapter 1

INTRODUCTION

1.1. General

Load and Resistance Factor Design (LRFD) has been gaining popularity over Allowable Stress Design (ASD) for several decades. While the LRFD method considers load factors as well as resistance factors to be applied to the limit state inequalities, the ASD method combines both of the factors into a single factor of safety. Consideration of two separate factors for load and resistance has made the LRFD method more consistent than the ASD method (Abu Farsakh et al. 2010). After the publication of the first edition of AASHTO LRFD Bridge Design Specifications, the major challenge was to make the transition from ASD to LRFD. To begin the transition from ASD to LRFD, the Federal Highway Administration (FHWA) released a policy in 2000 that required all new federally-funded bridges to be designed using the AASHTO LRFD specifications by October 2007 (Fortier, 2016). Despite this steady progression into LRFD, however, deep foundation design still does not take full advantage of the probabilistic framework in many parts of the United States due to a lack of area-specific resistance factors derived using reliability theory–based calibrations. Instead, many regions rely on values given in specifications from AASHTO (2010) which were developed by fitting to allowable state design (ASD) safety factors (Stanton et al. 2017). Studies like Abu-Farsakh et al. (2012), Long et al. (2009), Roling et al. (2011); Garder et al. (2012), Rahman et al. (2002), and McVay et al. (2005) were performed with an objective of calibrating region region-wise load and resistance factors for foundation design. Perusing all the studies, it was observed that the resistance factors did not improve with the

consideration of region region-based soil properties, in fact, they decreased in some cases. The low resistance factor values may occur from different uncertainties like inaccuracy in load test data, inaccurate soil test data, the effect of outlier cases, etc. The objective of this study is to develop a reliability framework incorporating the uncertainties for a more rigorous calibration of resistance factors for drilled shafts.

To meet the challenge of transitioning the design from ASD to LRFD, AASHTO LRFD specifications was published in 2007. At In the beginning, all the regions utilized the resistance factors provided in the AASHTO specifications to design drilled shafts following LRFD method. The drawback to this step was that the resistance factors were not developed based on the soil properties of different regions. They were developed by fitting to ASD safety factor values. Later, several DOT's conducted studies to calibrate the resistance factors based on specific regions. University of Florida conducted a study on calibrating resistance factors for both drilled shafts and driven piles. They collected 61 conventional static as well as statnamic load tests performed on drilled shafts and driven piles. The analysis for the calibration of the resistance factors included 37 load test cases which reached the failure criteria. At In the end, the study proposed a resistance factor of 0.35 for clay and 0.65 for rock and non-cohesive soils with a reliability index of 3.0 (Mc Vay et al. 2003). Garder et al. (2012) accumulated a database of 41 load tests on drilled shafts from 11 different states. 28 load test data were usable out of the total of 41. The majority of the database included Osterberg Cell load test. There were also a few statnamic load test results. Ng et al. (2014) performed calibration of resistance factors on the same database. They proposed resistance factor values between 0.40 to 0.55 for sand and clay for a reliability index value of 3.0. The New Mexico Department of Transportation accumulated a database of load tests on drilled shafts in cohesionless soil from New Mexico and other states. The filtered database included 24 drilled shaft load tests

including Osterberg Cell and Static load tests. Ng & Fazia (2012) proposed resistance factor values in the range of 0.45 to 0.49 based on the New Mexico database. Abu Farsakh et al. (2013) performed LRFD calibration on a load test database consisting of 34 drilled shaft cases from Louisiana and Mississippi. Most of the load tests included were Osterberg Cell load tests. Resistance factors were calibrated for 2010 and 1999 FHWA design methods with a reliabltity index value of 3.0. Abu Farsakh et al (2013) suggested the total resistance factors to be 0.48 and 0.60 for 2010 and 1999 FHWA design methods, respectively. The side and end bearing resistance factors were suggested to be 0.26 and 0.53 using 2010 FHWA design method. Using 1999 FHWA design method, the side and end bearing resistance factors were proposed to be 0.39 and 0.52, respectively. Based on area specific calibrations as well as the ASD factor of safety values, AASHTO updated the resistance factor values for drilled shaft in 2012. It can be observed from all the studies that the resistance factor values have not improved from the initially proposed resistance factors in AASHTO (2012). The lower resistance factor values may result from the uncertainties in LRFD calibration. The uncertainties can occur from different sources such as data quality, load test procedures, inaccurate soil properties, presence of outliers in the database etc.

Observing the databases from different LRFD calibration studies, it was found that the majority of the load tests were Osterberg Cell (O-Cell) load test. O-cell is a hydraulic jack that is installed at or near the bottom of the drilled shaft to conduct the O-cell test. Fluid pressure can be applied to the cell through a pipe fixed at the top of the center of the cell. A bi-directional force can be applied to the shaft through the O-cell which causes both upward and downward movement to the shaft. Tell-tale pipes are used to measure the upward and the downward movements. A top movement curve is plotted from the upward movement data and a bottom movement curve is plotted from the downward movement data. In turn, the top and the bottom movement curves are

utilized to reconstruct the top top-down curve. It was assumed that the pile body is rigid in Osterberg (1998) to construct an equivalent top top-down curve from the top and bottom movement curves. Later, this method was improved by taking pile elastic compression in consideration by Loadtest (2001), Kwon et al. (2005) and Lee and Park (2008). To construct the equivalent top-down curve, a random displacement value is selected, and corresponding resistance values are taken from both top and bottom movement curves. Summation of the two different resistance values for the same displacement is a single point in the displacement vs. total resistance curve without considering elastic compression. The displacement vs. total resistance curve can be plotted following this procedure for different values of displacements. As the top and bottom movement curves don't have the same failure load, extrapolation is required to get load values at the same displacement from both curves. Chin's (Ooi et al. 2004) hyperbolic extrapolation method is usually used to get the necessary values. This creates uncertainties in the estimation of the total resistance from the O-cell test data.

Extrapolation is a method of estimating values beyond the observed range by following the trend of the existing data. Though this method is very useful to estimate values, it's subjected to uncertainties and may result in meaningless estimation. In case of O-cell test approach, extrapolation can result in erroneous equivalent top top-down curve due to insufficient displacement, inaccurate data and various other reasons. Paikowsky and Tolsoko (1999) performed an analysis on the non-failed load test. The procedure was based on a database of 63 driven piles tested to failure. Loading was assumed to be known up to 25%, 33%, 50%, 75% and 100% of the entire load settlement data points. It was observed during the study that the extrapolated capacity with 25% and 33% data was 1.5 times to 2.3 times the actual capacity in some cases. This procedure of truncating load test data can be fit to analyze the effect of extrapolation error on the

equivalent top down curve. Ooi' et al. (2004) also performed a similar analysis by incrementally truncating data from load vs settlement curve. The study compared the extrapolated measured capacities to the predicted capacities in order to point out some conditions where extrapolations can result in reasonable values in capacity. Kam Ng et al. (2013) proposed a procedure to construct equivalent top-down curve from load test data on drilled shafts socketed in rock. If top or bottom displacement doesn't reach the failure load, it was proposed in Kam Ng (2013) to limit the displacement to the maximum applied O-Cell load or to the estimated side or tip resistances based on static analysis methods.

Presence of outliers may significantly affect the LRFD calibration. Several studies have been performed to separate the outliers of the calibration databases. Most of the calibration studies applied some kind of filtration process on the databases to separate the most suitable load test cases. Ramin Motamed et al. (2016) performed a calibration on drilled shafts in Las Vegas Valley. They applied a scoring system to quantify the quality of each load test and associated geomaterial properties. They scored the data from 1 to 4, 1 being the worst and 4 being the best data quality. The load test cases with score 1 had extrapolation of more than 2% of the shaft diameter for both components of the bidirectional movements or more than 3% for the top top-down test. On the other hand, the load test cases with score 4 had extrapolation of less than or equal to 2% for one component of the bidirectional test. The combined dataset had mean score in the range of 2 to 2.5. After calibration of the resistance factors, they observed high difference between load test cases with scores of less than 2 and cases with scores of more than 2. Trevor Smith et al. (2011) performed a recalibration of LRFD factors for Oregon Department of Transportation (ODOT), in which, they applied range of +/- 2 S.D (Standard Deviation) for the bias values. This range was not considered valid as it produced artificial tail modifications. Richard J. Bathurst et al. (2008)

suggested that the outlier bias values can be identified by plotting the bias values against the predicted resistance values. It was mentioned that the bias values must be random variables and to meet that condition, there can't be any trends in the bias vs predicted resistance plot. Seok-Jung Kim et al. (2015) suggested introducing a lower bound to the bias value distribution can produce more accurate LRFD resistance factors. 13 sets of drilled shaft load test results were collected for this study. They estimated the lower bounds of the resistance values based on Hoek Brown failure criteria and downgraded Geomaterial properties. The lower bound resistance values were utilized to estimate the lower bound for the bias values. Introduction of the lower bounds increased the resistance factor values up to 8% for the shaft resistance and up to 13% for base resistance. Among the studies, applying lower bounds has been proved to be most effective to get more accurate resistance factor values though it has not been applied to estimate the bias distribution to any DOTs yet.

1.2. Problem Statement

It was observed in the region based LRFD calibration studies that a major portion of the considered databases included Osterberg Cell load test. It was also observed that extrapolation plays a significant part in reconstructing top top-down settlement curve from the Osterberg Cell load test data which may produce errors in the estimation of resistance of the drilled shafts. Though the error causing from extrapolation may affect the LRFD resistance factor calibration, very little consideration was given to it in the studies mentioned in the previous section. No model was suggested for estimating the errors occurring from the extrapolation. Also, finite element modeling was not applied in any of the studies in order to investigate the effect of extrapolation on LRFD calibration process. An analysis of the errors occurring from extrapolation of top and bottom movement curves can result in more accurate LRFD calibration of resistance factors.

Many of the previously mentioned studies on LRFD calibration of resistance factors applied different procedures to filter out load test data with questionable quality. The applied procedures included introduction of scoring system based on data quality, utilizing a range of +/- 2S.D. etc. As there is no available standard procedure to select better quality load test data, use of different procedures may affect the results of the LRFD calibration of resistance factors.

1.3. Objective

The primary objective of this study is to improve the calibration procedure of LRFD resistance factors for drilled shafts by addressing different uncertainties in the calibration process. The primary objective can be broken into the following goals –

1. Minimize the bias errors produced from the extrapolation of O-Cell load test data by proposing a method to estimate the errors and perform LRFD calibration based on the proposed method.
2. Numerical Simulation of O-cell load test in order to reach the failure load without extrapolation and perform LRFD calibration based on the simulated database.
3. Incorporate lower bound resistance of drilled shafts in the LRFD calibration.

1.4. Organization of the Dissertation

In total, seven chapters are included in this dissertation. Chapter 1 introduces the topic and provides some background information about the LRFD calibration of resistance factors for drilled shafts. The purpose and specific objectives of this research study are highlighted to emphasize the necessity and importance of this study.

In Chapter 2, the current design practice is discussed. The current method of reliability-based LRFD calibration can also be found in Chapter 2. It also includes discussions on previous

studies performed with an objective of calibrating resistance factors based on probabilistic reliability-based methods. Discussions on the drilled shaft databases included in several previous studies are also incorporated in this chapter. Several studies on sources of uncertainties in the LRFD calibration procedure are also discussed in Chapter 2.

In Chapter 3, the load test database utilized for this dissertation is discussed in details. The background of the database and different subcategories of the database are described in this chapter. A reliability based LRFD calibration was conducted based on this database. The steps to the calibration as well as the results are also discussed in Chapter 3.

Chapter 4 includes the analyses performed to the effect of extrapolation of the top and the bottom movement curves on LRFD calibration. A regression analysis is performed to enable the estimation of the error in bias values occurred from the extrapolation. The result from the regression analysis is also applied on the accumulated database. The effect of the consideration of extrapolation error is compared to the conventional LRFD calibration.

Chapter 5 summarizes the procedure of the finite element modeling of the bidirectional load tests. The load tests are simulated up to the failure point for top and bottom movement of the shafts and LRFD calibration is performed based on the simulated database. The calibration results from the simulated database are compared to the results in Chapter 4.

Chapter 6 discusses the importance of incorporating lower bounds to the distribution of resistance bias. The methods of estimating the lower bounds are also discussed here. LRFD calibration is performed considering the lower bounds and the results are compared to conventional LRFD calibration results.

Chapter 7 summarizes the findings of the research performed for the dissertation. The limitations and recommendations for studies on LRFD calibration are also discussed here

Chapter 2

LITERATURE REVIEW

2.1. Introduction

Deep foundations are referred to structural components that carry the load from the superstructure to soil layers in extensive depth compared to shallow foundations. Driven piles, drilled shafts, micropiles can be mentioned as examples of deep foundations. Initially, allowable stress design (ASD) method was followed to design the components of deep foundation of bridges. On the other hand, load factor design (LFD) method was followed to design the superstructures. While the LRFD method considers load factors as well as resistance factors to be applied to the limit state inequalities, the ASD method combines both of the factors into a single factor of safety. Consideration of two separate factors for load and resistance has made the LRFD method more consistent than the ASD method (Abu Farsakh et al., 2010). After the publication of the first edition of AASHTO LRFD Bridge Design Specifications, the major challenge was to make the transition from ASD to LRFD. To begin the transition from ASD to LRFD, the Federal Highway Administration (FHWA) released a policy in 2000 that required all new federally-funded bridges to be designed using the AASHTO LRFD specifications by October 2007 (Fortier, 2016). Despite this steady progression into LRFD, however, deep foundation design still does not take full advantage of the probabilistic framework in many parts of the United States due to a lack of area-specific resistance factors derived using reliability theory–based calibrations. Instead, many regions rely on values given in specifications from AASHTO (2010) which were developed by fitting to allowable state design (ASD) safety factors (Stanton et al. 2017). Studies like Abu-

Farsakh et al. (2012), Long et al. (2009), Roling et al. (2011); Garder et al. (2012), Rahman et al. (2002), and McVay et al. (2005) were performed with an objective of calibrating region wise load and resistance factors for foundation design. Perusing all the studies, it was observed that the resistance factors did not improve with the consideration of region-based soil properties, in fact, they decreased in some cases. The low resistance factor values may occur from different uncertainties like inaccuracy in load test data, inaccurate soil test data, effect of outlier cases etc.

As the study of this research is to develop a reliability framework incorporating the uncertainties for a more rigorous calibration of resistance factors for drilled shafts, it is necessary to discuss about the current practice of calibrating the resistance factors. Along with the current practice for calibration of resistance factors, this chapter includes discussions on the previous studies performed in order to calibrate resistance factors in area specific conditions. Previous studies on uncertainties of the calibration procedure will also be discussed in this chapter.

2.2. Drilled Shaft Design Practice

A drilled shaft is a foundation unit that is entirely or partially embedded in the ground. It's constructed by placing concrete in a drilled hole with or without steel reinforcement. Drilled shaft also known as canst-in-drilled hole (CIDH) can be used in cases where driven piles are not suitable. It can be used when large vertical or lateral resistance is required or to resolve constructability issues. The diameter of drilled shafts can be in between the range of 2 to 30 ft. It is possible for the length of a drilled shaft to be more than 300 ft. In recent years, the use of drilled shafts for bridge foundations have increased dramatically due to their capability to withstand high lateral pressure. Stability against scour depth requirements and economical construction methods also affected the increasing popularity of drilled shafts for bridge foundations (M. Gunaratne, 2006).

The total capacity of a drilled shaft can be divided into side resistance and tip resistance. When axial load is applied on top of the drilled shaft, it causes the shaft to move downwards by mobilizing the shearing resistance of soil. Thus, the load is transferred to the surrounding soil and as a result, reducing the load along the length of the shaft. If the shearing resistance in the surrounding soil along the shaft is completely mobilized, the rest of the load is transferred to the bottom of the shaft, which mobilizes the soil resistance at the tip of the shaft (F. H. Kulhawy, 1991). For this study, the side and tip resistance of the shafts were estimated based on the approach mentioned in Federal Highway Administration (FHWA) manuals (O'Neil and Reese, 1999; Brown et al., 2010).

As the design approach of drilled shaft varies with the difference in the type of the geomaterial, it is necessary to discuss about different types of soils according to the FHWA manuals. Types of geomaterials according to O'Neil and Reese (1999) are –

a) Cohesive Soil: This includes clay or silt with undrained shear strength value of less than 0.25 MPa or 2.5 tsf.

b) Granular Soil: It includes sand, gravel or non-plastic silt with average SPT value of less than 50 blow per feet for each layer.

c) Intermediate Geomaterial (IGM): This is the geomaterial that has strength properties in between soil and rock. It can also be classified based on the soil being cohesive or cohesionless.

Cohesive IGM- This is clay with undrained shear strength value with in the range of 0.25 to 2.5 MPa.

Cohesionless IGM- This is granular soil with average SPT value of more than 50 blows per feet for each soil layer.

d) Rock: This is cemented geomaterial with undrained shear strength (S_u) value of more than 2.5 MPa.

Design approaches for each of these soil layers according to FHWA specifications are discussed in this section.

2.2.1. Side and Tip Resistance in Cohesive Soil

According to O'Neil and Reese (1999), cohesive soil can be defined as clay or plastic silt with S_u value less than 0.25 MPa or roughly 2.5 tsf. Methods to determine side and tip resistance of drilled shaft are discussed in the following section.

2.2.1.1. Side Resistance in Cohesive Soil

According to both O'Neil and Reese (1999) and Brown et al. (2010), α-method can be used to determine the side resistance of drilled shafts. While calculating side resistance, some parts of the drilled shaft are excluded from the calculation. Such as, at least the top 5 ft of drilled shaft doesn't contribute in the side resistance. According to O'Neil and Reese (1999), a bottom length equal to the shaft diameter is also excluded in case of straight shafts. In case of a drilled shaft with belled end, periphery of the belled end as well as a length above the belled end equal to the drilled shaft is kept out of the side resistance calculation. On the other hand, Brown et al. (2010) recommended against neglecting a portion above the tip of the shaft from the estimation procedure of the side resistance.

The unit side resistance for a single drilled shaft in cohesive soil can be calculated as (Brown et al. 2010) -

$$q_s = \alpha S_u \quad (2\text{-}1)$$

Here,

q_s = Unit side resistance of drilled shaft

S_u = Undrained shear strength

α is a dimensionless coefficient that can be determined through the following procedure -

$\alpha = 0$; Between ground surface and 5 ft depth

$$\alpha = 0.55 \text{ for } \frac{S_u}{P_a} \leq 1.5$$

$$\alpha = 0.55 - 0.1\left(\frac{S_u}{P_a} - 1.5\right) \text{for } 1.5 \leq \frac{S_u}{P_a} \leq 2.5$$

According to Brown et al. (2018), the dimensionless coefficient α can be estimated by the following equation –

$$\alpha = 0.30 + \frac{0.17}{\frac{S_u(CIUC)}{P_a}}$$

Here, CIUC denotes to the consolidated isotropically undrained triaxial compression test. AASHTO (2017) and Loehr et al (2017) recommended CIUC over conventional UC or UU tests to estimate the undrained shear strength.

2.2.1.2. Tip Resistance in Cohesive Soil

Both O'Neil and Reese (1999), Brown et al. (2010) and Brown et al. (2018) have similar approach to estimate the tip resistance of drilled shaft in cohesive soil. If design undrained shear strength (S_u) is less than 96 KPa and the depth of the tip of shaft is more than three times of the diameter of the shaft, then the tip resistance can be estimated by the following equation –

$$q_p = 9S_u \quad (2\text{-}2)$$

If design undrained shear strength (S_u) is more than 96 KPa and the depth of the tip of shaft is more than three times of the diameter of the shaft, then the tip resistance can be estimated by the following equation –

$$q_p = (4/3)[\ln(I_r) + 1]S_u = N_c^* S_u \quad (2\text{-}3)$$

If design undrained shear strength (S_u) is more than 96 KPa and the depth of the tip of shaft is less than three times of the diameter of the shaft, then the tip resistance can be estimated by the following equation –

$$q_p = (2/3)[1 + (1/6)(D/B)]N_c^* S_u \quad (2\text{-}4)$$

Here,

D = Depth of drilled shaft base

B = Diameter of drilled shaft

q_p = Nominal unit tip resistance

S_u = Undrained shear strength

N_c^* = Bearing capacity factor

I_r = Rigidity index = ($E_s/3S_u$)

E_s = Young's modulus of soil for undrained loading

As the rigidity index (I_r) is depended on the elasticity as well as the shear strength of soil, the bearing capacity factor can be estimated based on the undrained shear strength as shown in Table 2-1. Linear interpolation may be required to get the appropriate values.

Table 2 - 1 Values of rigidity index and bearing capacity factor. (O'Neil and Reese, 1999)

Undrained shear strength (S_u), lb/ft^2	**Rigidity index, $I_r = E_s/3S_u$**	**Bearing capacity factor, N_c^***
500	50	6.5
1000	150	8.0
2000	250-300	9.0

2.2.2. Side and Tip Resistance in Cohesionless or Granular Soil

Cohesionless soil or granular soil is comprised of sand, gravel or non-plastic silt with N (average within layer) is less than or equal to 50B or 0.3 m (50 blows/ft) according to O'Neil and Reese, (1999). Side and tip resistance of drilled shaft in cohesionless soil determination approach is described in the following section.

2.2.2.1. Side Resistance in Cohesionless Soil

β-method is recommended to determine the side resistance in cohesionless or granular soil in both O'Neil and Reese (1999) and Brown et al. (2010). Nominal unit side resistance of drilled shaft in cohesionless soil can be calculated as-

$$q_s = \beta\sigma'_v \tag{2-5}$$

While determining the side resistance, β is different for sandy soil and gravel. For sandy soils,

$$\beta = 1.5 - 0.135\sqrt{z} \text{ for } N_{60} \geq 15 \tag{2-6}$$

$$\beta = \frac{N_{60}}{15}\left(1.5 - 0.135\sqrt{z}\right) \text{ for } N_{60} < 15 \tag{2-7}$$

For Gravelly sand and gravel,

$$\beta = 2.0 - 0.06\ (z)^{0.75} \tag{2-8}$$

Here,

q_s = Nominal unit side resistance of drilled shaft

β = Side resistance coefficient

z = Thickness of the soil layer

σ_v' = Vertical effective stress at the middle depth of soil layer

O'Neill and Reese (1999) recommends allowing β to increase to 1.8 in gravels and gravelly sands, however, it's also recommended to limit the unit side resistance to 4.0 ksf in all soils.

This approach of estimating β is based on field load tests derived by fitting to design curves. Brown et al. (2010) and Brown et al. (2018) presents a more rational approach to estimate β based on Chen and Kulhawy (2002). This method can be utilized for both cohesionless soil and cohesionless IGM soil. In this method, β is estimated based on the coefficient of horizontal soil stress (K) which is a function of the at rest value (K_o). As K_o is directly related to overconsolidation ratio, K_o can be approximated as –

$$K_o = (1 - \sin\varphi')\, OCR^{\sin\varphi'} \leq K_p \tag{2-9}$$

Overconsolidation ratio is the ratio between preconsolidation stress and overburden stress of soil. K_p is the coefficient of passive earth pressure. For cohesionless soil, K_p can be calculated as –

$$K_p = \tan^2\left(45^o + \frac{\varphi'}{2}\right) \tag{2-10}$$

Mayne (2007) recommended the following equation for a rational estimation of effective preconsolidation stress (σ_p').

$$\frac{\sigma_p{}'}{P_a} = 0.47\,(N_{60})^m \tag{2-11}$$

Here, m can be assumed as 0.6 for clean quartzitic sand and 0.8 for silty sand to sandy silt. P_a is the atmospheric pressure. So, the side resistance coefficient can be approximated by –

$$\beta = (1 - \sin\varphi')\left(\frac{\sigma_p{}'}{\sigma_v{}'}\right)^{\sin\varphi'} \tan\varphi' \leq K_p \tan\varphi' \tag{2-12}$$

2.2.2.2. Tip Resistance in Cohesionless Soil

According to both O'Neil and Reese (1999) and Brown et al. (2010), tip resistance of drilled shaft in cohesionless soil can be calculated as –

$$q_p = 0.60\ N_{60} \leq 30\ \text{tsf} \quad (2\text{-}13)$$

Where,

q_p = Nominal unit tip resistance of drilled shaft (tsf)

N_{60} = SPT blow count

If the SPT blow count value is more than 50, the equation will not be effective. In that case, load test is recommended. Otherwise, the upper value of 30 tsf should be assumed for the tip resistance.

2.2.3. Side and Tip Resistance in Intermediate Geomaterial

Resistance of drilled shaft in intermediate geomaterial is different for cohesive IGM and cohesionless IGM. Design approach for both cohesive IGM and cohesionless IGM follows O'Neil and Reese (1999), which is going to be discussed here.

2.2.3.1. Side Resistance in Cohesive IGM

Roughness of the borehole wall plays crucial role in case of side resistance in cohesive IGM. The borehole is considered smooth unless it's roughened artificially. The unit side resistance of drilled shaft in cohesive IGM with smooth borehole wall can be calculated from the following equation. α can be determined from Figure 2-1.

$$q_s = \alpha \varphi q_u \quad (2\text{-}14)$$

Here,

E_m = Young's Modulus of the IGM mass

q_u = Unconfined strength of the intact IGM

w_t = Settlement of the socket at which α is developed

Φ_{rc} = Angle of interface friction

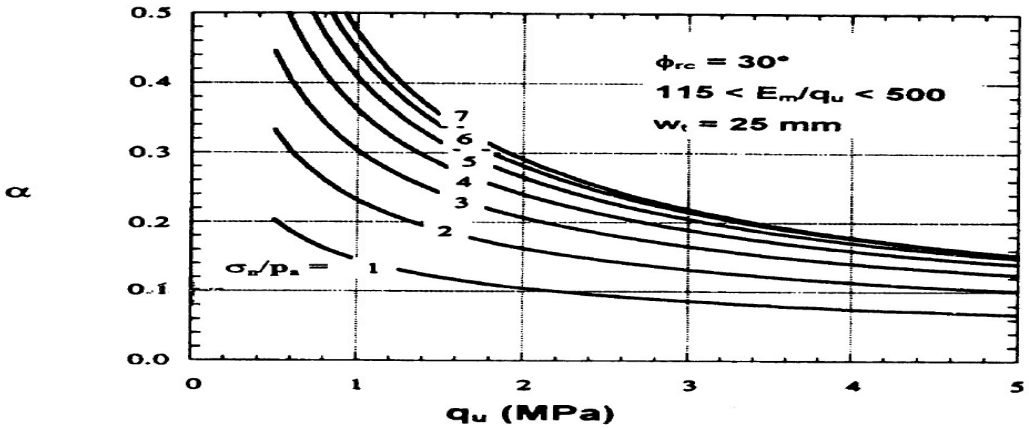

Figure 2 - 1 Factor α for cohesive IGM (O'Neil and Reese, 1999).

σ_n = Pressure imparted by fluid concrete at the middle of layer = $0.65\gamma_c z_i$

γ_c = Unit weight of concrete at or above 7 in

z_i = Depth below cutoff elevation

If Φ_{rc} is different from 30° then it can be calculated using the following equation-

$$\alpha = [\alpha(\text{Figure} - 1)].\left[\frac{\tan\emptyset_{rc}}{\tan 30^o}\right] \quad (2\text{-}15)$$

Table 2 - 2 Factors φ for cohesive IGM's.

RQD (percent)	Φ	
	Closed joints	Open or gouge-filled joints
100	1.00	0.85
70	0.85	0.55
50	0.60	0.55
30	0.50	0.50
20	0.45	0.45

φ is a joint effect factor and it can be determined from Table-1. If RQD is less than 20% for a cohesive IGM layer, load test is required to determine unit nominal side resistance. The unit side resistance of drilled shaft in cohesive IGM with rough borehole wall can be calculated as-

$$q_s = \frac{q_u}{2} \tag{2-16}$$

Generally, the average unconfined strength (q_u) within the layer is used to determine the unit side resistance but the median value is used in case of widely varying q_u.

2.2.3.2. Tip Resistance in Cohesive IGM

Tip resistance of drilled shaft in cohesive IGM is similar to tip resistance in rock according to O'Neil and Reese (1999). It will be discussed in a later section.

2.2.3.3. Side Resistance in Cohesionless IGM

According to O'Neil and Reese (1999), unit side resistance of drilled shaft in cohensionless IGM can be determined as –

$$q_s = \sigma'_{vi} K_{oi} \tan\varphi'_i \tag{2-17}$$

Here,

σ'_{vi} = Vertical effective stress at the middle of layer i

K_{oi} = Design value of earth pressure coefficient at rest in layer i

φ_i' = Design value for angle of friction in layer i

K_{oi} and φ_i' can be determined through field or laboratory tests or they can be estimated using the following equations. In this case, N_{60} should be limited to 100 blows/feet. Δz_i should be limited to 9m (30 ft).

$$\varphi_i' = \tan^{-1}\left[\left\{\frac{N_{60}}{12.3 + 20.3\left(\frac{\sigma_{vi}'}{P_a}\right)}\right\}\right]^{0.34} \quad (2\text{-}18)$$

$$K_{oi} = (1 - \sin\varphi_i')\left[\frac{0.2P_aN_{60}}{\sigma_{vi}'}\right]^{\sin\varphi_i'} \quad (2\text{-}19)$$

2.2.3.4. Tip Resistance in Cohesionless IGM

If the SPT (N_{60}) value is more than 50, then that soil is termed as cohesionless IGM. Nominal unit tip resistance of cohesionless IGM can be determined as –

$$q_p = 0.59\left[N_{60}\left(\frac{P_a}{\sigma_v'}\right)\right]\sigma_v' \quad (2\text{-}20)$$

Here,

P_a = Atmospheric Pressure (2.116 ksf)

σ_v' = Vertical effective stress at the tip

2.2.4. Side and Tip Resistance in Rock

AASHTO LRFD Bridge Design Specifications (2012) is followed to estimate the Side and Tip Resistance of a drilled shaft embedded in rock. These semi-empirical methods are based on load test data and site specific correlation between measured resistance and rock core strength.

2.2.4.1. Side Resistance in Rock

Unit Side Resistance of drilled shaft, q_s (ksf) in rock can be estimated as –

$$q_s = 0.65\alpha_E P_a \left(\frac{q_u}{P_a}\right)^{0.5} < 7.8 P_a \left(\frac{f_c'}{P_a}\right)^{0.5} \quad (2\text{-}21)$$

Here,

q_u = Uniaxial compressive strength of rock (ksf)

P_a = Atmospheric pressure (2.12 ksf)

α_E = Reduction factor to account for jointing in rock as shown Table 2 -3

f_c' = Compressive strength of concrete (ksi)

Table 2 - 3 Estimation of α_E (O'Neil and Reese, 1999)

E_m/E_i	α_E
1.00	1.00
0.50	0.80
0.30	0.70
0.10	0.55
0.05	0.45

The ratio of rock mass modulus to intact rock modulus (E_m/E_i) can be estimated from the following table –

Table 2 - 4 Estimation of E_m/E_i (O'Neil and Reese,1999)

RQD (Percent)	E_m/E_i	
	Closed Joints	Open Joints
100	1.00	0.60
70	0.70	0.10
50	0.15	0.10
20	0.05	0.05

2.2.4.2. Tip Resistance in Rock

Estimation approach of the tip resistance of drilled shaft in rock was also accumulated from O'Neil and Reese (1999). If the rock below the tip of the drilled shaft to a depth of 2B is intact or tightly jointed and the depth of the borehole or socket is more than 1.5B, then unit tip resistance, q_p (ksf) can be determined from –

$$q_p = 2.5 q_u \tag{2-22}$$

If the rock below the tip of the drilled shaft to a depth of 2B is jointed and the joints are randomly oriented, then unit tip resistance q_p (ksf) can be estimated as –

$$q_p = \left[\sqrt{s} + \sqrt{\left(m\sqrt{s} + s\right)}\right] q_u \tag{2-23}$$

Here,

q_u = Unconfined compressive strength of rock (ksf)

s,m = Fractured rock mass parameters from Table 2-5

Table 2 - 5 Approximate relationship between rock-mass quality and material constants used in defining nonlinear strength (AASHTO, 2012)

Rock Quality	Constants	Rock Type				
		A	B	C	D	E
Intact Rock Samples Laboratory size specimens free from discontinuities RMR=100	m	7.00	10.00	15.00	17.00	25.00
	s	1.00	1.00	1.00	1.00	1.00
Very Good Quality Rock Mass Tightly interlocked rock with unweathered joints at 3-10 ft RMR=85	m	2.40	3.43	5.14	5.82	8.567
	s	0.082	0.082	0.082	0.082	0.082
Good Quality Rock Mass Fresh to slightly weathered rock with joints at 3-10 ft RMR=65	m	0.575	0.821	1.231	1.395	2.052
	s	0.00293	0.00293	0.00293	0.00293	0.00293
Fair Quality Rock Mass Several moderately weathered joints at 1-3 ft RMR=44	m	0.128	0.183	0.275	0.311	0.458
	s	0.00009	0.00009	0.00009	0.00009	0.00009
Poor Quality Rock Mass	m	0.029	0.041	0.061	0.069	0.102
	s	3×10^{-6}	3×10^{-6}	3×10^{-6}	3×10^{-6}	3×10^{-6}

Rock Quality	Constants	Rock Type				
		A	B	C	D	E
Numerous weathered joints at 2-12 in RMR=23						
Very Poor Quality Rock Mass Numerous heavily weathered joints in < 2 in RMR =3	m s	0.007 1×10^{-7}	0.010 1×10^{-7}	0.015 1×10^{-7}	0.017 1×10^{-7}	0.025 1×10^{-7}

Table 2 – 5 (Cont.)

Different types of rocks acoording to AASHTO (2012) used in Table 2-5 are defined below

A = Carbonate rocks with well-developed crystal cleavage— dolomite, limestone and marble.

B = Lithified argrillaceous rocks—mudstone, siltstone, shale and slate (normal to cleavage).

C = Arenaceous rocks with strong crystals and poorly developed crystal cleavage sandstone and quartzite.

D = Fine grained polyminerallic igneous crystalline rocks— andesite, dolerite, diabase and rhyolite.

E = Coarse grained polyminerallic igneous & metamorphic crystalline rocks—amphibolite, gabbro gneiss, granite, norite, quartz-diorite.

RMR is Rock Mass Rating which is a geomechanical classification system for rocks. It specifies the quality of rocks. Table-5 show variation of rock quality with different RMR values.

Table 2 - 6 Geomechanics Rock Mass Classes Determined from Total Ratings (AASHTO, 2012).

RMR	Rock Quality
100-81	Very Good Rock
80-61	Good Rock
60-41	Fair Rock
40-21	Poor rock
<20	Very Poor Rock

2.2.5. Nominal Axial Resistance

After estimating both side and tip resistance of drilled shaft, the nominal axial bearing resistance can be determined. The factored nominal bearing resistance (R_R) can be calculated as (AASHTO, 2012.) –

$$R_R = \varphi R_n = \varphi_{qp} R_p + \varphi_{qs} R_s \quad (2\text{-}24)$$

$$R_p = q_p A_p \quad (2\text{-}25)$$

$$R_s = q_s A_s \quad (2\text{-}26)$$

Where,

R_n =Nominal bearing resistance of drilled shaft

R_p =Drilled shaft tip resistance (kips)

R_s =Drilled shaft side resistance (kips)

φ_{qp} =Resistance factor for tip resistance of drilled shaft

φ_{qs} =Resistance factor for side resistance of drilled shaft

q_p =Unit tip resistance of drilled shaft (ksf)

q_s = Unit side resistance of drilled shaft (ksf)

A_p = Area of drilled shaft tip (ft^2)

A_s = Surface area of drilled shaft side (ft^2)

2.2.6. Settlement of Drilled Shafts

After the assessment of diameter and length of the drilled shaft against axial nominal resistance, it is checked against settlement. In general, the total permissible settlement under the Service-I Limit State should be limited to one inch for multi-span structures with continuous spans or multi-column bents, one inch for single span structures with diaphragm abutments, and two inches for single span structures with seat abutments. For this study, the 5% B failure criterion will also be considered. 5%B means displacement of the shaft equivalent to 5% of the diameter of the shaft.

O'Neil and Reese (1999) has provided some curves summarizing the load settlement data for drilled shaft in dimensionless form. These can be used to determine the short term settlement of drilled shaft. Figure 2 - 2 shows the settlements at which side resistance is mobilized in cohesive soil. The shaft skin friction is typically fully mobilized at displacement of 0.2 percent to 0.8 percent of the drilled shaft diameter in cohesive soil. Figure 2 - 3 presents load settlement curves in end bearing in cohesive soil.

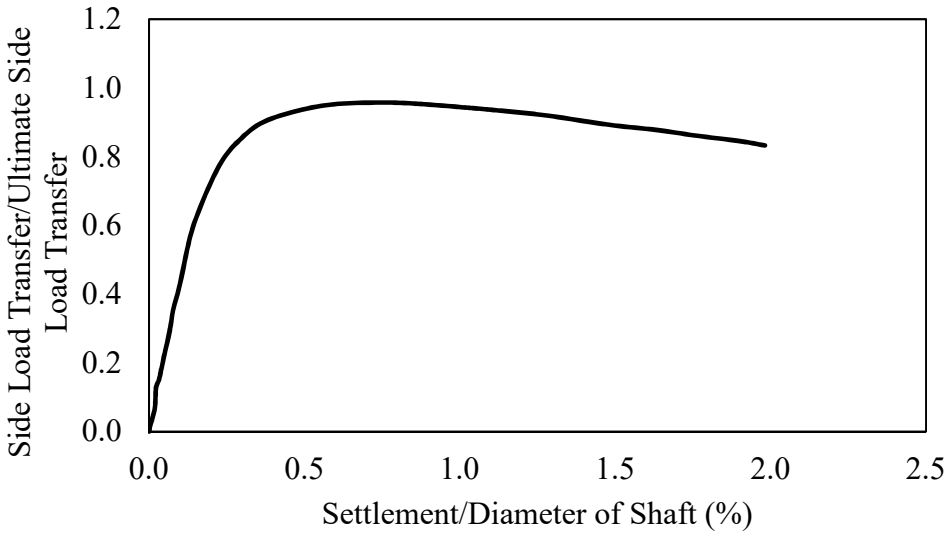

Figure 2 - 2 Normalized load transfer in side resistance vs settlement in cohesive soil (O'Neil and Reese, 1999)

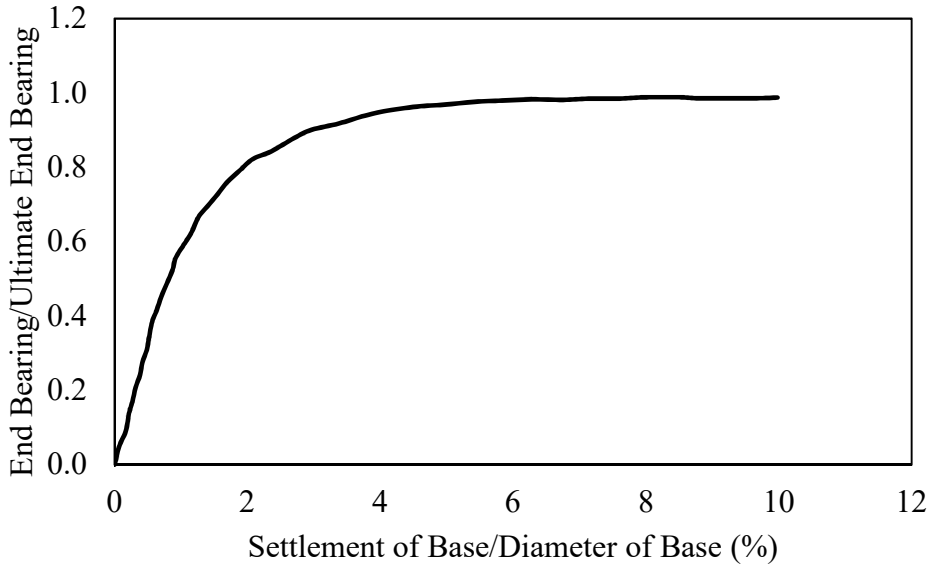

Figure 2 - 3 Normalized load transfer in end bearing vs settlement in cohesive soil (O'Neil and Reese, 1999).

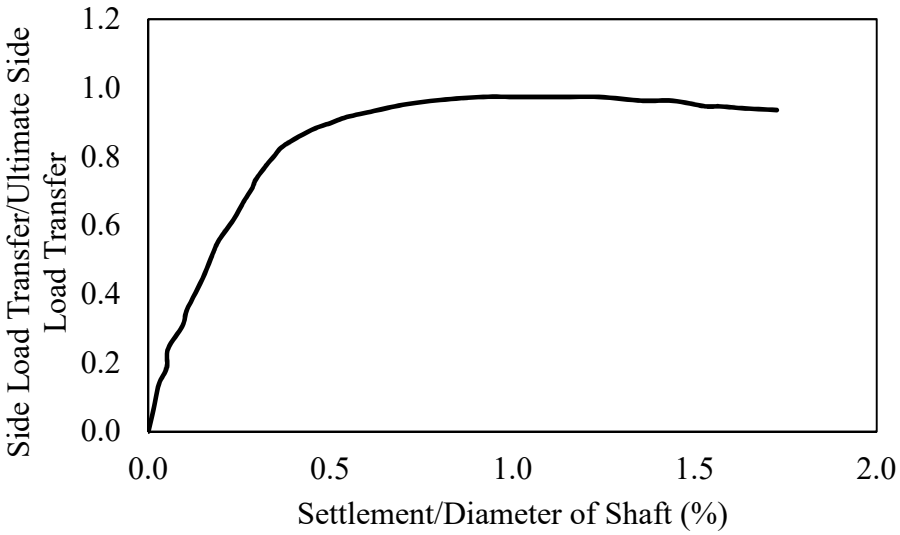

Figure 2 - 4 Normalized load transfer in side resistance vs settlement in cohesionless soil (O'Neil and Reese, 1999)

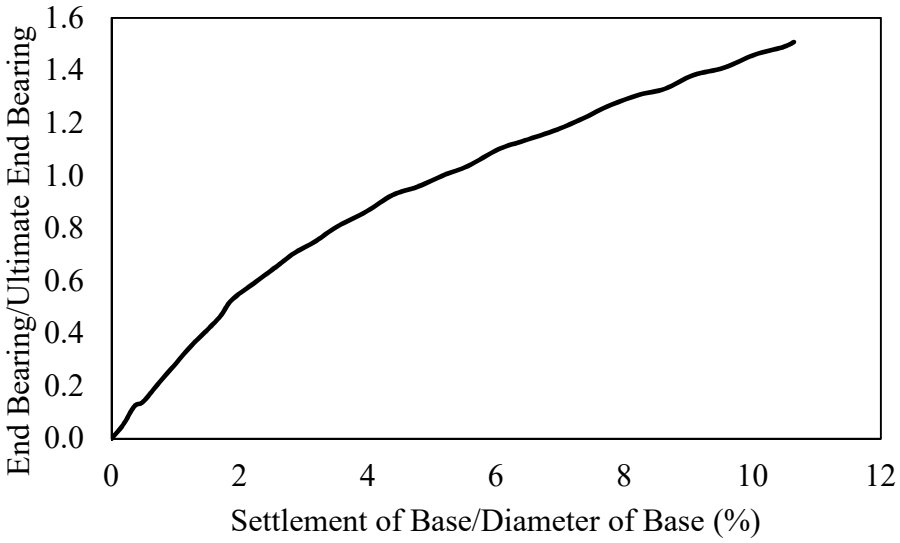

Figure 2 - 5 Normalized load transfer in end bearing vs settlement in cohesive soil (O'Neil and Reese, 1999)

Figure 2 - 4 and Figure 2 - 5 depicts load settlement curves in side bearing and end bearing in cohesionless soil. In cohesionless soil, drilled shaft skin friction is typically fully mobilized at displacement of 0.1 percent to 1.0 percent of the drilled shaft diameter. Load displacement curves

for side and tip resistance of a drilled shaft can be plotted for both cohesive and cohesionless soil after the estimation of the side and tip resistance values utilizing the aforementioned methods.

However, Brown et al. (2010) combined the load displacement curves for side and tip resistance into single curves for both chohesive and cohesionless soil based on the study of Chen and Kulhawy (2002). The combined curves were plotted by interpreting a larger amount of load test data than the previous method. These plots were also easier to use compared to the one mentioned before. Figure 2 – 6 presents the normalized load displacement plots for cohesive and cohesionless soil as it's presented in Brown et al. (2010).

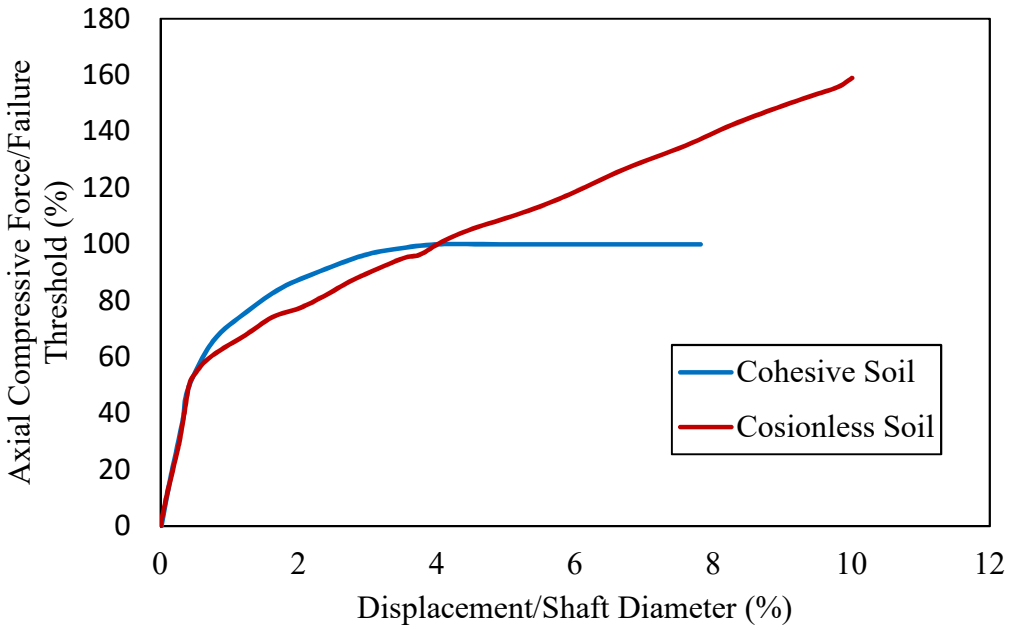

Figure 2 - 6 Combined normalized load displacement curve for side and tip resistance. (Chen and Kulhawy, 2002).

2.3. Load Tests on Drilled Shafts

Measured resistance of drilled shafts is a significant component in the procedure of calibration of the resistance factors. The most reliable way to get the measured resistance of drilled

shafts is to perform load tests on the shafts. There are several types of load tests that are performed to find out the actual capacity or measured resistance of drilled shafts. The most common load tests found on different studies on drilled shafts are static tests, statnamic tests, dynamic tests and bi-directional tests. A brief discussion on these load tests is presented in this section.

1.1.1. Static Load Test

Static test is the most accurate load test that can derive the axial capacity of a drilled shaft. It can be performed with uncomplicated equipment. In this case, the test drilled shaft or pile is loaded with weight. A platform is set up on the top of the shaft to support the weight and to transfer the load on top of the shaft. Usually, wedges are placed at the edges of the platform to support it while loading. Sides are provided on the platform, in case, any loose material like sand is used. Figure 2 – 7 shows typical set up for static load test on a pile.

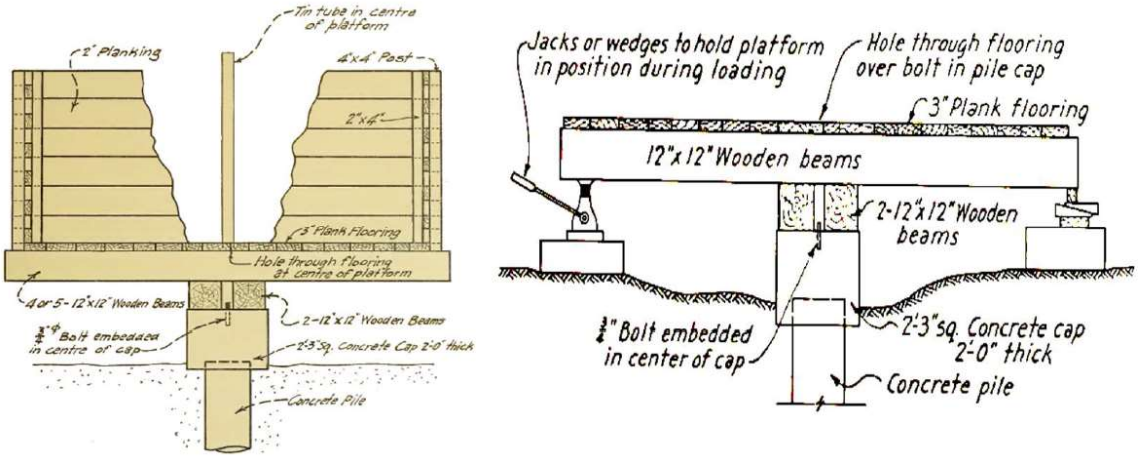

Figure 2 - 7 Static load test set up (Henly Abbot, 1915).

In modern static load tests, a reaction load arrangement is used to apply load on the shaft. Usually, the reaction load can be arranged in four ways i.e. kentledge system, kentledge combined

with anchored piles, system of anchored piles and system of tie down anchors (Prakash and Sharma, 1990). The arrangement makes sure that the load is stable during the load test.

Instrumentation is another significant aspect of a modern load test. A proper instrumentation leads to a stable and accurate completion of a load test. According to modern instrument system, the test shaft is loaded by the application of hydraulic jacks placed on top of the shaft head. Load cells are set up on the hydraulic jacks to measure the load. Steel plates and bourdon gages are also used to measure the applied load. Dial gages, wire gages, optical levelling system and linear displacement transducers are used to measure the displacement of the shaft had due to the applied load (Zenon et al., 1992). Figure 2 -8 shows the instrumentation of a typical static load test set up.

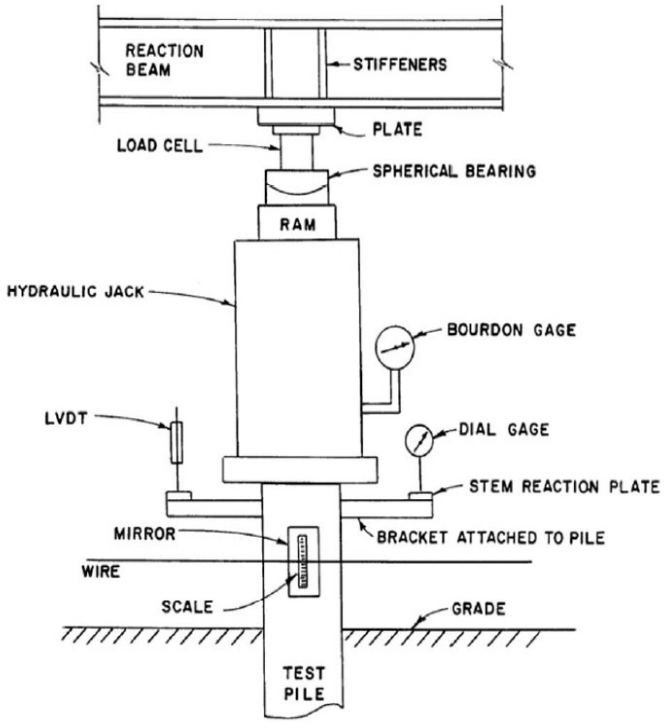

Figure 2 - 8 Instrumentation of static load test to measure applied load and displacement (Zenon et al., 1992)

Suitable loading procedure is another important aspect of static load test. Some of the most common loading procedures are going to be discussed here. The ASTM designation D1143-81(89) recommended a loading procedure, in which, the shaft is loaded in eight equal increments. The loading is continued up to 200% of the design load of the shaft. Each load increment is held until the displacement rate reaches 0.25 mm/h. The final load increment is held for 24 hours and then, the unloading is performed in four equal decrements in one-hour intervals. This procedure is known as slow maintained method. Another loading procedure, also recommended by ASTM D1143-81(89), is quick maintained method. In this method, the load is applied in twenty equal increments in 5 mins intervals up to 300% of the design load. The unloading is also performed in five minutes interval with four equal decrements. In constant rate of penetration method, a displacement rate of 1.25/min is forced on the shaft head. The procedure is continued up to total displacement of 50 to 75 mm.

The results from the static load tests are presented as load settlement curves. The capacity of the shaft is determined from the load settlement curve procured from the load test result. The capacity is equivalent to the failure load of the shaft. There are several ways to determine the failure load from the load settlement curve. Hansen (1963), Chin (1970), Fuller and Hoy (1970), Davisson (1972), Mazurkiewicz (1972), Butler and Hoy (1977) and DeCourt (1999, 2008) have discussed about some of the ways of the estimation of the failure load from the load settlement curve. For this study, 5% B criterion recommended by Federal Highway Administration is going to be used to estimate failure load of drilled shafts. In this method, the load corresponding to the displacement of 5% of the diameter of the shaft is accepted as the failure load.

1.1.2. Bidirectional Load Test

As it was mentioned before that the conventional static load test needs a proper reaction system to apply the load on the shaft, it can cause difficulties, in terms of expense as well as time, in case of shafts with very high load capacity. It's also inconvenient to set up a reaction system when the drilled shaft or pile is under water. Bidirectional load test can be the answer to these difficulties. A jack like device is installed at or near the bottom of the shaft to perform a bidirectional load test. Bidirectional load is applied from the device in both upward and downward direction of the shaft which causes displacement of the shaft head as well as the tip. Figure 2 – 9 shows the comparison between the static test and the bidirectional test based on the location of the jack.

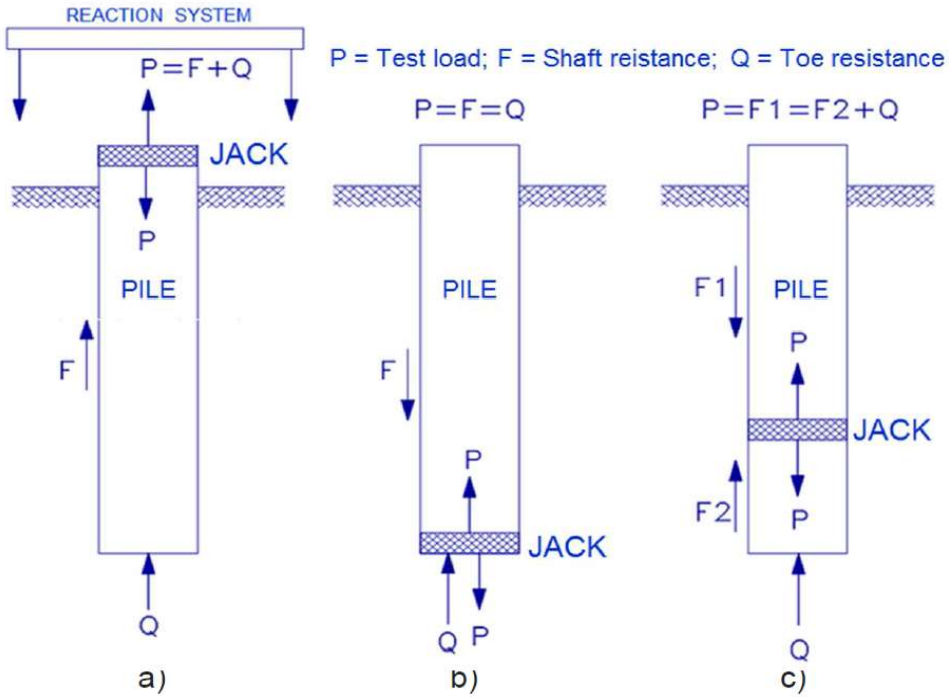

Figure 2 - 9 Location of jack in a) static load test, b) bidirectional test with jack at the bottom and c) bidirectional test with jack in the middle (Nguyen, 2017)..

2.3.2.1. Development of Bidirectional Test

Gibson et al. (1973) described, for the first time, a new load test method in order to reduce the cost related to the setup of a reaction system for a conventional static load test. The study recommended the load test to be performed during site investigation. According to the procedure, a hydraulic jack had to be placed at the bottom of the borehole and plugged by concrete. Load was applied from the jack until failure occurred. Amir (1981) also proposed a load test method using a hydraulic jack placed inside the pile. This method was proposed for piles embedded in rock. Tell-tales had to be installed connecting the jack to the pile head to measure the displacement. Upward and downward displacements of the pile could be measured after the bidirectional load was applied from the jack.

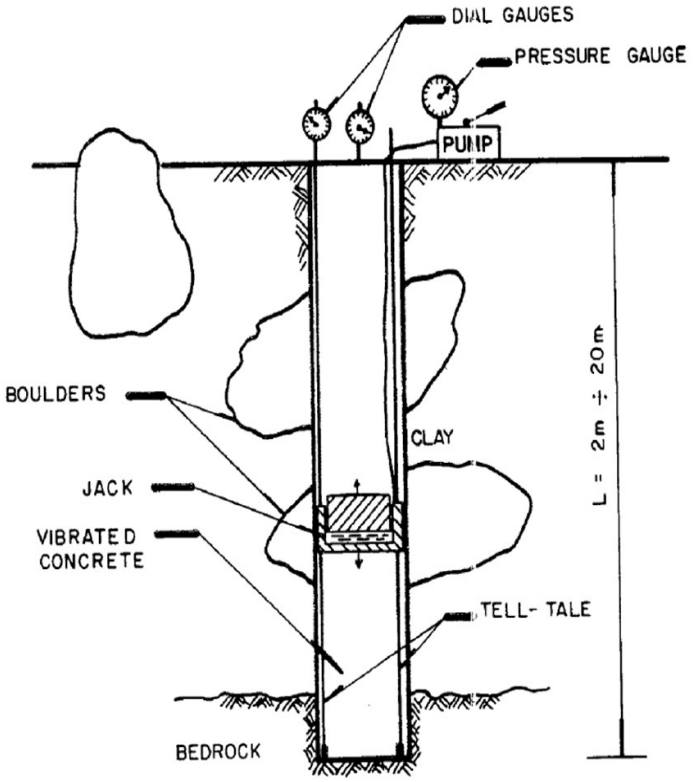

Figure 2 - 10 Bidirectional load test method proposed by Amir (1981).

Elisio (1983) performed a bidirectional load test on a pile with 13 m length and 0.52 m diameter. The pile was placed in sandy clay and silt. The jack was placed 2 m above the base of the pile (Fellenius, 2015). Osterberg (1986) proposed a device to carry out the bidirectional load test. The shaft resistance and the tip resistance of the pile could be measured separately using the proposed device, known as Osterberg cell or O-cell. The device was placed at the bottom of the shaft and load was applied by pressurizing the device using fluids. Thus, the upward movement of the shaft and the downward movement of the tip could be measured. The ultimate side resistance as well as the ultimate tip resistance could be estimated from the upward movement curve and downward movement curve, respectively. Figure 2 – 11 shows the proposed load test system by Osterberg.

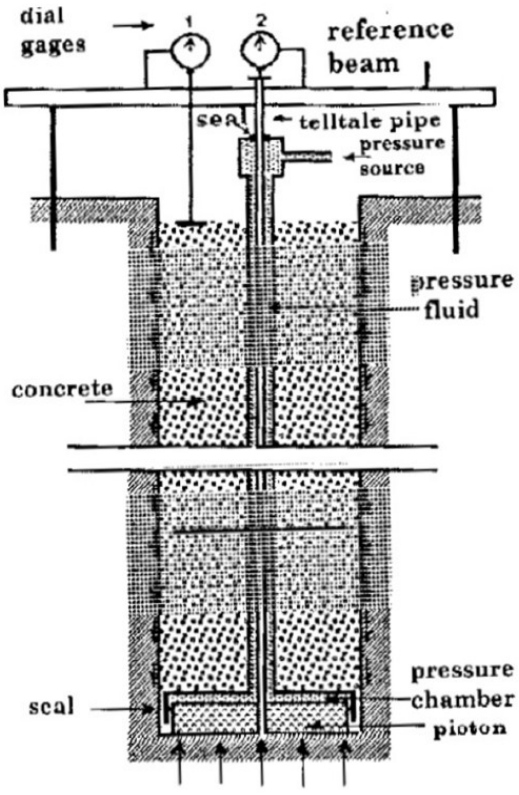

Figure 2 - 11 Bidirectional load test device proposed by Osterberg (Osterberg, 1996).

Osterberg revised the design of the device in Osterberg (1996). In the new version of the device, an expansion chamber was installed at the bottom of the shaft to displace the entrapped air and fluid while the fluid and grout are pumped into the chamber. Tell tales were also installed to supervise the movement of the chamber. Figure 2 – 12 shows the revised device for bidirectional load test.

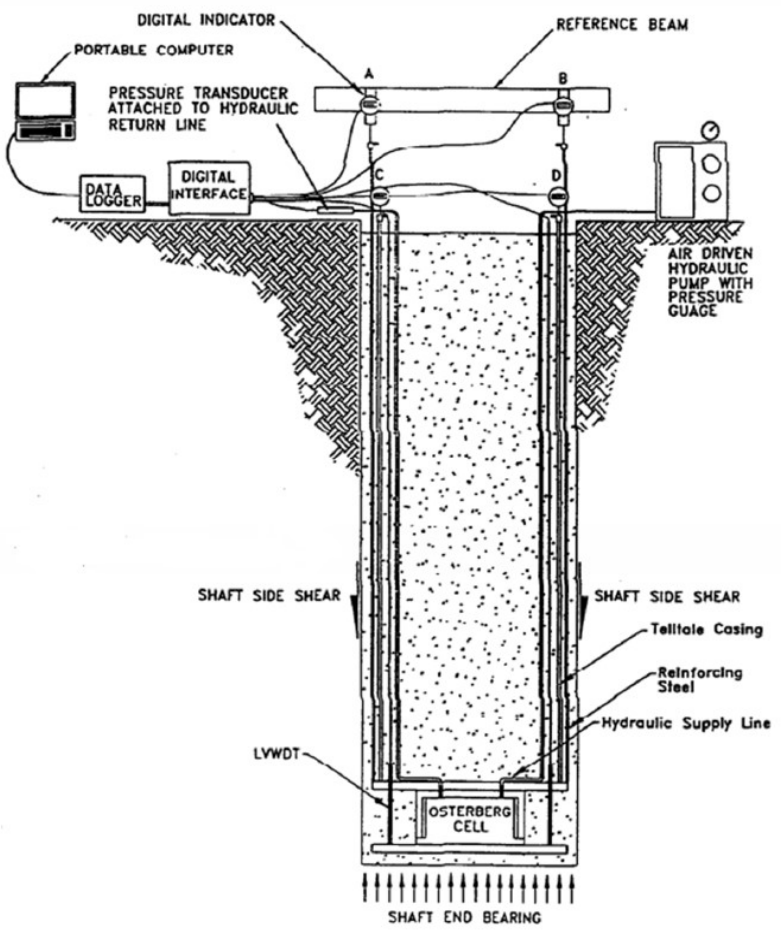

Figure 2 - 12 Revised design of Osterberg cell load test (Osterberg , 1996).

2.3.2.2. Instrumentation and Loading of Bidirectional Load Test

The instruments required to perform a bidirectional load test are jacks and hydraulic control system, telltales and linear displacement transducers, strain gages, dial gages and data logger. The

jack and hydraulic control system are used to apply load on the shaft. Both upward and downward movement of the shaft are measured by measuring the opening of the jacks using the linear displacement transducer and the telltales. Strain gages are used to measure the strain in the shaft in turn, to measure the shaft resistance. The dial gages are utilized to measure the applied load and displacement of the shaft. The data logger is used to record the data in a computer while the test is being performed.

ASTM D1143 -81 (89) is followed for the loading procedure of the load test. Both slow and quick maintained loading methods are applied to perform the test. As it was mentioned before, the loading is performed in eight equal increments for the slow maintained method, and it's performed in twenty equal increments for the quick maintained method. Figure 2 – 13 presents a typical arrangement for a bidirectional load test.

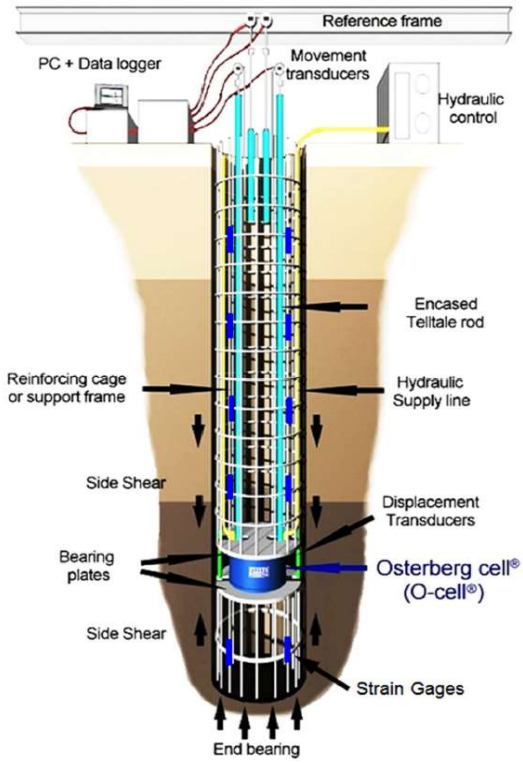

Figure 2 - 13 Typical arrangement for a bidirectional load test (www.Loadtest.com).

2.3.2.3. Interpretation of Bidirectional Test Result

The outputs of a bidirectional load test are top movement vs side resistance plot as well as bottom movement vs tip resistance plot. Like a conventional static load test, bidirectional load test does not provide a load settlement curve which can be defined as the settlement of the shaft vs total resistance plot. Figure 2 – 14 shows the comparison between the results from conventional static load test and bidirectional load test.

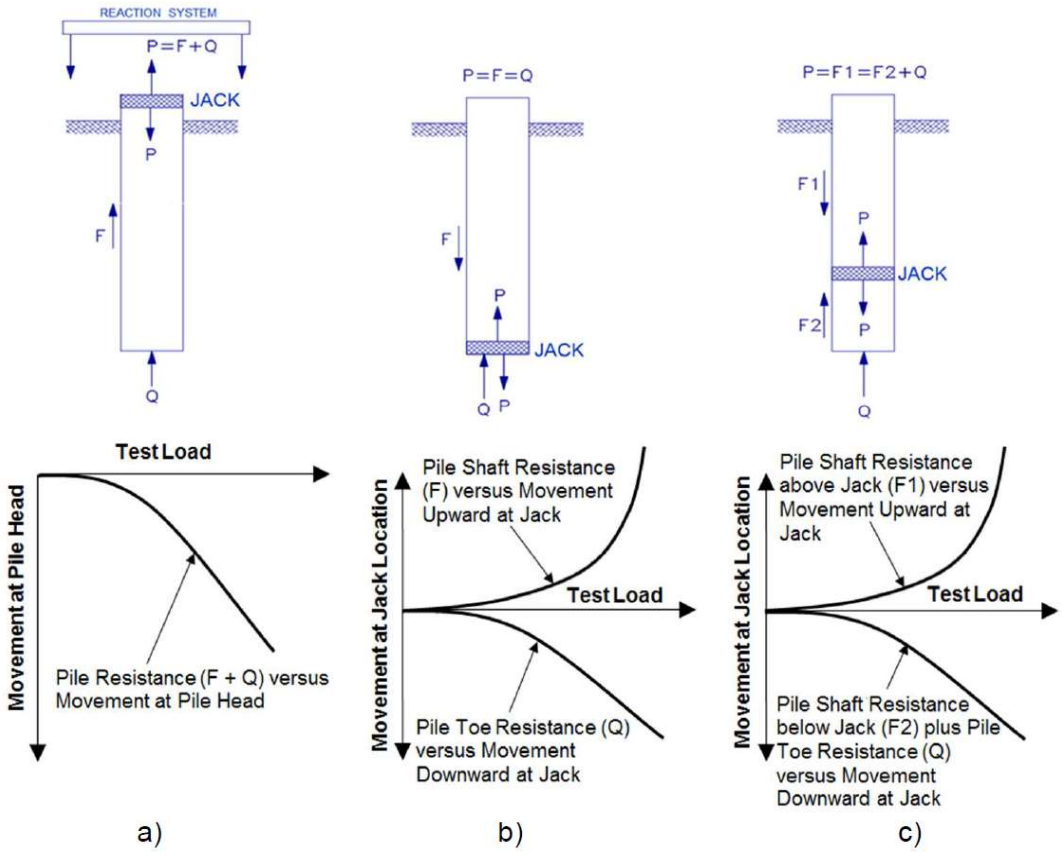

Figure 2 - 14 Curves plotted from a) static load test result, b) bidirectional test result with the jack at the bottom and c) bidirectional test result with the jack in the middle of the shaft (Nguyen, 2017).

It is required to plot a load settlement curve from the upward and downward movement curves in order to obtain the failure load of the shaft. A method to obtain the load settlement curve

from the top and bottom movement curves can be found in Osetrberg (1996). The plotted curve following the aforementioned method was termed as “Equivalent Top Down Curve”. The method to construct the equivalent top down curve was proposed based on three assumptions. The first assumption is that the pile is considered to have a rigid body. It’s also assumed that the upward movement curve from the bidirectional test is similar to the downward movement curve from a static load test. Also, the downward movement curve obtained from the bidirectional test is similar to the toe movement curve obtained from the static load test. To obtain the equivalent top down curve, same movement points are selected in the upward and the downward movement curve. The loads, for the same movement points, from both of the curves are added to get a point in the equivalent top down curve. This process is repeated for different movement points to construct the equivalent top down curve. Figure 2 – 15 shows the procedure to construct the equivalent to down curve from the upward and downward movement curves.

In Figure 2 – 15, all the curves have points denoted from 1 to 12. Same numbered points have the same amount of movement in all the curves. For example, point number 4 has the same movement of 10 mm in all the curves. To obtain the point number 4 in the equivalent top down curve, loads corresponding to point 4 are taken from both the upward and bottomward movement curves. In the upward movement curve, the load corresponding to point 4 is 18.6 MN and in the downward movement curve, the load is 9.4 MN. These loads are summed up and the load corresponding to point 4 is obtained for the equivalent top down curve as 28 MN. This process is repeated for all the points from 1 to 12 to get the corresponding loads in the equivalent top down curve.

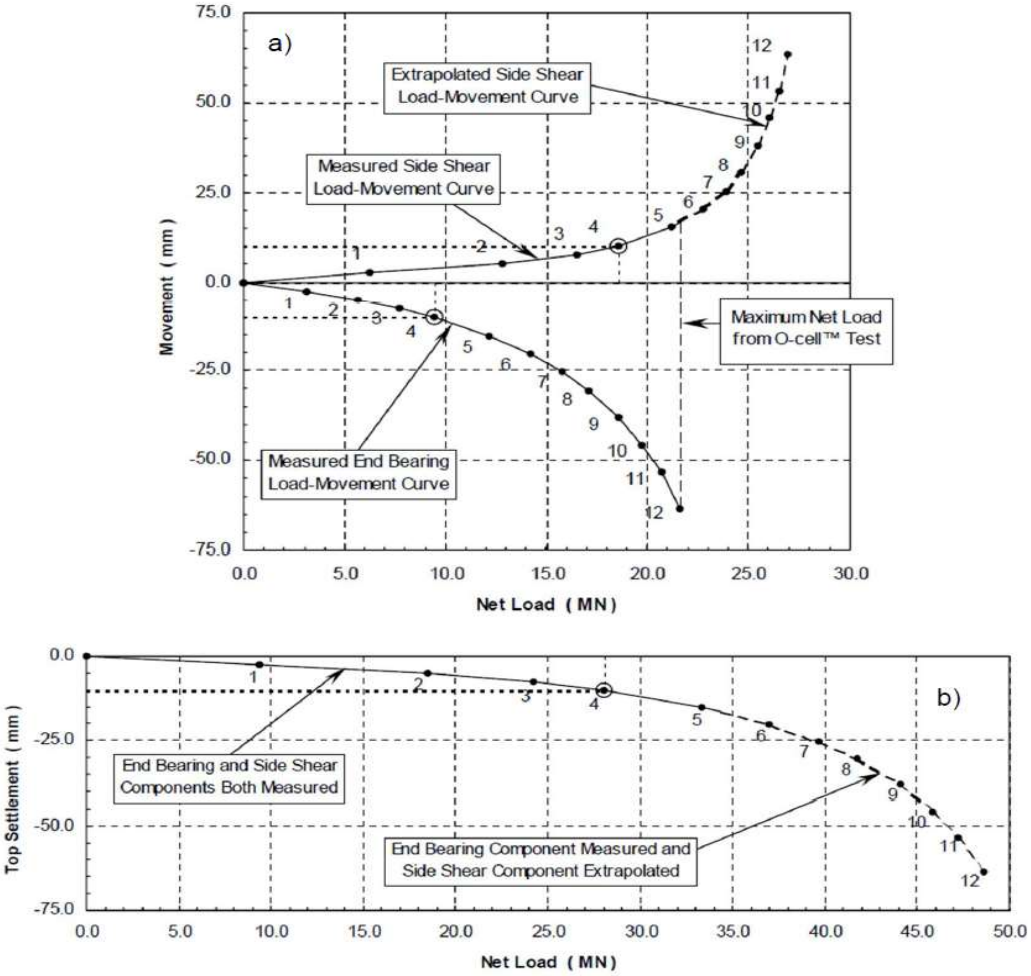

Figure 2 - 15 Method of constructing equivalent top down curve (Loadtest International Pte. Ltd., 2013)

It can be observed in Figure 2 – 15 that the upward movement curve stopped at point 5 after the completion of the load test. As it is required for the upward movement to reach the failure point like the downward movement curve to obtain the equivalent top down curve, the upward movement curve was extrapolated to reach up to point 12. Chin (1970) proposed a procedure which can be followed to extrapolate the top or bottom movement curves. Chin (1970) proposed the method based on a study of Kondner (1963). Kondner (1963) proposed a hyperbolic stress strain relationship for a consolidated-undrained triaxial compression test performed on a remolded

cohesive soil. The relationship was found to be a rectangular hyperbola which is passing through the origin in a two-dimensional stress-strain plot as shown in Figure 2 – 16. Kondner wrote the hyperbolic equation as –

$$\varepsilon\sigma - \beta\varepsilon + \alpha\sigma = 0 \qquad (2\text{-}27)$$

Here, ε is the axial strain and σ is the deviator stress, which can be defined as $(\sigma_1 - \sigma_3)$. If equation 2 – 27 is divided by σ, it can be rearranged as,

$$\frac{\varepsilon}{\sigma} = a + b\varepsilon \qquad (2\text{-}28)$$

Here, $a = \frac{\alpha}{\beta}$ and $b = \frac{1}{\beta}$

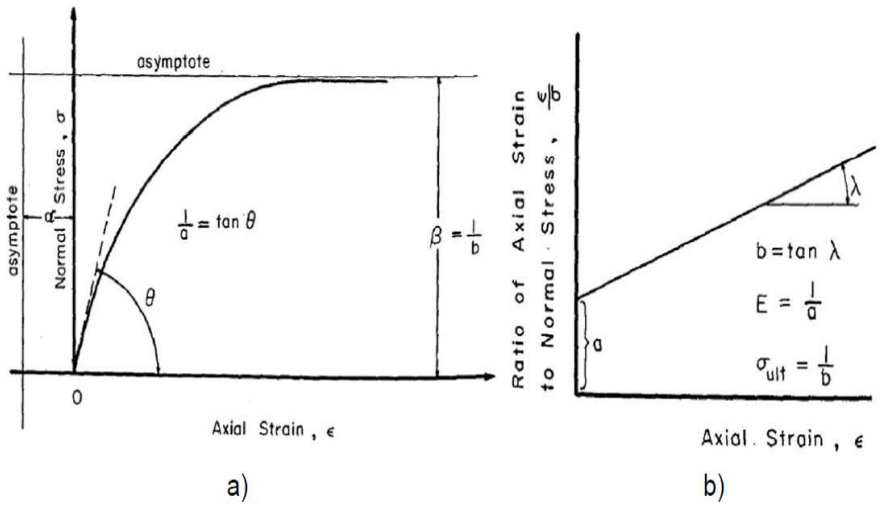

Figure 2 - 16 a) Rectangular hyperbolic relation of stress-strain, b) transformed hyperbolic relation of stress-strain. (Kondner, 1963).

The ultimate value of the stress can be estimated by taking the limit of equation 2 – 28 as ε becomes very large. So, the ultimate strength can be measured by the inverse of the slope of the straight line shown in Figure 2 – 16(b).

Chin (1970) followed this method to extrapolate the upward and downward movement curve by assuming a hyperbolic relation between load and movement. The recommendation by Chin (1970) was to construct a movement/load (δ/Q) vs movement (δ) linear plot and use the inverse slope of the linear relationship to extrapolate the upward and downward curve. The process can be expressed by -

$$Q_u = \frac{1}{C_1} \tag{2-29}$$

Here, Q_u is the ultimate load of the shaft and C_1 is the slope of the line in the movement/load (δ/Q) vs movement (δ) plot. The plot is shown in Figure 2 – 17.

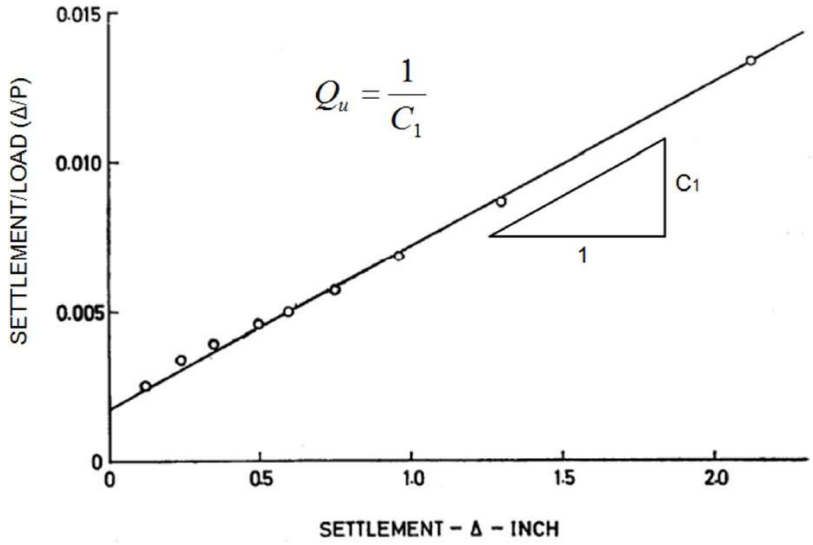

Figure 2 - 17 Movement/load (δ/Q) vs movement (δ) plot (Chin, 1970).

2.3.2.4. Correction for Elastic Shortening

To construct the equivalent top down curve from the result of a bidirectional test, it is assumed that the shaft body is rigid (Osterberg, 1998) but, in reality, the elastic shortening of the shaft material can affect the equivalent top down curve significantly. Khoo (2007) recommended

a method to perform correction on the equivalent top down curve for elastic shortening. Elastic shortening of a shaft for performing bidirectional load test can be estimated by the following relationship.

$$\delta_{BLT} = C\frac{(Q - W_{L1} - W_{L0})L_1}{AE} \quad (2\text{-}30)$$

Here, δ_{BLT} is the elastic shortening of the drilled shaft material because of the bidirectional load. Q is the applied load on the shaft. W_{L1} and W_{L0} are weights of the pile segments L_1 and L_0, respectively, as shown in Figure 2 – 18. L_1 is the length of the pile from the ground surface to the top of the jack or the bidirectional device. A is cross sectional area of the drilled shaft and E is the elastic modulus of the drilled shaft material. C is the centroid factor. C is 1/3 for a triangular resistance distribution as shown in Figure 2 – 18 (a) and 1/2 for a rectangular resistance distribution as shown in Figure 2 – 18 (c).

The elastic shortening of a shaft can be estimated by the following equation for a conventional static load test.

$$\delta_{CLT} = \frac{PL_0}{AE} + (1 - C)\frac{PL_1}{AE} + C\frac{(Q - W_{L2})L_1}{AE} \quad (2\text{-}31)$$

$$P = 2Q - W_{L1} - W_{L0} + W_{L2} \quad (2\text{-}32)$$

Here, δ_{CLT} is the elastic shortening of the drilled shaft material because of the conventional load test. Q is the applied load on the shaft. W_{L0}, W_{L1} and W_{L2} are weights of the pile segments L_0, L_1 and L_2, respectively, as shown in Figure 2 – 18. L_1 is the length of the pile from the ground surface to the top of the jack or the bidirectional device. A is cross sectional area of the drilled

shaft and E is the elastic modulus of the drilled shaft material. C is the centroid factor. C is 1/3 for a triangular resistance distribution as shown in Figure 2 – 18 (a) and 1/2 for a rectangular resistance distribution as shown in Figure 2 – 18 (c).

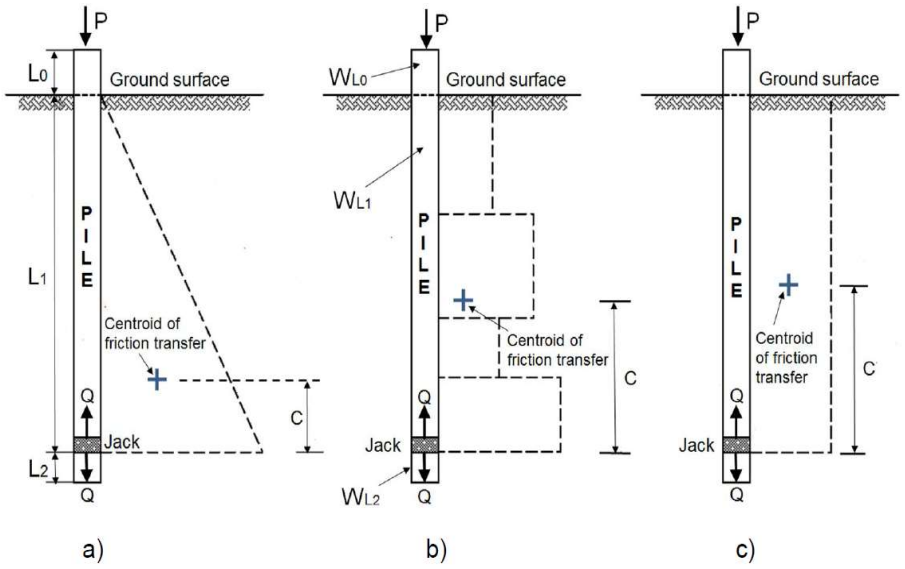

Figure 2 - 18 Distribution of shaft resistance for estimation of elastic shortening in a) cohesionless soil, b) layered soil and c) cohesive soil (Loadtest International Pte. Ltd., 2013).

So, the elastic shortening of the shaft material can be considered for the equivalent top-down curve by utilizing the following equation.

$$\delta_{adj} = \delta_{eq} + (\delta_{CLT} - \delta_{BLT}) \quad (2\text{-}33)$$

Here, δ_{adj} is the correction in the displacement of the shaft due to elastic shortening, δ_{eq} is the displacement of the shaft from the equivalent top-down curve. δ_{CLT} is the theoretical elastic

shortening of the shaft due to conventional load test and δ_{BLT} is the theoretical elastic shortening of the shaft due to bidirectional load test.

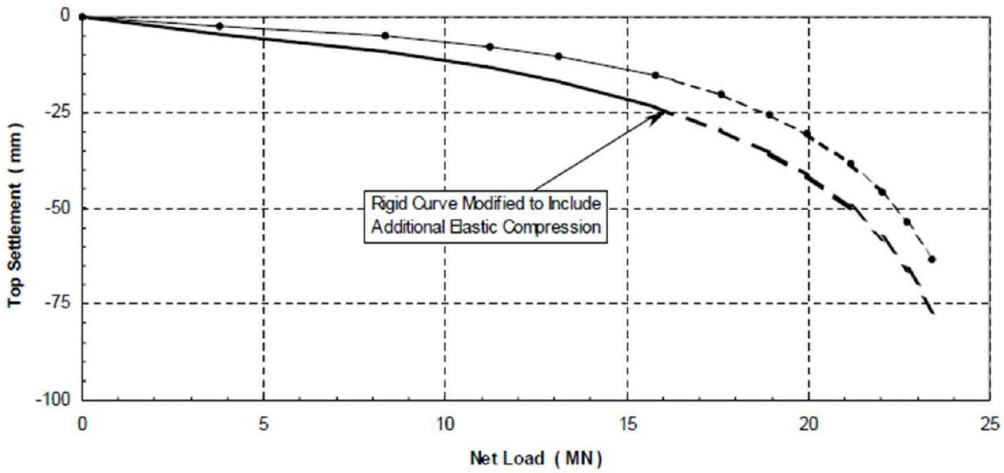

Figure 2 - 19 Correction for elastic shortening in equivalent top-down curve (Loadtest International Pte. Ltd., 2013)

2.4. LRFD Calibration of Resistance Factors

2.4.1. Load and Resistance Factor Design

Allowable stress design (ASD) method was used for foundation design before the introduction of load and resistance factor design (LRFD) method. The basic characteristic of ASD is that a global factor of safety (FS) is considered with the estimated capacity of the foundation. It can be presented by the following equation according to Brown et al. (2010).

$$Q_{des} \leq Q_{all} = \frac{Q_{ult}}{FS} \tag{2-34}$$

Here, Q_{des} is the design load applied on the foundation, Q_{all} is the allowable load, Q_{ult} is the ultimate capacity of the foundation and FS is the global factor of safety. In this method, the factor of safety is always more than one so that it can provide a capacity of the foundation higher than the applied load. The drawback of using this method of foundation design is that all the uncertainties related to variations in loads and resistance of the foundation are considered with only one factor of safety. This method cannot consider different level of uncertainties occurring from separate sources like applied loads, strength of material, construction method etc.

These limitations of allowable stress design can be overcome by implementing limit state design in the design method. Limit states are assigned to each sources of the uncertainties. A check is performed for each of the limit state to ensure adequate improbabilities for failure. Limit states can be incorporated in the design by assigning partial factors. Partial factors are applied to the applied load on the foundation as well as to the resistance of the foundation. Rather than increasing the total capacity of the foundation like allowable stress design, the partial factors increase the applied load and decrease the resistance of the foundation. The method of applying partial factors was first developed in 1950's. One of the criteria to apply partial factors was that a more uncertain quantity should have higher partial factor. The challenge to incorporate partial factors to limit state design was to demonstrate same level of adequate improbability of occurring of all the limit states. Probability reliability analysis was introduced to the design method in order to which made it possible to properly consider the variability and uncertainty of all the components of force and resistance. Due to incorporation of probability reliability analysis, similar level of probability of failure for all components of the structure can be ensured for a given limit state. Partial factors are applied for load and resistance in the load and resistance factor design (LRFD) method. According

to Brown et al. (2010), the LRFD format for a drilled shaft under axial loading can be expressed by the following equation.

$$\gamma_D Q_{DL} + \gamma_L Q_{LL} \leq \varphi_s R_s + \varphi_p R_p \quad (2\text{-}35)$$

Here, γ_D and γ_L are the load factors for dead load and live load, respectively. Q_{DL} and Q_{LL} are the nominal axial dead load and nominal axial live load, respectively. φ_s and φ_p are the resistance factors for side and tip resistance of the shaft. R_s and R_p are the side and tip resistance of the shaft, respectively. It can be stated from equation 2-35 that the summation of the factored loads on the shaft has to be smaller than the summation of the factored resistance of the shaft. It can be expressed by the following equation (Brown et al).

$$\sum \eta_i \gamma_i Q_i \leq \sum \varphi_i R_i \quad (2\text{-}36)$$

Here, η_i is a load modifier which accounts for ductility, redundancy and operational importance of the structure. γ_i is the load factor. Q_i is the load applied on the shaft. φ_i is the resistance factor and R_i is the resistance of the shaft.

2.4.2. Resistance Factor Development

Calibration of load and resistance factors can be performed by several ways, i.e., by judgement, by fitting to past experience, by reliability analyses or by a combination of approaches (Withiam et al., 1998). A calibration by judgement can be performed by changing the load and resistance factors recommended by standard code based on the past experience of inconvenience of the code. Calibration by judgement cannot be recommended as a standard as the same level of probability of failure cannot be ensured for all the components.

2.4.2.1. Calibration by Fitting to Past Practice

Calibration by fitting to past practice denotes to simply transforming the design format from the previously practiced design method. This method of calibration cannot specifically determine the probability of failure for each component, but it can be a starting point to perform reliability based calibration. The transformation of ASD to LRFD first began by transforming the global factor of safety into resistance factors by keeping the same level of reliability. The transformation of factor of safety for ASD to resistance factor for LRFD can be performed by the following equation.

$$\varphi = \frac{\gamma_D\left(\frac{Q_{DL}}{Q_{LL}}\right) + \gamma_L}{FS\left(\frac{Q_{DL}}{Q_{LL}} + 1\right)} \tag{2-37}$$

Here, φ is the resistance factor, FS is the global factor of safety, Q_{DL} and Q_{LL} are the applied dead load and live load on the shaft, γ_D and γ_L are the load factors for dead load and live load, respectively. Some resistance factors estimated based on selected factor of safety values are presented in Table 2 – 7.

Table 2 - 7 Resistance factors estimated based on global factors of safety (O'Neil and Reese, 1999).

FS	$Q_{DL}/Q_{LL} = 1$	$Q_{DL}/Q_{LL} = 2$	$Q_{DL}/Q_{LL} = 3$	$Q_{DL}/Q_{LL} = 4$
1.5	1.00	0.94	0.92	0.90
2.0	0.75	0.71	0.69	0.68
2.5	0.60	0.57	0.55	0.54
3.0	0.50	0.47	0.46	0.45
3.5	0.53	0.40	0.39	0.39
4.0	0.38	0.35	0.34	0.34

2.4.2.2. Calibration by Reliability Analyses

In order to perform a calibration based on probabilistic reliability analyses, the load and resistance factors are estimated based on a target probability of failure. For load and resistance factor design method, failure can be defined as the condition where the applied load (Q) on the shaft is higher than the resistance (R). Load (Q) and resistance (R) can be considered as random variables with normal or lognormal distribution. The characterization of random variables load (Q) and resistance (R) is possible by the statistical parameters like mean, standard deviation and coefficient of variation of both Q and R. Figure 2 – 20 shows the distributions of load (Q) and resistance (R). The shadowed are between the two distributions is the space where failure occurs.

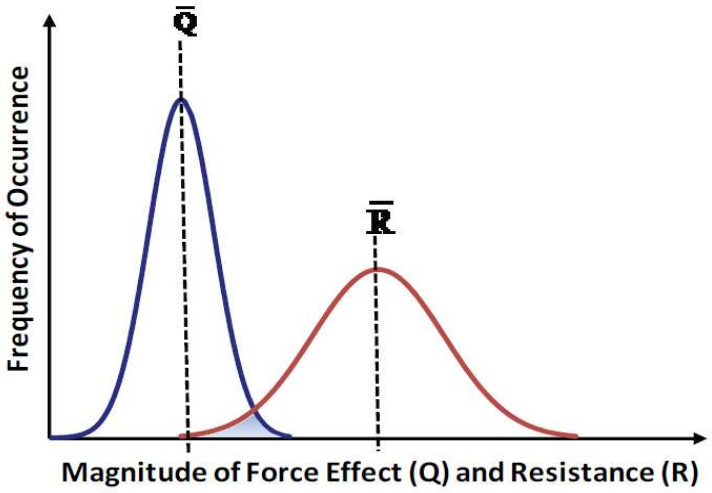

Figure 2 - 20 Distribution of load (Q) and resistance (R) (Withiam et al., 1998).

The mean or the average value for a random variable can be estimated as –

$$\bar{x} = \frac{\sum x_i}{N} \tag{2-38}$$

Here, $\bar{x}$ is the mean value, x_i is the random variable under consideration and N is the number of the random variable. The standard deviation of the random variable can be estimated by the following equation.

$$\sigma = \sqrt{\frac{\sum(x_i - \bar{x})^2}{N-1}} \tag{2-39}$$

Here, σ is the standard deviation of the random variable. The coefficient of variation (COV) can be estimated by the following equation.

$$COV = \frac{\sigma}{\bar{x}} \tag{2-40}$$

The occurrence of failure can be expressed by a single term (g), which is the difference between the resistance (R) and load (Q). It can be termed as the limit state function, which can be expressed by its own distribution. Figure 2 – 21 presents the distribution of the limit state function. In terms of the limit state function, the failure occurs when g is zero (R=Q). The failure region is shown as a shaded area in the distribution of the limit state function. The failure region can also be termed as the probability of failure (P_f).

The reliability index (β) can also be used to express the occurrence of failure. The distance between the mean of the limit state function and the boundary of the failure region can be expressed by reliability index in term of the standard deviation. Table 2 – 8 shows reliability index values for selected probability of failure values.

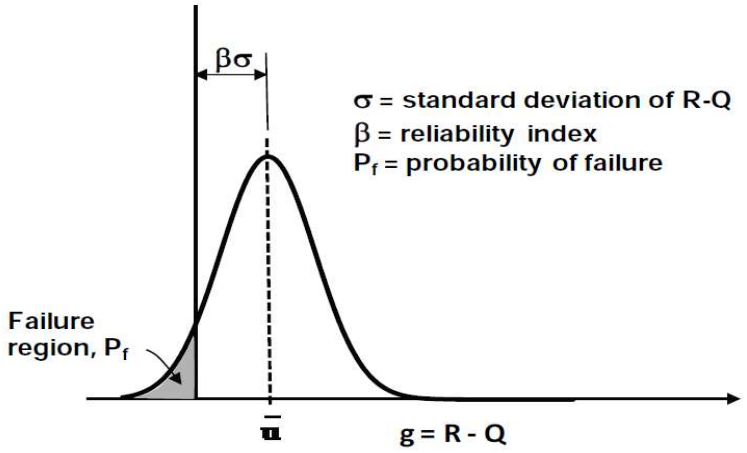

Figure 2 - 21 Distribution of the limit state function (Allen, 2005).

Table 2 - 8 Relation between reliability index and probability of failure (Brown et al., 2010).

Reliability Index, β	Probability of Failure, P_f
2.0	1/10
2.5	1/100
3.0	1/1,000
3.6	1/10,000
4.1	1/100,000
4.6	1/1,000,000

The predicted resistance is needed to be evaluated against the measured resistance in order to develop a reliability based design equation. To perform the evaluation, the ratio of the measured resistance and the predicted resistance are taken as the bias values. Predicted resistance can be estimated based on the process described in section 2.2. Measured resistance values are obtained from load tests performed on the drilled shafts. Based on the probability of the bias value to be equal to or less than a given value, the calibration of the resistance factor is performed for a target reliability index. AASHTO specified load factors are used for the calibration of the resistance factor.

In summary, for the calibration of resistance factor, the statistical parameters i.e. mean, standard deviation and coefficient of variation are estimated for all the variables of resistance and load. A target reliability index is selected based on the current practice of safety specifications. Finally, resistance factors are estimated based on the selected reliability index and the AASHTO specified load factors. From this point on, the resistance factor can be calculated through several methods. These methods are discussed below.

Mean Value First Order Second Moment (MVFOSM): This is the least accurate method of estimating resistance factor. In this method, mean and standard deviation of the limit state function (g) is estimated based on Taylor series expansion. Only the first order terms are considered in this method. All the random variables are characterized by only the first two moments i.e. mean and standard deviation.

Advanced First Order Second Moment (AFOSM): Rackwitz and Fiessler (1978) developed this method, in which, the limit state function (g) is considered at the failure point where, applied load is equal to the resistance. In this method, a reliability index value is assumed initially to select a primary design point. The calculations are performed to obtain a new reliability index value. The procedure is repeated until two successive trials result in reliability index values with very small difference. The mean, standard deviation and distribution function of the variables are considered for this method.

Monte Carlo Simulation (MCS): Monte Carlo simulation method of estimating resistance factor for a target reliability index was discussed in Allen (2005). In this method, random numbers

are generated and cumulative distribution function (CDF) values are estimated for each random variable. Mean, standard deviation and the type of the distribution are used to specify the cumulative distribution function. Using this method, resistance factor can be estimated for a target reliability index, even if, adequate amount of measured data is not available. Spreadsheet software can be used to perform a Monte Carlo simulation.

3.5. Studies on Calibration of Resistance Factor

When resistance factors for LRFD method was first published in AASHTO specifications (1994), the resistance factors were calibrated by fitting the global factor of safety of ASD method. This calibration did not consider the same level of reliability for all the uncertainties related to load and resistance. Also, this calibration did not reflect uncertainties for different geomaterial in different area specific conditions. Several studies were performed to calibrate the resistance factors by collecting drilled shaft load test data from different locations by considering are specific condition. Some of those studies are discussed in this section.

3.5.1. Florida DOT

Florida Department of Transportation (FDOT) performed a study on calibration of resistance factors for deep foundations in 1998. The database of the study only consisted of conventional static load tests as FDOT used a very limited amount of Osterberg Cell and statnamic load test. For any other load test, they used the result of the study on the conventional load test. The objective of this study was to estimate resistance factors by fitting to ASD global factor of safety and compare the result to AASHTO (1994) specifications (McVay et al., 1998). Table 2 – 9 presents the results of the study performed in 1998.

Table 2 - 9 Resistance Factors for Drilled Shafts in all types of soil (McVay et al. 1998).

AASHTO (1994)	Reliability	Fitting
0.45-0.65	0.50-0.65	0.55

Over the years, the use of conventional static load test was decreased due to its inconvenience against larger diameter of drilled shaft and higher applied load. FDOT replaced a lot of the conventional load tests with statnamic load test. The increase in statnamic load testing posed a problem as the previous database for resistance factor calibration did not include any statnamic load test data. To solve this problem, FDOT conducted another study with a database in 2003 that included both conventional static load test and statnamic load test data. The new database included both drilled shafts and driven piles. Different soil materials were also considered separately in the database (McVay et al., 2003).

3.5.1.1. Collected Database

Before the beginning of the study, FDOT had already collect a database with thirteen statnamic load tests performed on drilled shafts and fifteen statnamic as well as conventional load test data performed on piles. Seven of the load test data performed on piles were collected from Florida. Eight of the piles were located in Taiwan and Japan. More load test data were collected from AFT and Berminghammer and the Federal Highway Administration (FHWA) in order to perform the new study in 2003. The final database had 27 load test data performed on drilled shafts and 34 test data performed on piles. The study used Davisson failure criteria to estimate the measured load and 37 of the load tests reached the Davisson failure criteria. Table 2 – 10 presents

the load tests included in the database collected by FDOT. In the table, CLT is the conventional static load test and SLT denotes to the statnamic load test.

Table 2 - 10 Database for the study performed by FDOT (McVoy et al., 2003).

Pile Type	Soil Type	Location	CLT Capacity (kN)	SLT Capacity(kN)
Drilled Shaft	Rock	USA	6200	6480
Drilled Shaft	Rock	USA	5600	4950
Pipe Pile	Rock	JPN	4380	5087
Driven Pile	Sand	USA	3380	5000
Driven Pile	Sand	USA	3820	3322
Driven Pile	Sand	USA	3500	3957
Pipe Pile	Sand	JPN	1100	1042
Other	Sand	JPN	446	489
Drilled Shaft	Silt	USA	1420	2191
Drilled Shaft	Silt	USA	1700	2450
Drilled Shaft	Silt	USA	2230	3530
Drilled Shaft	Silt	USA	2800	2890
Drilled Shaft	Silt	USA	1013	1730
Drilled Shaft	Silt	USA	2230	2890
Drilled Shaft	Silt	USA	2400	2970
Pipe Pile	Silt	USA	1230	1790
Pipe Pile	Silt	USA	1300	1380
Pipe Pile	Silt	USA	1210	1404
Pipe Pile	Silt	USA	1300	1750
Pipe Pile	Silt	USA	1810	N/F
Pipe Pile	Silt	USA	2380	3850
Driven Pile	Clay	USA	1830	3070
Driven Pile	Clay	USA	2470	N/F
Pipe Pile	Clay	USA	1668	N/F
Pipe Pile	Clay	USA	2190	2600
Drilled Shaft	Clay	USA	1214	1244
Drilled Shaft	Clay	USA	965	1617
Drilled Shaft	Rock	CAN	4550	3500
Pipe Pile	Sand	CAN	1310	1350
Pipe Pile	Rock	CAN	1560	1800

Pile Type	Soil Type	Location	CLT Capacity (kN)	SLT Capacity(kN)
Driven Pile	Silt	USA	2470	2360
Pipe Pile	Clay	CAN	1040	2550
Pipe Pile	Rock	CAN	2200	2550
Drilled Shaft	Sand	USA	7130	6370
Pipe Pile	Clay	USA	1360	892
Driven Pile	Sand	JPN	2770	2700
Pipe Pile	Sand	JPN	1890	1490

Table 2 – 10 (Cont.)

3.5.1.2. Calibration Approach

Statistical analyses were conducted on the database collected in order to calibrate the resistance factors. To ensure proper characterization of statnamic load test, the database was separated based on different types of soil condition as well as different kinds of foundations. The statistical analyses were performed for each of the criteria. Bias values were estimated for each of the load test cases. For the statistical characterization, mean of the bias values, standard deviation and coefficient of variation were calculated. Table 2 – 11 presents the estimated statistical parameters of the resistance values. In table 2 – 11, λ_R is the resistance bias value, σ_R is the standard deviation of the resistance and V_R is the coefficient of variation of the resistance. A rate factor (RF) was introduced to further characterize the database based on Mullins (2002). The rate factors were taken as 0.91 for sand, 0.65 for clay, 0.69 for silt and 0.96 for rock. It can be observed from Table 2 – 11 that the bias factors without the rate factors are all less than one, which signifies the over prediction of the predicted capacity for statnamic load tests. Application of the rate factors resulted in higher bias values, but it did not affect the coefficient of variation values.

Table 2 - 11 Statistical parameters for resistance for statnamic load tests (McVay et al. 2003).

Case	With Clay						Without Clay					
	With RF			Without RF			With RF			Without RF		
	λ_R	σ_R	V_R	λ_R	σ_R	V_R	λ_R	σ_R	V_R	λ_R	σ_R	V_R
All data	1.11	0.28	0.25	0.88	0.24	0.27	1.10	0.18	0.16	0.89	0.20	0.22
Rock	-	-	-	-	-	-	1.07	0.17	0.16	1.00	0.18	0.18
Sand/ Silt	-	-	-	-	-	-	1.10	0.18	0.16	0.87	0.19	0.22
Clay	1.18	0.52	0.44	0.82	0.40	0.49	-	-	-	-	-	-
Drilled shaft	1.10	0.20	0.18	0.87	0.23	0.26	1.08	0.16	0.15	0.88	0.23	0.26
Driven pile	1.12	0.32	0.29	0.89	0.25	0.28	1.10	0.21	0.19	0.89	0.18	0.20

Table 2 – 12 presents the statistical parameters used for the loads in the calibration approach. In the table, γ_D and γ_L denotes to load factors for dead load and live load, λ_D and λ_L denotes to the bias factors for dead load and live load, COV_D and COV_L presents the coefficient of variation of dead load and live load and Q_D/Q_L is the ratio between dead load and live load.

Table 2 - 12 Statistical parameters for loads (McVay et al. 2003).

γ_D	1.250
γ_L	1.750
λ_D	1.080
λ_L	1.150
COV_D	0.128
COV_L	0.180
Q_D/Q_L	2.000

The next step to the calibration approach was to select target reliability index. The target reliability index was selected based on the previously mentioned study performed by FDOT (McVay et al. 1998) because of unavailability of data for factor of safety for the statnamic load test in allowable stress design method. Finally, a target reliability index (β) was selected as 2.5 for driven piles and 3.0 for the drilled shafts. Assuming a lognormal distribution of the bias values, the resistance factors were estimated based the relationship between probability of failure (Pf) and reliability index (β) (Rosenblueth and Esteva, 1972). Calibrated resistance factors for seven different cases are presented in Table 2 – 13.

Table 2 - 13 Calibrated resistance factors (McVay et al. 2003).

Case	Resistance Factor (ϕ) w/ β = 2.5				Resistance Factor (ϕ) w/ β = 3.0			
	With Clay		Without Clay		With Clay		Without Clay	
	w/ RF	w/o RF	w/ RF	w/o RF	w/ RF	w/o RF	w/ RF	w/o RF
All data	0.62	0.47	0.72	0.52	0.52	0.40	0.63	0.45
Rock	-	-	0.72	0.52	-	-	0.63	0.44
Sand and silt	-	-	0.71	0.64	-	-	0.62	0.56
Clay	0.43	0.27	-	-	0.34	0.21	-	-
Drilled shaft	0.70	0.47	0.73	0.48	0.61	0.38	0.64	0.41
Driven pile	0.58	0.47	0.69	0.55	0.49	0.40	0.60	0.47

Some of the load test cases were consisted of mostly clayey soil for the geomaterial. It was found during the study that these cases with high amount of clayey soil had a significant effect on the calibrated resistance. These cases were separated from the rest of the load test cases. Table 2 – 14 presents a summary of the calibrated resistance factors excluding the cases with high amount of clayey soil. After the completion of the study, resistance factors of 0.70 and 0.65 were recommended for piles and drilled shafts in noncohesive soil, respectively, for statnamic load test.

A resistance factor of 0.60 was recommended for both drilled shafts and driven piles in cohesive soil.

Table 2 - 14 Recommended Resistance Factors (McVay et al. 2003).

Foundation Type	Rock and Noncohesive Soils	Clays	Sand-Clay-Rock Mixed Layers
Driven Pile ($\beta = 2.5$)	0.70	0.45	0.60
Drilled Shaft ($\beta = 3.0$)	0.65	0.35	0.60

3.5.2. Iowa DOT

Iowa Department of Transportation conducted a study in order to develop a procedure for LRFD calibration of resistance factors. The objective of the study was to calibrate area specific resistance factors based on probabilistic reliability theory. The study was conducted based on a database developed in 2012, which consisted of load tests performed on drilled shafts. A literature review was performed on current practice of design of Iowa DOT. By analyzing the data from the collected database, the measured resistances of all the drilled shafts were obtained and primary area specific resistance factors were calibrated.

3.5.2.1. Collected Database

Garder et al. (2012) developed an electronic database in Microsoft Office Access consisting of thirty-two load tests performed on drilled shafts. The load test data were collected from Iowa, Illinois, Minnesota, Missouri, Nebraska and Tennessee. The database was developed by collecting detailed information for each of the load test cases. The information collected for each load test included location of the shafts, type of construction, subsurface condition, details of the drilled shafts, types of load tests performed, concrete quality and results from the load tests. Later, more

load test cases were collected and added to the original database. During the study conducted by Iowa DOT, the database consisted of 41 load tests performed on drilled shafts from 11 different states. Out of 41 cases, 28 drilled shafts had information available required for the study. The load tests were separated into several categories based on type of soil at the tip of shafts, type of soil along the side of shafts, construction method and type of load tests. Table 2 – 15 presents the information on the usable drilled shaft load test included in the database collected by Garder et al. (2012).

3.5.2.2. Data Quality

All the collected load test data were thoroughly scrutinized to ensure the quality of the data included in the database. The quality check was performed based on the report of each load test case, type of load tests, and available information on subsurface condition and cross-hole sonic logging (CSL). A category termed as 'Usable Data' was added to the database in order to identify the load tests with complete information. A few of the incomplete load tests were also added to the database with a target to complete the dataset when information is available.

Table 2 - 15 Summary of usable load test databased (Garder et al. 2012).

State	D (ft)	L (ft)	Concrete f'_c (ksi)	Soil Type		Construction Method	Load Test
				Shaft	Base		
IA	3.0	12.7	5.86	Rock	Rock	Wet	Osterberg
IA	4.0	65.8	3.80	Clay+Rock	Rock	Wet	Osterberg
IA	3.5	72.7	3.44	Mixed+IGM	IGM	Casing	Osterberg
IA	4.0	79.3	3.90	Clay+IGM+Rock	Rock	Wet	Osterberg
IA	2.5	64.0	3.48	Clay	Clay	Casing	Osterberg
IA	3.0	34.0	4.10	Clay+Rock	Rock	Wet	Osterberg
IA	5.5	105.2	3.80	Mixed+Rock	Rock	Casing	Osterberg
IA	5.0	66.3	5.78	Sand	Sand	Wet	Statnamic
IA	5.0	55.4	5.58	Mixed	Sand	Wet	Statnamic
IA	5.0	54.8	5.77	Mixed	Sand	Wet	Statnamic
KS	6.0	49.0	6.01	IGM	IGM	Dry	Osterberg
MO	6.0	40.6	6.00	IGM+Rock	IGM	Dry	Osterberg
KS	3.5	19.0	4.55	IGM	IGM	Wet	Osterberg
KS	6.0	34.0	5.62	IGM	IGM	Dry	Osterberg
KY	8.0	105.2	N/A	IGM+Rock	Rock	Wet	Osterberg
KS	6.0	26.2	5.42	IGM	IGM	Dry	Osterberg
MN	6.0	55.3	5.90	Sand	Sand	Casing	Osterberg
IL	3.5	37.5	4.10	Clay+IGM	Rock	Dry	Osterberg
IA	5.0	75.2	6.01	Sand	Sand	Wet	Osterberg
IA	5.0	75.0	5.63	Sand	Sand	Wet	Osterberg
TN	4.0	16.0	5.77	Rock	Rock	Dry	Osterberg
TN	4.0	23.0	5.90	Rock	Rock	Dry	Osterberg
CO	3.5	22.6	3.42	IGM	IGM	Dry	Osterberg
CO	3.5	16.0	3.19	Clay	IGM	Dry	Osterberg
CO	4.0	25.3	3.41	IMG	IGM	Casing	Osterberg
CO	3.5	40.6	3.94	Rock	Rock	Casing	Osterberg
CO	3.0	11.3	4.88	Rock	Rock	Dry	Osterberg
CO	4.0	20.0	3.54	Rock	Rock	Casing	Osterberg

3.5.2.3. Calibration Approach

In order to calibrate the resistance factors, the modified First Order Second Method (FOSM) was selected for this study. A verification was performed to ensure the lognormal distribution of the data. A hypothesis test was performed to verify the lognormality based on Anderson-Darling normality method. The verification of lognormality can also be performed by Chi-square test and the Kolmogorov Smirnov test, but the Anderson-Darling (AD) method was selected because of capability of performing the test with small sample size (Romeu, 2010). The hypothesis test is based on the logic that if the AD value is less than the critical value (CV), it can be concluded that the assumption of lognormal distribution is correct. The required equation to estimate AD and CV are shown below.

$$AD = \sum_{i=1}^{N} \frac{1-2i}{N} \{\ln(F_o[Z_i]) + \ln(1 - F_o[Z_{N+1-i}])\} - N \quad (2\text{-}41)$$

$$CV = \frac{0.752}{1+\frac{0.75}{N}+\frac{2.25}{N^2}} \quad (2\text{-}42)$$

Here,

$F_o[Z_i]$ = cumulative probability density function of $Z_i = P_r(Z \leq z_i)$

$P_r(\ )$ = probability function

Z = standardized normal distribution of expected resistance bias λ_R or $\ln(\lambda_R)$

z_i = standardized normal distribution of estimated resistance bias λ_R or $\ln(\lambda_R) = \frac{R_i - \mu_R}{\sigma_R}$ or $\frac{\ln R_i - \mu_{\ln}}{\sigma_{\ln}}$

λ_R = resistance bias, a ratio of estimated and measured pile resistances

N = sample size

The ratio between dead load and live load was assumed to be 2.0 for this study. To consider a wide range of possibilities for the design of drilled shafts, several reliability indices were selected

to perform the calibration. The selected target reliability indices were 2.00, 2.33, 2.50, 3.00 and 3.50. Separate calibrations were conducted to obtain separate resistance factors for both side resistance and tip resistance in each type of soil. Predicted resistance for each of the drilled shafts were estimated based on several methods. The utilized methods to predict the side and tip resistance for the study are shown in Table 2 – 16.

Table 2 - 16 Methods utilized to estimate predicted resistance of the drilled shafts (Ng et al. 2014).

Soil Type	Unit Side Resistance (q_s)	Unit End Bearing (q_p)
Clay	α-method (O'Neill and Reese, 1999)	Total stress method (O'Neill and Reese, 1999)
Sand	β-method (O'Neill and Reese, 1999)	Effective stress method (O'Neill and Reese, 1989)
Cohesive IGM	O'Neill and Reese, 1999	Various
Cohesionless IGM	O'Neill and Reese, 1999	O'Neill and Reese, 1999
Rock	Horvath and Kenney, 1979	Various

There are nine analytical methods available for predicting the unit end bearing resistances in cohesive IGM and rock, and six of those methods were chosen to be used in this study because of the variability of rock mass conditions that could occur beneath a drilled shaft. A combination of these methods was also proposed in this study to simplify the end bearing prediction. The predicted side resistances in clay, sand, IGM, and rock were compared to three different failure criteria of the measured resistance – the measured resistance obtained directly from the load test report, the measured resistance defined by the one-inch top displacement criterion, and the measured resistance defined by the 5% of shaft diameter for top displacement criterion. An

example of this comparison for clay is shown in Figure 2-22. The data sets were found to most closely represent lognormal distributions based on the AD method.

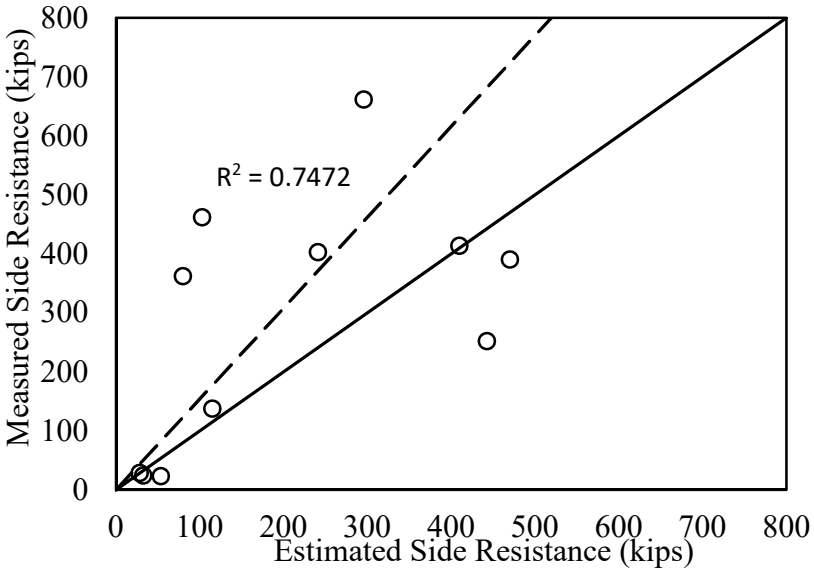

Figure 2 - 22 Measured side resistance vs predicted side resistance in clay (Ng et al. 2014).

A statistical analysis was not performed for tip resistance in clay, as there was only one available data form measured tip resistance in clay. Predicted tip resistance in sand cases were similar to the measured resistances as well as for the side resistances. The methods of predicting tip resistance in rock and IGM were different. The tip resistance in rock and IGM were predicted by utilizing six different methods. Three failure criteria were used to get the resistance values for each of the method of prediction. The majority of this data was also lognormally distributed. The total nominal resistance was also analyzed for the drilled shafts with 27 data points to compare. After determining all of the resistance factors for side, end bearing, and total nominal resistance for the various reliability indices, a target reliability index of 3.0 was chosen because a typical drilled shaft cap has four or fewer shafts, which is considered a non-redundant drilled shaft foundation. The total, side, and end bearing resistance factors based on this target reliability index

were then compared to the recommended resistance factors by AASHTO (2010), NCHRP (1991, 2004), and FHWA-NHI (2005). Efficiency factors were also generated to compare the three different failure criteria for the drilled shafts. After comparing the various resistance factors and efficiency factors, the one-inch top displacement criterion was selected to have the most efficiency, and the recommended resistance factors for various resistance components based off of this are summarized in Table 2-17.

Table 2 - 17 Recommended resistance factors for reliability index value of 3.0 (Ng et al. 2014).

Resistance Type	Soil Type	Analytical Method	Resistance Factors
Total Resistance	All	Combination of methods depending on subsurface profile	0.60
Side Resistance	Clay	α-method (O'Neill and Reese, 1999)	0.45
	Sand	β-method (Burland, 1973 & O'Neill and Reese, 1999)	0.55
	IGM	Cohesive: Eq. 2-11 (O'Neill and Reese, 1999) and Cohesionless: Eq. 2-14 (O'Neill and Reese, 1999)	0.60
	Rock	Eq. 2-16 (Horvath and Kenney, 1979)	0.55
End Bearing	Clay	Total stress method (O'Neill and Reese, 1999)	0.40
	Sand	Effective stress method (O'Neill and Reese, 1989)	0.50
	IGM	Cohesive: Proposed method and Cohesionless: Eq. 2-22 (O'Neill and Reese, 1999)	0.55
	Rock	Proposed method	0.35
All	All	Static Load Test	0.70

3.5.3. New Mexico DOT

The New Mexico Department of Transportation (NMDOT) conducted a study for LRFD calibration in cohesionless soils. Load test data was collected primarily from New Mexico. Some load test data were also collected from other states if the subsurface condition was similar to the

soil of New Mexico. The objective of this study was to develop area specific resistance factors for drilled shafts replacing the resistance factors prescribed by AASHTO. The study was performed only for the side resistance of drilled shafts. Three analytical methods were utilized to estimate the predicted side resistance values. Calibration was performed for each of the three analytical methods and the results were compared to each other. The three analytical methods are O'Neill and Reese method (O'Neill and Reese, 1999), the NHI 2010 method recommended by FHWA (Brown et al. 2010) and the Unified Design Equation (Chua et al. 2000). The O'Neill and Reese method and the FHWA method were discussed earlier in section 2.2. In this section, the Unified Design Equation has been discussed.

3.5.3.1. The Unified Design Equation

This method of estimating predicted resistance of drilled shaft was recommended by Chua et al. (2000). Resistance of drilled shaft both in cohesive and cohesionless soil can be obtained by utilizing this method. The internal friction angle and the unit weight are required parameters to estimate the side resistance in cohesionless soil. According to the Unified Design Equation, the side resistance of a drilled shaft in cohesionless soil can be estimated by the following equation.

$$f_s = \beta \sigma'_z \tag{2-43}$$

$$\beta = (1 - \sin\phi)\tan\phi\left(1 + \frac{\frac{K_p}{K_o} - 1}{\sqrt{1+z}}\right) \tag{2-44}$$

$$\phi = 30 + 0.15 D_R \tag{2-45}$$

$$D_R = 20.4\left(\frac{\sigma'_z}{p_a}\right)^{-0.223} N^{0.41} \tag{2-46}$$

Here, f_s is the unit side resistance of the drilled shaft, σ'_z is the overburden pressure, ϕ is the internal friction angle of soil, K_p and K_o are coefficient of passive lateral earth pressure and coefficient of lateral earth pressure at rest, respectively, z is the depth of soil layer, D_R is the relative density and N is SPT blow count.

The relationship between relative density and SPT blow counts was developed based the study Gibbs and Holtz (1957). The relationship to estimate the friction angle from relative density was established by Chua et al. (2000). U.S. Navy (1971) developed another relationship between internal frictional angle and relative density which is more accurate, as it considers the type of soil based on soil classification. The relationship is presented in Figure 2 - 23.

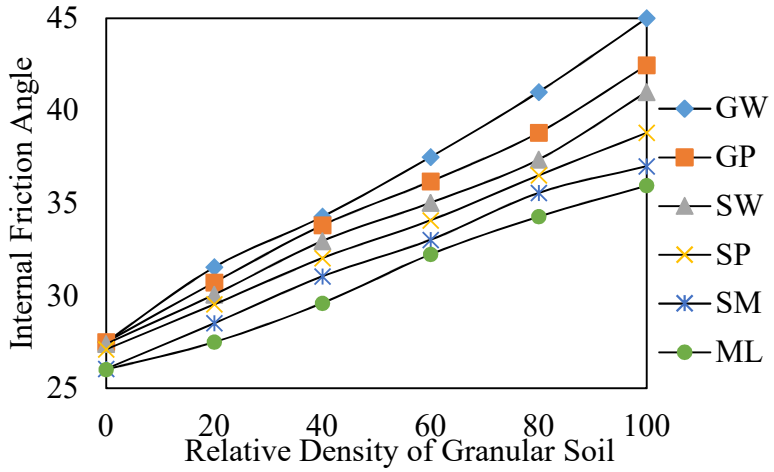

Figure 2 - 23 Relationship between internal friction angle and relative desity (Ng & Faiza, 2012).

3.5.3.2. Collected Database

A database was collected from New Mexico DOT and other states to conduct this study. Primarily, the database had ninety-five load tests performed on drilled shafts. Five of the load test data were obtained from New Mexico. The rest of the load tests were collected from other states. After initial filtering of data, twenty-four load tests were selected for this study. The side resistance values obtained from the load test results were compared to the predicted side resistance values

estimated by the three aforementioned methods. Table 2 – 18 presents the summary of the database utilized for this study.

Table 2 - 18 Summary of the New Mexico DOT database (Ng & Faiza, 2012).

Location	Measured (ton)	O'Neill & Reese (ton)	Unified (ton)	NHI (ton)	Load Condition	D (ft)	L (ft)
Iowa	83.6	146.4	81.3	81.2	Bottom with O-cell	4.0	59.8
Georgia	152	324.3	337	292.6	Bottom with O-cell	5.5	60
Texas	166	244.3	216.9	274.8	Bottom with O-cell	3.0	34
Florida	445	383.6	480.4	389.4	Bottom with O-cell	4.0	46.8
New Jersey	871	1905.2	1547.9	1767.2	Top load	1.5	68
Georgia	493	287.2	255.9	263.6	Top load	3.0	60
New Mexico	571	627.7	380.3	324	Top load	2.8	30
Alabama	662	625	670.4	664.3	10 ft from tip with O-cell	4.0	33.2
New Mexico	1620	1429.2	848.6	1079.4	Bottom and middle with O-cell	6.0	81
New Mexico	1800	2559.4	2491.7	2526.1	Bottom and middle with O-cell	4.5	52
Georgia	873.5	1399.7	1115.5	1019.6	Top load	2.6	47
Arizona	2964	1354.5	1662.6	1580.5	42 ft from tip with O-cell	6.0	62
Arizona	778	730.1	942.5	942.5	42 ft from tip with O-cell	6.0	53
Arizona	2626.5	2281.4	2608.5	1676.3	22 ft from tip with O-cell	6.0	90
Arizona	1947	1945	1672.7	1439.6	14 ft from tip with O-cell	6.0	48
Arizona	1627	1271.9	1308.9	1298.5	24 ft from tip with O-cell	6.0	77
Arizona	276	352	653.3	527.6	24 ft from tip with O-cell	6.0	24.3

Location	Measured (ton)	O'Neill & Reese (ton)	Unified (ton)	NHI (ton)	Load Condition	D (ft)	L (ft)
Arizona	1771	1503.4	1475.1	1152.6	37 ft from tip with O-cell	7.0	115
New Mexico	705	605.9	613.6	732.3	Bottom with O-cell	4.0	74.6
Japan	2527.7	2048.7	2695	1898.9	No data	3.9	134.5
New Mexico	950	265.7	306.7	240.9	Top load	2.7	40
Florida	456.8	328.3	332	426.6	O-cell	5.0	90
Florida	354.8	661.2	481.7	746.5	O-cell	6.0	90
Florida	404.2	298.2	556.4	503.9	O-cell	5.0	100

Table 2 – 18 (Cont.)

3.5.3.3. Calibration Approach

To carry on with the calibration procedure, bias values were obtained for each of the three analytical methods. Measured resistances were estimated from the load test results. After getting the bias values for each of the drilled shaft cases, a statistical analysis was performed by estimating the mean, standard deviation and coefficient of variation of the bias values. The statistical parameters for each of the three analytical methods are presented in Table 2 – 19. It can be observed that the Unified Design Equation provided with the smallest value of coefficient of variation. Figure 2 -24 to 2- 26 presents the relationship between predicted side resistance and field side resistance for O'Neill and Reese method, Unified design method and NHI method.

Table 2 - 19 Statistical parameters for the NMDOT study (Ng & Faiza, 2012).

Design Method	Mean	Standard Deviation	COV
O'Neill & Reese	1.14	0.66	0.58
Unified	1.13	0.59	0.52
NHI	1.21	0.73	0.60

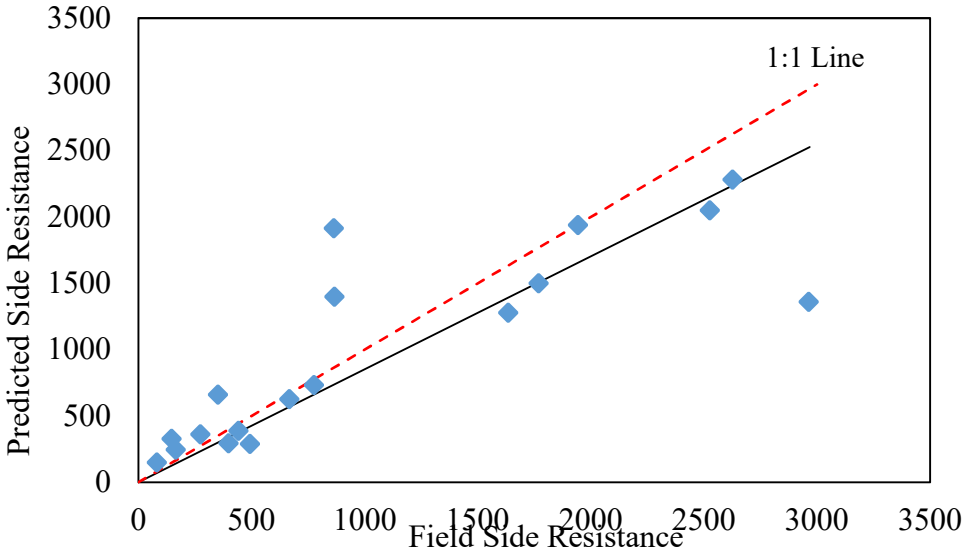

Figure 2 - 24 Predicted side resistance vs field side resistance for O'Neill and Reese method (Ng & Faiza, 2012).

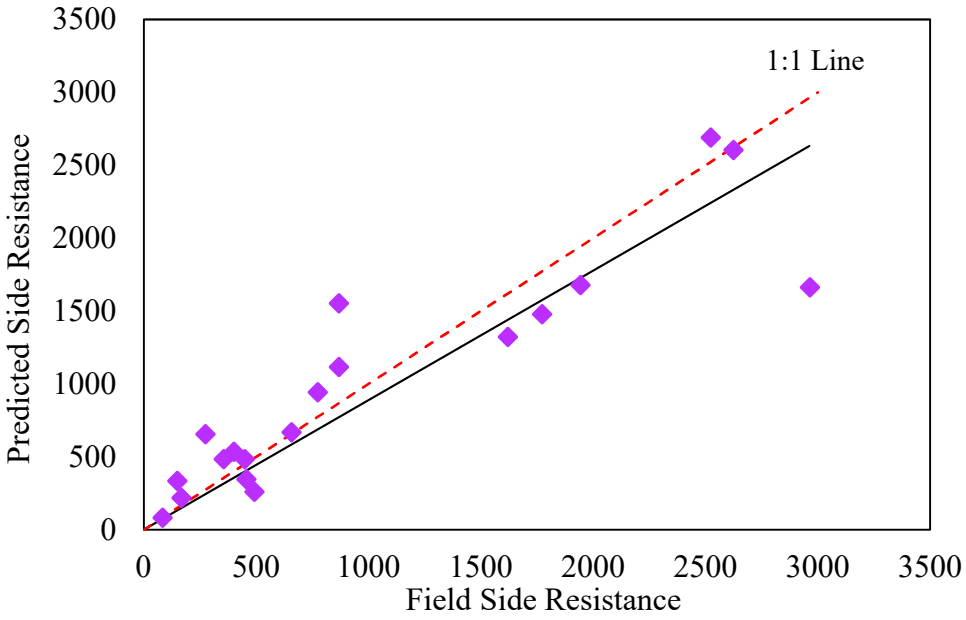

Figure 2 - 25 Predicted side resistance vs field side resistance for Unified design method (Ng & Faiza, 2012).

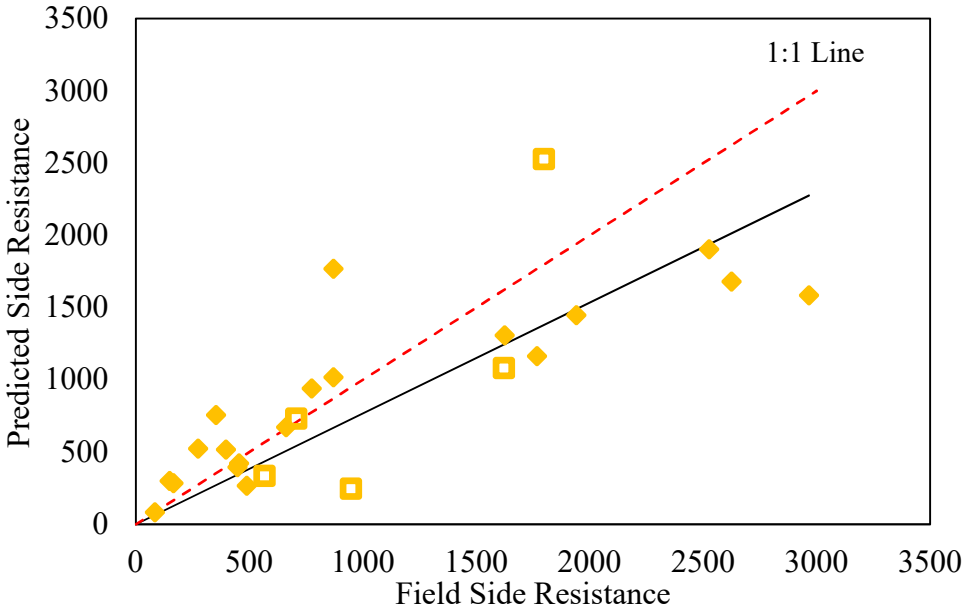

Figure 2 - 26 Predicted side resistance vs field side resistance for NHI method (Ng & Faiza, 2012).

It was assumed that the estimated bias values follow a lognormal distribution. Based on this assumption, the statistical parameters were characterized based on the best fit to tail lognormal distribution method (Allen et al. 2005) as presented in Table 2 – 20. For the calibration procedure, the statistical parameters shown in Table 2 – 20 were utilized.

Table 2 - 20 Statistical parameters based on best fit to tail lognormal distribution (Ng & Faiza, 2012).

Design Method	Mean	Standard Deviation	COV
O'Neill & Reese	0.95	0.39	0.41
Unified	1.20	0.68	0.57
NHI	0.88	0.31	0.35

The load factors and related statistical parameters were collected from Paikowsky (2004). The live and dead loads were also assumed to have a lognormal distribution. The load factors are

presented below. Here, γ_D and γ_L are the dead and live load factors, respectively. λ_D and λ_L are the bias factors for dead load and live load, respectively. COV_D and COV_L are coefficient of variation for dead and live load, respectively.

$$\gamma_D = 1.25 \quad \lambda_D = 1.05 \quad COV_D = 0.10$$
$$\gamma_L = 1.75 \quad \lambda_L = 1.15 \quad COV_L = 0.20$$

Along with the assumption of the resistance biases to be lognormally distributed, a curve-fitted polynomial regression model was also considered for the bias values. A Monte Carlo simulation method was used to calibrate the resistance factors. Statistical parameters obtained from both the lognormal distribution and polynomial distribution fitting were utilized to perform the calibration with a target reliability index of 3.0. Table 2 – 21 presents the results obtained from the resistance factor calibration. After the completion of the calibration, Ng & Faiza (2012) concluded that the resistance factors are higher with the assumption of polynomial distribution of bias values.

Table 2 - 21 Results from calibration of resistance factors (Ng & Faiza, 2012).

Design Method	Lognormal	Polynomial
O'Neill & Reese	0.32	0.45
Unified	0.26	0.49
NHI	0.37	0.47

3.5.4. Louisiana DOTD

Several studies on LRFD calibration of resistance factors were performed over the years by the Louisiana Transportation and Research Center (LTRC), Louisiana Department of Transportation and Development (LADOTD) and Louisiana State University. They performed their first study solely on driven piles in 2009. Fifty-three load tests performed on prestressed concrete pile were collected for the first study. The second study, also in 2009, was conducted on load test data on drilled shafts. Sixteen drilled shafts load tests were collected from LADOTD for

the study. As the number of collected load test data was not adequate, data on fifty more load tests were collected from Mississippi Department of Transportation. After the completion of this study, a new LRFD method was published by FHWA in 2010. Based on the 2010 FHWA method, LATDOTD conducted a new study to update the previous one. This time, LADOTD provided eight more load test data on drilled shafts to add to the previous database, increasing the total number of cases to seventy-four.

3.5.4.1. Collected Database

For the first study conducted on drilled shafts, only sixteen drilled shaft cases were collected from LADOTD. Out of the sixteen load tests, only eleven cases were found to reach the failure criteria provided by FHWA. Because of the inadequate number of collected load tests, fifty additional drilled shaft load test were collected from Mississippi DOT. Out of the fifty cases collected from Mississippi, twenty-six load tests were selected to include in the study based on the similarity of the subsurface condition to the soil in Louisiana. Out of the twenty-six cases, fifteen load test cases were found to reach the failure criteria recommended by FHWA. Finally, twenty-six cases out of sixty-six were selected to include in the study. Eight additional load test data were added to the database for the study performed in 2013. The diameter of the drilled shafts included in the database was within the range of 2 to 6 ft. the lengths of the shafts ranged from 35 to 138.1 ft. Conventional static load test was performed on only four of the collected drilled shafts. Osterberg cell load test was conducted on the rest of the drilled shafts. The subsurface condition found in the database included sand, clay, gravel, silty clay and clayey sand. Table 2 – 22 presents a summary of the drilled shaft cases selected for the study.

Table 2 - 22 Summary of drilled shafts data collected (Abu-Farsakh et al. 2013).

Location	D (ft)	L (ft)	Soil Type	Load Test
Caddo, LA	2.5	53.1	Silty Clay, Sand Base	Top Down
Caddo, LA	2.5	35.1	Clay and Sand, Sand Base	Top Down
E. Baton Rouge, LA	3	54.1	Clayey Silt, Sand Base	O-cell
Ouachita, LA	5.5	76.1	Silty Sand, Sand Base	O-cell
Calcasieu, LA	6	86.9	Stiff Clay, Clay Base	O-cell
Winn, LA	2.5	77.4	Sand Clay, Sand Base	O-cell
Winn, LA	2.5	65	Sand, Clay Base	O-cell
E. Baton Rouge, LA	2.5	49.9	Silt, Clay, Clay Base	O-cell
Beauregard, LA	5.5	40.7	Clay, Silt, Clay Base	O-cell
Caddo, LA	3	44.9	Clay, Silty Clay, Clay Base	Top Down
Caddo, LA	3	62	Clay, Sand Base	Top Down
Union, MS	4.5	49.9	Sand, Sand Base	O-cell
Union, MS	4	73.1	Sand, Clay/Sand Base	O-cell
Washington, MS	4	123	Clay, Sand, Sand Base	O-cell
Washington, MS	4	138.1	Sand, Sand Base	O-cell
Washington, MS	4	119.1	Clay, Sand, Sand Base	O-cell
Washington, MS	5.5	94.1	Sand, Clay, Sand Base	O-cell
Washington, MS	4	96.1	Sand, Sand Base	O-cell
Washington, MS	4	82	Sand, Gravel, Sand Base	O-cell
Washington, MS	4	97.1	Sand, Clay, Sand Base	O-cell
Washington, MS	4	82	Sand. Sand Base	O-cell
Lee, MS	4	89	Clay, Clay Base	O-cell
Forrest, MS	6	47.9	Sand, Sand Base	O-cell
Perry, MS	4.5	64	Sand, Clay, Clay Base	O-cell
Wayne, MS	4	64	Sand, Clay Base	O-cell
Madison, MS	2	40	Clay, Clay Base	O-cell
E. Baton Rouge, LA	4	67.5	Clay, Clay Base	O-cell
E. Baton Rouge, LA	2.5	81.5	Clay, Clay Base	O-cell
E. Baton Rouge, LA	4	77.5	Clay, Clay Base	O-cell
Caddo, LA	6	43	Clay, Sand, Sand Base	O-cell
Caddo, LA	5.5	47.5	Sand, Sand Base	O-cell
Caddo, LA	5.5	48	Sand, Clay, Sand Base	O-cell
Caddo, LA	5.5	53.85	Clay, Sand, Sand Base	O-cell
Caddo, LA	5.5	51.12	Clay, Sand, Sand Base	O-cell

3.5.4.2. Calibration Approach

In the first study of LRFD calibration conducted by LTRC, the 1999 FHWA drilled shaft design method (O'Neill and Reese, 1999) utilized to obtain the predicted resistance of the drilled shafts. In addition, the second study utilized the 2010 FHWA drilled shaft design method (Brown et al. 2010) to estimate the predicted resistance values. To ascertain the load-settlement behavior of drilled shafts, the resistance of the drilled shafts were predicted for different settlement values based on the normalized trend curves for cohesive and cohesionless soil provided by both of the FHWA manuals. As discussed in section 2.2, O'Neill and Reese (1999) provides the normalized curves separately for side and tip resistance for both cohesive and cohesionless soil. On the other hand, Brown et al. (2010) provides a single curve for both side and tip resistance in cohesive and cohesionless soil.

Top and bottom movement curves were used to obtain the equivalent top down curves for each of the O-cell load test data. These curves were utilized to determine the measured side resistance, tip resistance and total resistance values. 5% D failure criteria provided by FHWA was utilized to obtain the measured nominal side, tip and total resistance. 5% D denotes to the settlement value equal to 5% of the diameter of the drilled shaft. 5% D method was selected because of its proved superiority over other criteria by several studies. Figure 2-27 shows the predicted load-settlement curves generated using the 1999 and 2010 methods and the measured load-settlement curve from the load test of one of the drilled shaft cases.

A few drilled shaft load tests did not meet the 5%B settlement criterion so it was necessary to extrapolate the load-settlement curves to estimate the load corresponding to the needed settlement. The exponential curve fitting method was chosen as the best method for extrapolating the load-settlement curves over the hyperbolic, Chin's, cubic spline, and exponential curve fitting

methods. Figure 2-28 compares the extrapolated load-settlement curve to measured curve to show the accuracy of the method. The extrapolation, however, was only performed on tests that were near the 5%B settlement criterion. Load tests that needed large extrapolations were thrown out.

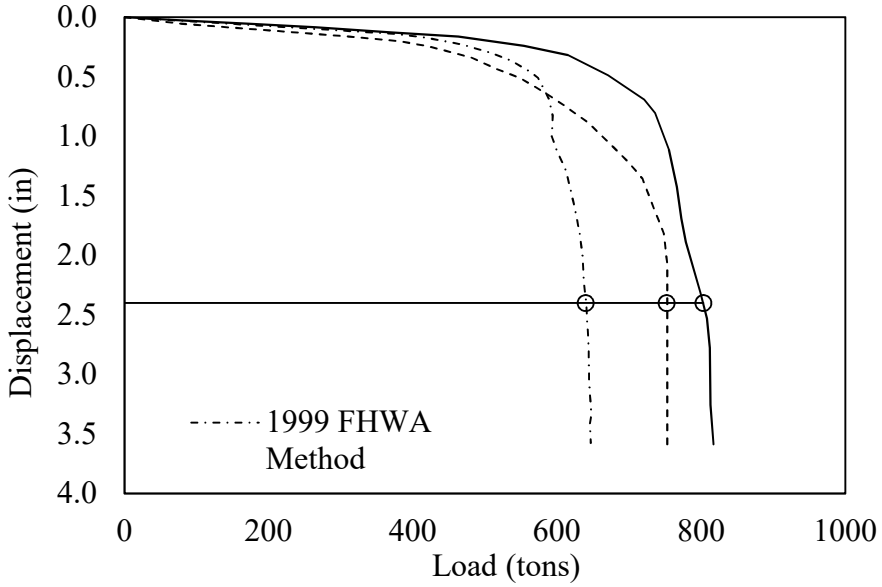

Figure 2 - 27 Predicted and measured load-settlement curves (Abu-Farsakh et al. 2013)

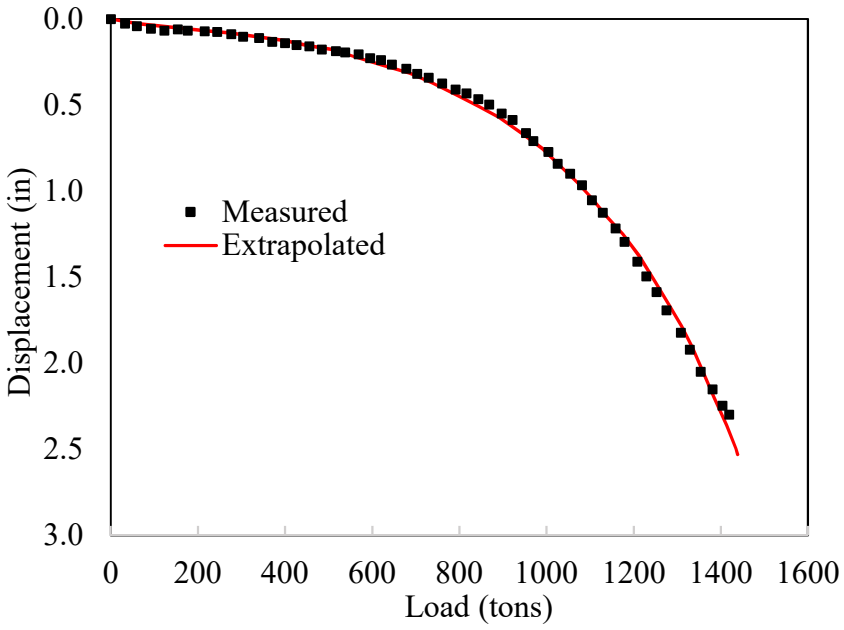

Figure 2 - 28 Extrapolated top-down load-settlement curve (Abu-Farsakh et al. 2013).

The resistance bias factor, which is the measured to predicted resistance ratio, was determined for each case, and a statistical analysis was performed to determine the statistical characteristics from each design method, which are summarized in Table 2-41below. The predicted resistances were plotted against the measured resistances, and a simple regression analysis was performed to determine the line of best fit of the data trend. The regression analysis showed the slope of the best fit line for the 2010 FHWA design method to be 1.02, which indicates the method overestimates the drilled shafts' resistances by 2%. On the other hand, the analysis showed the slope of the best fit line for the 1999 FHWA design to be 0.79, which indicates the method underestimates the resistances by 21%. The average resistance bias for the 1999 design method decreased from the 1.35 determined in the previous LTRC study, however the slope of the best fit line stayed the same.

Table 2 - 23 Statistical Analysis Summary (Abu-Farsakh et al. 2013).

2010 FHWA Design Method			
Summary Statistics			Best Fit Calculations
R_m/R_p			
Mean	Standard Deviation	COV	R_{fit}/R_m
0.99	0.30	0.30	1.02
1999 FHWA Design Method			
Summary Statistics			Best Fit Calculations
R_m/R_p			
Mean	Standard Deviation	COV	R_{fit}/R_m
1.27	0.38	0.30	0.79

The Anderson-Darling goodness of fit test was performed on the resistance biases from the 1999 and 2010 design methods, and it showed that both normal and lognormal distributions fit the

data with a significance level of 0.05. Histograms were also generated for the resistance biases, and the lognormal distribution seemed to better fit the data – the lognormal distribution was chosen to be used in the calibration. The same process was conducted on the side and end bearing resistances biases, and the lognormal distribution was a better fit for the data.

The Monte Carlo simulation method was used in this study to calibrate the resistance factors. The equation used in the simulation is given as:

$$g(R,Q) = \left(\frac{\gamma_D + \gamma_L \frac{Q_L}{Q_D}}{\varphi}\right)\lambda_R - \left(\lambda_D + \lambda_L \frac{Q_L}{Q_D}\right) \quad (2\text{-}47)$$

The statistical characteristics selected for the dead and live loads are the following values:

$$\gamma_D = 1.25 \quad \lambda_D = 1.08 \quad COV_D = 0.13$$

$$\gamma_L = 1.75 \quad \lambda_L = 1.15 \quad COV_L = 0.18$$

A dead to live load ratio of 3.0 was also used, and the target reliability index was 3.0. 50,000 simulations were generated, and the total resistance factors for the 2010 and 1999 FHWA design methods were determined to be 0.48 and 0.60, respectively. While the resistance factor for the 2010 design method is much lower than the 1999 method, the 2010 method gives a relatively higher efficiency factor. The simulation was also conducted on the side and end bearing resistances to determine the resistance factors for each. The side and end bearing factors using the 2010 design method were determined to be 0.26 and 0.53, respectively, and the side and end bearing resistance factors using the 1999 design method were determined to be 0.39 and 0.52, respectively.

2.5.5. Nevada DOT

Nevada Department of Transportation (NDOT) conducted a research on a LRFD calibration of resistance factors for drilled shafts in the Las Vegas Valley. The subsurface condition of Las Vegas Valley mostly consists of cemented sandy soil. This type of soil are also termed as

caliche. As the effect of caliche on resistance factors is hardly predictable, the objective of the study was to propose a method to treat caliche for calibration of resistance factors for drilled shafts. A Monte Carlo simulation was utilized to perform the calibration of the resistance factors. In addition to the traditional Monte Carlo simulation, the study also proposed a new method for calibration which considers the uncertainties developed from the material properties obtained from in-situ tests. The achieved results of the study were compared to the current practice of LRFD design of Nevada DOT. (Motamed et al. 2016)

2.5.5.1. Collected Database

To carry out the study, 41 load test cases on drilled shafts were from a database consisting of 45 load test cases. The selection of the drilled shafts was achieved based on the availability of geotechnical investigation (GI) data and adequate mobilization of the axial resistance of the drilled shafts. The diameter of the shafts included in the selected databased ranged from 2 to 8 ft and the length of the shafts were in the range of 31.6 to 128 ft. All the drilled shafts except one were subjected to bidirectional load test. A few of the included drilled shafts were constructed with dry method whereas, most of the shafts were constructed with wet method. During the study, no significant effect of the drilled shafts with dry construction method was found on the calibrated resistance factors.

For the filtering process of the data, a scoring system was applied to quantify the quality of the load test data as well as the relevant geotechnical investigation (GI) data. The scoring system is developed in such a way that a load test case with high score denotes to high quality of data. The drilled shaft cases were scored from 1 to 4, 1 being the worst and 4 being the best, based on the load test data and GI data. Based on the load test data, if both the top and bottom movement

curves needed extrapolation amount more than 2% of the shaft diameter or the top-down curve needed more than 3% of the shaft diameter, the case was scored 1. For extrapolation of more than 2% in only one of top and bottom movements or in between 2.5% to 3% for the top-down curve, the cases were scored 2. For extrapolation of less than 2% in both top and bottom movements or in between 2% to 2.5% for the top-down curve, the cases were scored 3. Load test data with less than 2% of extrapolation were scored 4. Based on the geotechnical investigation data, if boring log were found incomplete and no lab test data were available for some load test cases, they were scored 1. For the load test data with boring log including minimal SPT data but unavailable lab test data, the score provided was 2. Cases with complete boring log and limited lab test or in-situ test data were given a score of 3. Load tests with complete boring log and proper lab test and in-situ test data were scored 4. The calibration of the resistance factor was performed in three categories based on the scoring system. The categories included all data, data with mean score more than 2 and data with mean score value of more than or equal to 3. Figure 2 – 29 presents the distribution of the load test cases based on the scores. The distance from the GI to the shaft was also considered for the quality of the data. Table 2- 24 presents a summary of the collected load test.

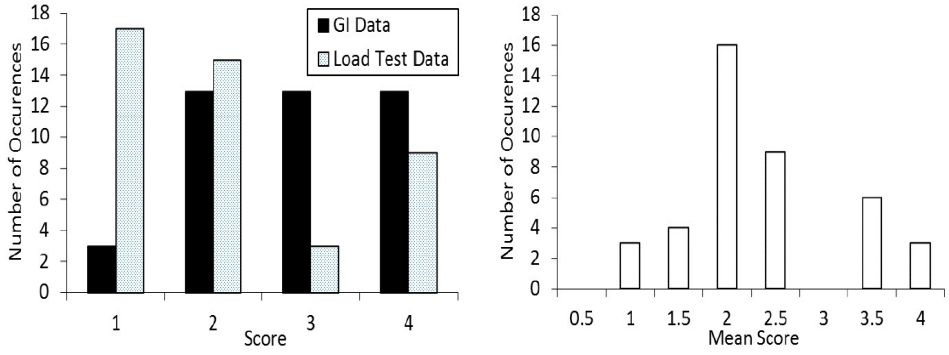

Figure 2 - 29 Distribution of the load test data based on provided scores (Motemed, 2016).

Table 2 - 24 Summary of the load tests collected from NDOT (Motamed, 2016).

No.	Load test score	GI score	D (ft)	L(ft)	R_m (kip)
1	2	2	4.00	103.00	10707
2	4	4	5.00	40.00	3423
3	1	4	7.67	74.43	13989
4	3	4	8.00	32.00	7905
5	3	4	2.00	31.60	1125
6	1	2	2.00	82.50	3812
7	1	4	2.00	43.00	1426
8	1	2	4.00	106.00	19299
9	2	2	4.00	105.00	12641
10	2	2	4.00	116.80	10940
11	2	2	4.00	112.50	12699
12	2	3	4.00	123.00	20937
13	2	3	4.00	122.50	20109
14	1	3	3.00	102.00	5260
15	1	4	4.00	100.00	10616
16	1	4	4.00	101.00	11848
17	3	4	6.00	122.00	13215
18	2	2	4.00	121.70	8112
19	2	2	4.00	121.80	15935
20	1	3	3.50	90.70	22110
21	1	3	3.50	105.50	20669
22	1	2	4.00	128.00	15964
23	2	2	4.00	117.00	13286
24	1	3	3.50	100.00	12185
25	1	4	4.00	82.00	7142
26	4	4	4.00	90.50	3682
27	4	3	5.00	95.50	9965
28	4	3	5.00	96.00	10822
29	2	1	4.00	62.00	6611
30	1	3	4.00	101.60	8876
31	1	3	6.00	112.70	18519
32	2	2	3.75	104.33	15268
33	4	3	3.50	70.00	7923
34	2	2	3.50	70.00	10943
35	4	4	3.50	75.00	7712
36	2	3	3.50	105.50	16945
37	4	1	3.50	112.00	9918
38	4	2	5.00	101.00	10276

No.	Load test score	GI score	D (ft)	L(ft)	R_m (kip)
39	1	3	4.00	106.00	11001
40	4	4	4.00	84.00	3376
41	4	4	3.00	83.00	2204

Table 2 – 24 (Cont.)

2.5.5.2. Predicted Resistance

The FHWA 2010 drilled shaft design method (Brown et al. 2010) was primarily used to estimate the predicted resistance of the drilled shafts for this study. In addition, the study also considered four different methods for the cemented geomaterial available in Las Vegas Valley. According to ASTM (2000), the cemented geomaterial can be classified into three types. Weak cemented material breaks under little finger pressure. Moderate cemented material breaks with moderate finger pressure. Strong cemented material cannot be crumbled under finger pressure. Caliche is a strong cemented sand which is very commonly found in the region included in the study. The four design approaches considered for cemented sand are discussed below.

M_1 method – This is the current practice to estimated predicted resistance, in which, caliche is considered as very dense sand. This method is mainly followed with recommendations from local practitioners.

M_2 Method – According to this method, the caliche is treated as cohesive IGM. The procedure recommended in Brown et al. (2010) is followed to estimate the predicted resitance of drilled shafts.

M_3 Method - In this procedure, caliche is considered as rock. Brown et al. (2010) is also followed in this case to estimate the predicted resistance.

M_4 Method – In this method, the following equation is used to estimate side resistance.

$$\frac{f_S}{p_a} = 0.85\sqrt{\frac{q_u}{p_a}} \leq 15.8 \quad (2\text{-}48)$$

Here, f_S is the unit side resistance, p_a is the atmospheric pressure and q_u is the unconfined compressive strength in caliche (Motamed et al. 2016). The base resistance is obtained from the rock model or 100 ksf, whichever is smaller.

2.5.5.3. Calibration Approach

Two calibration approaches were used to estimate the resistance factors of the drilled shafts. The approaches are termed as L_1 and L_2. L_1 is basically the current practice of calibration procedure using a Monte Carlo simulation. According to the L_1 method, the resistance bias values were calculated for all the drilled shafts included in the database. The mean and coefficient of variation (COV) of the bias values were obtained. It was found that a lognormal distribution can define the bias values properly. Statistical parameters for the load factors were obtained from Paikowsky (2004). The dead load to live load ratio was assumed to be 3.00. The difference between the L_1 and L_2 method was in the estimation of the bias values. For the estimation of bias values, values of unit weight, unconfined compressive strength, internal friction angle, SPT values are taken treated as random variables. The mean and COV values for these parameters were estimated based on the data collected in this study. An additional Monte Carlo simulation was performed whenever on of the mentioned parameters were faced in the design to get the bias values. Table 2 -25 presents the result from the study on calibration of resistance factors. The results are shown for a reliability index value of 3.0. It was found from the study that M_1, M_2 and M_3 method underestimate the predicted resistance values. That could be the reason for the difference in the resistance factor values.

Table 2 - 25 Resistance factors obtained from the study in Las Vegas Valley (Motamed et al. 2016).

Calibration Approach	Analytical Method	All Data	Mean score > 2	Mean score ≥ 3
L_1	M_1	1.05	0.78	0.79
	M_2	0.81	0.85	0.85
	M_3	0.90	0.91	0.91
	M_4	0.73	0.77	0.72
L_2	M_1	1.09	0.86	1.02
	M_2	0.84	0.87	0.76
	M_3	0.90	0.91	0.77
	M_4	0.71	0.74	0.66

2.5.6. FHWA Recommendations

FHWA 2010 LRFD design method of drilled shafts (Brown et al. 2010) collected calibrated resistance factors from different sources and recommended resistance factors for drilled shafts in different conditions. Most of the resistance factors recommended by Brown et al. (2010) were obtained from AASHTO (2007). The resistance factor values collected from AASHTO (2007) were also recommended by FHWA 1999 LRFD design method of drilled shafts (O'Neill and Reese, 1999). Brown et al. (2010) included some conditions where resistance factors were selected based on newer studies. The recommended resistance factors for axial strength limit states of drilled shafts were collected from Allen (2005). Studies conducted by Barker et al. (1991) and Paikowsky et al. (2004) were considered by Allen (2005) for the recommendation of the resistance factors. For the recommended resistance factor values by Brown et al. (2010), a target reliability index (β) of 3.00 was selected which corresponds to a probability of failure value of 1 in 1000. Table 2 – 26 presents the resistance factors for axially loaded drilled shafts recommended by Brown et al. (2010).

Table 2 - 26 Resistance factor recommended by FHWA 2010 (Brown et al. 2010).

Limit State	Resistance Component	Type of Soil	Analytical Method	Resistance Factor
Strength I through Strength V	Side resistance compression/uplift	Cohesionless soil	Beta method (Brown et al. 2010)	0.55/0.45
		Cohesive soil	Alpha method (Brown et al. 2010)	0.45/0.35
		Rock	(Brown et al. 2010)	0.55/0.45
		Cohesive IGM	Modified alpha method (Brown et al. 2010)	0.60/0.50
	Tip resistance	Cohesionless soil	N – value	0.50
		Cohesive soil	Bearing capacity	0.40
		Rock & cohesive IGM	CGS (1995)	0.50
	Static compressive resistance	All soils		≤ 0.70
	Static uplift resistance	All soils		0.60
	Group block failure	Cohesive soil		0.55
	Group uplift resistance	Cohesive and cohesionless soil		0.45

In the Table 2 – 26, side resistances are presented for both compression and uplift. Resistance factors for uplift was considered to be 0.10 less than the resistance factor of compression according to Allen et al. (2005). For the side resistance in cohesionless soil, the resistance factors were estimated based on fitting to global factor of safety considered in ASD method. For a live load factor value of 1.75, dead load factor value of 1.25 and factor of safety value of 2.5, the resistance factor for side resistance in cohesionless soil was estimated to be 0.55 following the procedure mentioned before. The resistance for uplift an also be calculated to be

0.45 for a factor of safety value of 3.0. The resistance factors for side resistance in cohesive soil were also obtained by fitting to ASD method with a factor of safety of 2.5 for compression and factor of safety of 3 for uplift. Resistance factors for side resistance of drilled shafts located in rock were also estimated with fitting ASD global factor of safety values with a factor of safety value 0f 2.5 for compression and factor of safety value of 3.0 for uplift. These resistance factor values were recommended as interim values until valid reliability based analysis was performed for drilled shafts in rock. Resistance factors for side resistance in cohesive IGM were obtained from the reliability calibration studies performed by Allen (2005).

To obtain the resistance factors for tip resistance in cohesionless soil, both ASD fitting method and Reliability based analysis conducted by Paikowsky (2004) were considered. Also for tip resistance in cohesive soil, both ASD fitting and Paikowsky (2004) were considered. For tip resistance in rock and cohesive IGM, a resistance factor value of 0.5 was recommended based on Barker et al. (1991). The resistance factor value for the axial static compression resistance for load tests was recommended based on AASHTO (2007). The resistance factor for the static uplift for load tests was assumed to be 0.60, which is 0.10 less than the resistance factor recommended for static compression resistance. This resistance factor value was assumed because of lack of data. Resistance factors for group axial resistance were estimated based on ASD fitting with a factor safety value of 2.5.

2.6. Studies on Uncertainties in LRFD Calibration

The procedure to calibrate LRFD resistance factors considers uncertainties developing from applied load and the resistance of the drilled shaft by the utilization of the load and resistance factors. Load factors are usually collected from the AASHTO specifications for the studies on

LRFD calibration. Resistance factors are calibrated based on the distribution of bias values, which is the ratio of the measured resistance and the predicted resistance of the drilled shafts. So, the uncertainties developing from the resistance of the shaft can occur from the predicted resistance and the measured resistance. Predicted resistance values are estimated based on theoretical relationships including the soil and drilled shaft parameters. The methods used for the estimation of the predicted resistance values can affect the calibration of the resistance factors differently. The in-situ and lab test data on the subsurface condition, which are utilized to estimate the predicted resistance may cause some uncertainties in the calibration of resistance factors. Uncertainties may also occur from the location of the drilled shafts, construction methods, presence of water body near the drilled shaft etc. Motamed et al. (2016) recommended a procedure to conduct calibration of resistance factors by considering the uncertainties occurring from the parameters related to the subsurface condition, which was discussed in section 2.5.5. The uncertainties in the measured resistance may occur from the type of the load test performed on the drilled shafts. It may also occur from the interpretation procedure of the load test data. Extrapolation of the top and bottom movement curves to develop the equivalent top-down curve is a usual procedure to interpret data resulted from the application of bidirectional load test on drilled shafts. As extrapolation is a procedure with possibilities of making errors in developing the equivalent top-down curve, it may also affect the calibration of resistance factors. The assumption of the distribution of the resistance bias values also affects the calibration procedure as random numbers are generated for the bias values based on its type of distribution. Some studies on the possible sources of uncertainties affecting the LRFD calibration are discussed in this section.

2.6.1. Studies on Extrapolation

Top and bottom movement curves are developed from the results achieved from a bidirectional load test performed on drilled shafts. To interpret the data, an equivalent top-down curve is developed from the top and the bottom movement curves. Extrapolation of the top and the bottom movement curves is often necessary in order to ensure that the curves reach the failure criteria. This section concentrates on studies performed on the extrapolation of load test studies.

2.6.1.1. Paikowsky and Tolosko (1999)

Paikowsky and Tolosko (1999) conducted a study on the extrapolation of non-failed load tests performed on driven piles. A non-failed load test is a type of load test in which, a load equivalent to a given factor times the design load is applied on the pile. In case of a non-failed load test, extrapolation is required to be performed in order to estimate the measured load beyond the applied load in the load test. Paikowsky and Tolosko (1999) recommended a procedure to practically estimate the measured resistance based on extrapolated load-settlement curves. They compared the proposed method with two other possible methods i.e. Chin's method (Chin, 1971) and Brinch-Hansen method (Brinch-Hansen, 1963). To carry out the study, they collected database of 63 driven piles with conventional static load test data performed to the failure point. In the study, it was assumed that the data points of the load tests were known up to 25%, 33%, 50%, 75% and 100% of the bearing capacity as well as the maximum applied load. The assumed known data was extrapolated based on the three methods and the results were compared to the actual capacity of the driven piles. Statistical analysis was performed on the results to estimate the reliability of the proposed methods.

In this study, Davisson's criterion (Davisson, 1972) was utilized to estimate the failure load of the driven piles. According to Davisson's criterion, the failure load is estimated as the load corresponding to the displace of the pile that exceeds the elastic compression of the pile by a offset of 0.15 inches in addition to the pile diameter divided by 120. It can expressed by –

$$\mathrm{X} = 0.15 + \mathrm{d}/120 \tag{2-49}$$

Here, X is the offset displacement of the elastic compression line and d is the diameter of the pile. The failure load is obtained from the intersection of the Davisson's criterion line and the load-settlement curve. The Davisson's criterion line is parallel to the elastic compression line.

The Chin's method of extrapolation was discussed in section 2.3.2.3. According to the Brinch-Hansen's 80% method, the failure load is estimated based on the assumed hyperbolic relation between the load and the settlement. This method can be expressed by the following equation.

$$\mathrm{Q}_u = \frac{1}{2\sqrt{C_1 + C_2}} \tag{2-50}$$

$$\delta_u = \frac{C_2}{C_1} \tag{2-51}$$

Here, Q_u is the load at the failure point and δ_u is the displacement at the failure point. C_1 and C_2 are the slope and y-intercept of the straight line obtained by plotting the $\frac{\sqrt{\delta}}{Q}$ vs the displacement.

In addition to the Chin's method and Brinch-Hansen method, Paikowsky and Tolosko (1999) proposed another method to extrapolate the load-settlement curves. For this proposed method, a plot is developed for Δ/Q vs Δ. Δ is the displacement and Q is the corresponding load.

This plot forms a straight line. A linear regression is performed on the plot to get the ratio of the best fit line and the coefficient of regression. For the regression analysis, the ratio of the displacement and the load is assumed to be the predictor variable and the displacement is considered to be the dependent variable. Data points at the beginning of the plot are removed to get a coefficient of regression value of at least 0.8. The procedure can be expressed by the following equation.

$$\frac{\Delta}{Q} = a\Delta + b \qquad (2\text{-}52)$$

Here, Δ is the displacement and Q is the load corresponding to the displacement. Here, a is the slope of the straight line and b is the y-intercept. The slope and y-intercept can be estimated by linear model analysis.

The analysis included in the study started with 100% of the data achieved from the load test. Then the data points were subsequently decreased perform the analysis with 75%, 50%, 33% and 25% of the available data. For each step of the analysis, the failure load of the driven piles were estimated based on Chin's method, Brinch-Hansen method as well as the proposed method. The achieved failure loads from extrapolated data were compared to the actual failure load of the driven piles by calculating the ratio of the extrapolated capacity and the actual capacity for each of the three methods. Table 2 – 27 presents the ratio of extrapolated failure load and actual failure for Chin's method. In this case, the data was removed by the percentage of the total applied load in load test. It can be observed from the mean of the ratios that Chin's method significantly over predicts the failure load even when 100% data is used to estimate the failure load.

Table 2 - 27 Ratio of extrapolated failure load to actual failure load for Chin's method (Paikowsky and Tolosko, 1999).

Percentage of Data	100%	75%	50%	33%	25%
No of cases	63	63	63	62	59
Mean	1.56	1.64	1.62	1.81	1.29
Standard Deviation	0.62	0.77	0.90	2.21	0.85

Table 2 – 28 presents the ratio of extrapolated failure load and actual failure for Brinch-Hansen method. In this case, the data was removed by the percentage of the total applied load in load test. It can be observed in from the mean and standard deviation of the ratio of the extrapolated load to the actual load that Brinch-Hansen method can close estimate the failure load when requirement for extrapolation is very little. On the other hand, this method over predicts the failure load by about two times the actual load when the amount of extrapolation is significant.

Table 2 - 28 Ratio of extrapolated failure load to actual failure load for Brinch-Hansen method (Paikowsky and Tolosko, 1999).

Percentage of Data	100%	75%	50%	33%	25%
No of cases	61	61	61	61	61
Mean	0.99	1.15	2.06	2.37	2.35
Standard Deviation	0.31	0.99	2.07	2.00	2.08

Table 2 – 29 presents the ratio of extrapolated failure load and actual failure for the proposed method by Paikowsky and Tolosko (1999). In this case, the data was removed by the percentage of the total applied load in load test. It can be observed in from the mean and standard deviation of the ratio of the extrapolated load to the actual load that proposed method can closely estimate the failure load when requirement for extrapolation is very little. When the amount of extrapolation required is large, the proposed method underestimate the extrapolated failure load compared to the actual failure load.

Table 2 - 29 Ratio of extrapolated failure load to actual failure load for the proposed method by Paikowsky and Tolosko (1999).

Percentage of Data	100%	75%	50%	33%	25%
No of cases	63	62	61	54	48
Mean	1.02	0.99	0.89	0.74	0.64
Standard Deviation	0.21	0.26	0.41	0.46	0.44

2.6.1.2. Ooi et al. (2004)

Ooi et al (2004) conducted a study for the extrapolation of non-failed test performed on drilled shafts. They used a load test data for drilled located in the island of Oahu in Hawaii supporting the H-3 freeway viaduct. Truncation of the data points collected from the load test data was performed and six different extrapolation techniques were utilized to estimate the failure loads. More reliable of the six different techniques were recommended by Ooi et al (2004). They also discussed about the limitations of the techniques to extrapolate the load-settlement curves achieved from the load tests. The objective of the study was to improve the confidence in using the extrapolation methods to estimate measured loads from non-failed tests.

In addition to the Chin's method (Chin, 1971a and 1971b) and Brinch-Hansen's 80% criteria (Brinch-Hansen, 1963) of extrapolation. Ooi et al. (2004) utilized the polynomial method recommended by Brinch-Hansen (1963). Chin's method and Brinch-Hansen's 80% criteria were discussed earlier in this paper. The polynomial method discussed by Brinch-Hansen will be discussed here. The polynomial method can be expressed by the following equation.

$$\frac{\delta}{Q^2} = M_1\delta + M_2 \qquad (2\text{-}53)$$

$$Q_{ult} = \frac{1}{\sqrt{M_1}} \tag{2-54}$$

Here, δ is the displacement value, Q is the applied load. M1 and M2 are constants, which can be estimated by linear regression analysis. Ooi et al. used Davisson's criteria (Davisson, 1972) and 5% of the drilled shaft dimeter criteria (O'Neill and Reese, 1999) to estimate the failure load from the load-settlement curves.

The collected database for the study consisted of 19 drilled shafts with ten load tests to failure and nine non-failed tests. Three out of the ten load tests failed prematurely. The remaining seven load test data were selected for the study under consideration. The Osterberg cell load test was conducted on five of the seven load tests. Conventional static load test was performed on the remaining two selected drilled shafts.

The six methods considered for the extrapolation in this study are, A) Chin's method, B) Brinch-Hansen 80% criterion, C) Brinch-Hansen's polynomial method, D) Chin's/Davisson's method, E) Brinch-Hansen 80% criterion/Davisson's method and F) Brinch-Hansen's polynomial/Davisson's method. In the first three methods, the failure loads are estimated based on the equations for Chin's method, Brinch-Hansen method and Brinch-Hansen's polynomial method. For the last three methods, the failure loads are estimated from the intersection points of the extrapolated load-settlement curves based on the corresponding methods and the offset line of the Davisson's criterion.

To perform the study, the data points were truncated consecutively in between the elastic line and the offset line from Davisson's criteria. The analysis was conducted for 100%, 75%, 50% and 25% data coverage. The data coverage was estimated by $\frac{\delta_{max}-\delta_{ec}}{\delta_0-\delta_{ec}}$, where, δ_{max} is the maximum displacement value in the load-settlement curve, δ_{ec} is the displacement value at the

intersection of the load-settlement curve and the elastic line and δ_0 is the displacement value at the intersection of the load-settlement curve and the offset line. The failure loads were estimated from the extrapolated load-settlement curve for each of the steps of the truncation using all six aforementioned methods. The estimated failure loads from extrapolated load-settlement curves were compared to the actual failure load by estimating the capacity ratio between the extrapolated failure load and the actual failure load. Table 2 – 30 presents the mean and standard deviation of the capacity ratios for the seven load test cases for each of the steps of the truncation of data points as well as for the six different methods of extrapolation.

Table 2 - 30 Statistical parameters for the capacity ratio (Ooi et al. 2004).

Method	Mean				Standard Deviation			
	100%	75%	50%	25%	100%	75%	50%	25%
A	1.053	1.065	1.119	1.191	0.06	0.05	0.11	0.18
B	1.012	1.001	1.019	1.249	0.01	0.01	0.05	0.61
C	1.047	1.077	1.141	1.543	0.06	0.06	0.13	0.95
D	1.000	1.000	1.015	1.036	0.00	0.01	0.02	0.06
E	0.995	0.988	0.993	1.024	0.02	0.02	0.03	0.16
F	1.000	1.001	1.016	1.070	0.00	0.01	0.02	0.13

It was observed from the study that methods D, E and F estimated the failure loads in a narrower range compared to method A, B and C. Methods E and F over predicted the failure loads of the drilled shafts by about 36% of the actual loads. Method D over predicted the failure load by about 17%. Also, method D has smaller standard deviation value than method E and F.

2.6.1.3. Ng et al. (2013)

Ng et al. (2013) proposed an improved procedure to develop the equivalent top-down curve from the top and the bottom movement curves achieved from bidirectional load tests performed on drilled shafts. They performed the study on the database mentioned in Garder et al. (2012). The database consisted of 41 drilled shaft load test cases collected from 11 states, 28 of which were usable for the study. The study used the approach recommended by Loadtest Inc (2006) to develop the equivalent top-down curves from the top and the bottom movement curves. They proposed a method for the top and the bottom movement curves to reach the failure load. Based on the proposed procedure, the study estimated the measured loads and the predicted loads and finally, performed LRFD calibration of the resistance factors.

Methods prescribed in O'Neill and Reese (1999) were used to estimate the side resistances in clay, sand as well as base resistance in clay and sand. A combination of approaches recommended by Rowe et al. (1987) and Carter et al. (1988) were used to estimate the resistances in cohesive IGM and rock.

As it often happens that the top and bottom movement curves from a bidirectional load test data does not reach the failure criteria, Ng et al. (2013) recommended an improved procedure to develop the equivalent top-down curve based on three different load-settlement behavior scenarios. Case A was defined as the scenario, when the side resistance reaches the failure load before the tip resistance and Case B occurs when tip resistance reaches the failure load before the side resistance. Case C occurs, when neither side resistance nor tip resistance reaches the failure load. Figure 2 – 30 presents the flowchart describing the procedure to obtain the ultimate resistnace value for case A.

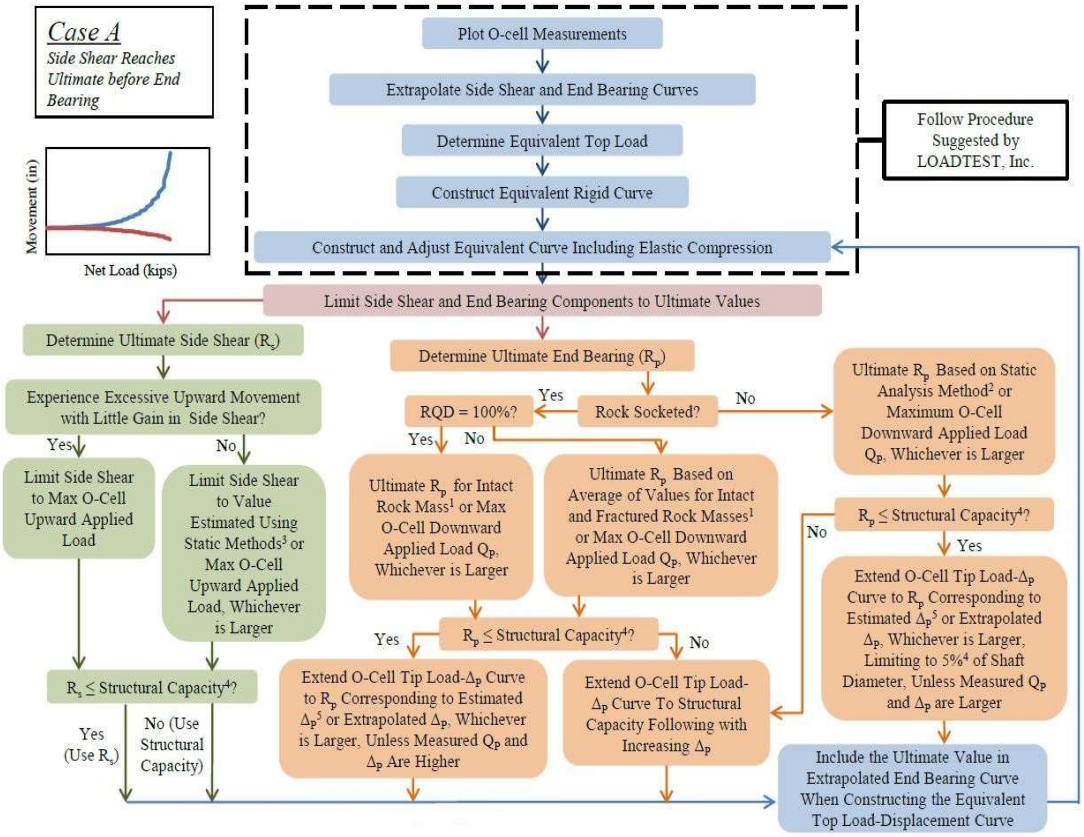

Figure 2 - 30 Proposed procedure to estimate failure loads for side and tip resistance (Ng et al. 2013).

In figure 2 – 30, the current practice of extrapolation of the top and bottom movement curves is presented. The procedure to obtain the ultimate side resistance is presented on the left side of the flowchart. The procedure to obtain the ultimate tip resistance is presented on the right side of the flowchart. For the estimation of ultimate side resistance, if there's excessive upward movement with little increase in the load value, the side resistance value is limited to the maximum upward applied load. Then it's compared to the structural capacity, which is estimated based on AASHTO Specifications (2010). The smaller value between the O-cell load and the structural capacity is selected as the ultimate side resistance. For case A, tip resistance does not reach the ultimate value. If the tip is not located in rock, the maximum downward applied load is compared

to the ultimate tip resistance estimated based on static analysis methods (O'Neill and Reese, 1999) and the larger value is selected. The selected tip resistance is then compared to the structural capacity. If the selected tip resistance is smaller than the structural capacity, the bottom movement curve is extended to the larger value between the estimated tip displacement and the extrapolated displacement. The estimated tip displacement can be obtained by Vesic (1977) for all soils, O'Neill and Reese (1999) for cohesive IGM, Mayne et al. (1993) for cohesionless IGM and Kulhawy et al. (1992) for rock. If the structural capacity is smaller than the selected tip resistance, then the bottom movement curve is extended to the structural capacity. If the side resistance does not reach the ultimate value, the top movement curve can be extended in a similar procedure. The measured resistance values for each of the drilled shafts were estimated by following the aforementioned procedure.

Ng et al. (2013) also conducted a LRFD calibration of resistance factors for drilled shafts. The modified FOSM method of calibration was utilized for the estimation of the resistance factors. The Anderson-Darling (1952) method was used to find out the type of distribution of the bias values obtained from the collected load tests. The statistical parameters for the load factors were collected from AASHTO (2010). The dead load live load ratio was assumed to be 2.0. A range of target reliability index values were selected including 2.00, 2.33, 2.50, 3.00 and 3.50. After the completion of the calibration approach, the recommended resistance factor values for a reliability index of 3.0 are presented in Table 2 -31.

Table 2 - 31 Summary of the calibrated resistance factors (Ng et al. 2013).

Soil Type	Side Resistance Factors	Tip Resistance Factors
Clay	0.22	N/A
Sand	0.47	0.70
IGM	0.69	0.70
Rock	0.62	0.70

2.6.2. Studies on Outliers

The calibration procedure of resistance factors include estimation of the measured and predicted resistance for drilled shafts. The predicted resistance factors are estimated by following various analytical methods like O'Neil and Reese (1999) and Brown et al (2010). The measured resistance factors are obtained from the results of load tests performed on drilled shafts. For the probabilistic reliability analyses, the statistical parameters (mean, standard deviation and coefficient of variation) for resistance bias and load bias values are utilized while it is assumed that the resistance bias values follow a lognormal distribution. The statistical parameters for the load factors can be obtained from AASHTO Specifications (2010). The resistance bias is the ratio of the measured resistance to the predicted resistance of drilled shaft. Several studies performed with an objective of calibration of resistance factors for drilled shafts included some kind of analysis on the resistance bias values in order to achieve more reliable resistance factor values. Oregon Department of Transportation performed a study to calibrate resistance factors for driven piles in 2011 (Smith et al. 2011). The study included an analyses to remove the bias values outside the range of +/- 2 times of the standard deviation from the mean bias value in order to optimize the calibration of resistance factors. Though in the final calibration approach, they did not apply this method due to lack of justification in removing the extreme data points. Iowa Department of

Transportation performed a study on the calibration of resistance factors for drilled shafts based on database developed by Garder et al. (2012). A data quality check was conducted based on type of load tests, accuracy of load test result and availability of information on subsurface condition in order to perform an accurate calibration. Nevada Department of Transportation also performed a study on calibration of resistance factors, in which, they developed a scoring system of the drilled shaft cases included in the database to separate the cases with better data quality and more accurate load test results (Motamed et al. 2016). New Mexico Department of Transportation (Ng and Fazia, 2012) performed a study on calibration with the assumption of the resistance values following a polynomial distribution, in addition to the calibration with lognormality of the bias values. After the completion of the study, the calibration approach with the polynomial function of the bias values yielded higher resistance factor values compared to the calibration approach with the lognormal function of the bias values. They concluded that the polynomial distributions are more rational. Bathurst et al. (2008) recommended a process to recognize the extreme load test cases by plotting the bias values against the predicted resistances. The data points in the developed plots should be randomly distributed. The study recommended to separate the extreme data points in the bias vs predicted resistance plot as the outlier cases. Kim et al. (2016) performed a calibration study by introducing lower bound capacity to the calibration procedure. They estimated the lower bounds of the side as well as tip resistances and considered the lower bounds for the calibration procedure. The consideration of lower bounds for the calibration resulted in the increase of the side resistance factors by up to 8%. The tip resistance factors also increased by up to 13% due to the involvement of the lower bounds in the calibration approach.

Najjar and Gilbert (2009) also recommended consideration of lower bound capacities for the calibration of resistance factors. They performed a study, in which, the effect of lower bounds

was investigated for driven piles in cohesive and cohesionless soil. The study utilized a database of driven piles presented by Olson and Dennis (1982). Methods proposed by Najjar (2005) were used to obtain the lower bound capacities for the driven piles in cohesive and cohesionless soil. Najjar and Gilbert (2009) concluded with the proof of the presence of lower bounds in the capacity distribution and they suggested to incorporate lower bound capacity in the LRFD calibration of resistance factors.

2.7. Summary

This chapter introduced the background for the studies included in the dissertation. As the LRFD calibration of drilled shafts is included in the scope of this study, the current practice of LRFD calibration was discussed in this chapter. The current practice of reliability based LRFD calibration of resistance factors requires the estimation of predicted resistance and measured resistance for the drilled shafts included in the given database. In case of the predicted resistance, the procedures to calculate the side and tip resistance of drilled shafts located in different types of subsurface condition are enclosed in this chapter. The measured resistance is obtained from the load tests performed on the drilled shafts. This chapter also includes descriptions of different load tests as well as the procedure to interpret the load test data. The current practice of reliability based LRFD calibration procedure is described based on the predicted and measured resistance of drilled shafts.

As the AASHTO specified resistance factors for LRFD design of drilled shafts were mostly obtained by fitting the global factors of safety for allowable stress design method, several studies were conducted to perform LRFD calibration for drilled shafts based on the different conditions in different regions. These studies performed by different Department of Transportation are

discussed in this chapter. It was observed from the area specific LRFD calibrations that the obtained resistance factors varied from the resistance factors recommended by AASHTO specifications. Several studies were discussed to find out some possible reasons behind the difference in the resistance factors. It was discerned from the studies that the possible reasons are different types of load tests performed on drilled shafts, interpretation of load test data, presence of outlier load test cases, considered type of distributions for resistance and load etc.

Chapter 3

DATABASE

3.1. Introduction

As the objective of this study is to optimize the reliability based LRFD calibration of resistance factors of drilled shafts, a database of load tests performed on drilled shafts is required to perform the calibration based on the necessary analysis. In order to conduct the study, a database was compiled based on Abu Farsakh et al. (2013) and Fortier (2016). The database included load test data performed on only drilled shafts. Sixty-four drilled shafts load test cases were included in the database. Thirty of the drilled shafts were located in Louisiana and 34 of the drilled shafts were located in Mississippi.

3.2. Background

The accumulation of the database was first started for a study conducted by Abu Farsakh et al. (2013). In the beginning, only sixteen drilled shafts from Louisiana were included in the database. Twenty-six additional drilled shafts data were collected from Mississippi based on the similarity between the subsurface conditions of the surrounding soil of the drilled shafts. Later, eight more drilled shaft load test case were obtained for the LRFD calibration study performed in 2013. Finally, for this study, the database included a total of 64 drilled shaft load test cases. 30 of the drilled shafts were from Louisiana and 34 of them were from Mississippi. Out of the sixty-four cases, a bidirectional load test was performed on 60 of the drilled shafts and conventional static

load test was performed on only four of the drilled shafts. The bidirectional load test and conventional static load test were discussed in Chapter 2. Table 3 – 1 presents a summary of the accumulated drilled shaft load test cases. The summary includes the test shaft ID, location of the shafts, the diameter of the shafts, length of the shafts, type of load test performed on the shafts and construction method of the shafts.

Table 3 - 1 Summary of the accumulated load test database of drilled shafts.

Test Shaft ID	Location	D (ft)	L (ft)	Load Test	Construction Method
LT-8193-1	Monroe County, MS	5.0	35.5	Bidirectional	Wet
LT-8193-2	Monroe County, MS	4.5	33.8	Bidirectional	Wet
LT-8194	Lee County, MS	4.0	38.3	Bidirectional	Dry
LT-8212	Pontotoc County, MS	4.5	31.3	Bidirectional	Wet
LT-8341	Wayne County, MS	5.5	18	Bidirectional	Dry
LT-8371-1	Clarke County, MS	4.0	26.5	Bidirectional	Dry
LT-8371-2	Clarke County, MS	6.0	36.1	Bidirectional	Dry
LT-8373	Oktibbeha County, MS	3.5	29	Bidirectional	Dry
LT-8461-1	Oktibbeha County, MS	4.0	42.5	Bidirectional	N/A
LT-8461-2	Oktibbeha County, MS	4.0	49.16	Bidirectional	N/A
LT-8488-1	Wayne County, MS	4.0	42.3	Bidirectional	Dry
LT-8488-2	Wayne County, MS	4.0	23	Bidirectional	Wet
LT-8578	Jackson County, MS	7.5	125.5	Bidirectional	Wet
LT-8618	Jefferson County, MS	4.0	17.16	Bidirectional	Dry
LT-8655	Washington County, MS	6.5	91.5	Bidirectional	Wet
LT-8745	Hancock County, MS	5.0	33.61	Bidirectional	Wet

Test Shaft ID	Location	D (ft)	L (ft)	Load Test	Construction Method
LT-8786	Forrest County, MS	6.0	47.64	Bidirectional	Wet
LT-8788	Madison County, MS	2.0	40	Bidirectional	Dry
LT-8800	Washington County, MS	4.2	92.48139	Bidirectional	Wet
LT-8825	Harrison County, MS	6.0	74.9	Bidirectional	Wet
LT-8829-1	Desoto County, MS	5.0	49.87	Bidirectional	Wet
LT-8829-3	Desoto County, MS	4.0	16.99	Bidirectional	Dry
LT-8905	Covington County, MS	4.5	16.9	Bidirectional	Dry
LT-8912-1	Pontotoc County, MS	4.0	39.5	Bidirectional	Dry
LT-8912-2	Pontotoc County, MS	4.0	34.2	Bidirectional	Dry
LT-8954-2	Desoto County, MS	4.0	53.2	Bidirectional	Wet
LT-8981	Union County, MS	4.5	49.5	Bidirectional	Wet
LT-9147	Adams County, MS	3.0	39	Bidirectional	Dry
LT-9191	Grenada County, MS	5.0	64	Bidirectional	Wet
LT-9262	Lauderdale County, MS	5.0	35	Bidirectional	Wet
LT-9263	Laurel, MS	4.0	89	Bidirectional	Wet
LT-9280-1	Warren County, MS	4.0	67.2	Bidirectional	Wet
LT-9280-2	Warren County, MS	7.0	175	Bidirectional	Wet
LT-9280-3	Warren County, MS	6.0	94.9	Bidirectional	Wet
LT-9459-2	East Baton Rouge Parish, LA	4.0	67.5	Bidirectional	Wet
LT-9459-3	East Baton Rouge Parish, LA	2.5	81.5	Bidirectional	Wet
LT-9459-4	East Baton Rouge Parish, LA	4	78.5	Bidirectional	Wet
LT-9473-1	Caddo Parish, LA	6.0	39.3	Bidirectional	Dry
LT-9473-2	Caddo Parish, LA	5.5	45.6	Bidirectional	Dry
LT-9597-1	Caddo Parish, LA	5.5	46.2	Bidirectional	Wet
LT-9597-2	Caddo Parish, LA	5.5	53.41	Bidirectional	Wet

Test Shaft ID	Location	D (ft)	L (ft)	Load Test	Construction Method
LT-9694-1	Caddo Parish, LA	5.5	50.1	Bidirectional	Wet
LT-8467	Beauregard Parish, LA	5.5	62.17	Bidirectional	N/A
LT-9694-3	Caddo Parish, LA	5.5	96.8	Bidirectional	N/A
LT-9694-4	Caddo Parish, LA	5.5	43.4	Bidirectional	N/A
LT-9934-1	Caddo Parish, LA	5.5	45	Bidirectional	Wet
LT-9934-3	Caddo Parish, LA	4.5	57	Bidirectional	N/A
LT-9934-4	Caddo Parish, LA	5.5	55.6	Bidirectional	Wet
LT-9934-5	Caddo Parish, LA	5.5	34.3	Bidirectional	Wet
LT-9938-1	Caddo Parish, LA	5.5	35.37	Bidirectional	Wet
LT-9938-3	Caddo Parish, LA	4.5	42.5	Bidirectional	Wet
LT-9950-1	Caddo Parish, LA	5.5	70.14	Bidirectional	Wet
LT-9950-2	Caddo Parish, LA	5.5	47.6	Bidirectional	Wet
455-08-20, #2	Caddo, LA	2.5	53.1	Conventional	N/A
455-08-20, #3	Caddo, LA	2.5	35.1	Conventional	N/A
LT -8412, #2	E. Baton Rouge, LA	3.0	54.1	Bidirectional	N/A
LT -8470	Ouachita, LA	5.5	76.1	Bidirectional	N/A
LT -8915	Calcasieu, LA	6.0	86.9	Bidirectional	N/A
LT -8961, #1	Winn, LA	2.5	77.4	Bidirectional	Wet
LT -8961, #2	Winn, LA	2.5	65	Bidirectional	Wet
LT -8412, #1	E. Baton Rouge, LA	2.5	49.9	Bidirectional	N/A
LT -8944	Beauregard, LA	5.5	40.7	Bidirectional	N/A
455-08-47, 2A	Caddo, LA	3.0	44.9	Conventional	N/A
455-08-47, 2B	Caddo, LA	3.0	62	Conventional	N/A

Table 3 – 1 (Cont.)

3.3. Breakdown of the Database

The database considered for the study was separated based on the type of soil and different construction methods. The soil classification was performed based on the classifications provided in O'Neil and Reese (1999) as well as Brown et al. (2010). Table 3 - 2 presents a summary of the

subcategories developed from the database. In the table, Sand 2010 and clay 2010 are the categories developed based on Brown et al. (2010). Sand 1999, clay 1999, Cohesionless IGM 1999 and Cohesive IGM 1999 were separated based on O'Neill and Reese (1999). Cohesive IGM can be defined as the cohesive soil with an undrained shear strength value of 0.25 to 2.5 MPa. Cohesionless IGM can be defined as cohesionless soil with more than 50 SPT blows per feet for each soil layer.

Table 3 - 2 Subcategories of the drilled shaft database.

Parameters	Subgroups	MS Database	LA Database
		Number of Cases	Number of Cases
Soil Properties	Sand 2010	18	17
	Clay 2010	16	13
	Sand 1999	4*	14
	Clay 1999	5*	12
	Cohesionless IGM 1999	14	5*
	Cohesive IGM 1999	9*	1
	Sand +Clay 1999	9*	25
Construction Method	Wet	19	15
	Dry	13	2
	N/A	2	13

* Calibration of resistance factors based on less than 10 cases.

3.4. Calibration Approach

To perform the calibration of the resistance factors based on the drilled shaft load test cases included in the aforementioned database, the predicted resistance and the measured resistance values were estimated for each of the drilled shafts. The predicted resistances were estimated based on Brown et al. (2010) for both cohesive and cohesionless soil. The measured resistances were obtained from the load teste results in the form of load-settlement curve. Later, resistance bias

values were estimated, which is the ratio of measured resistance to predicted resistance. Finally, Monte Carlo simulation was utilized to perform calibration of resistance factors (Yu et al. 2011).

3.3.1. Predicted and Measured Resistance

The predicted resistances of the drilled shafts included in the database were estimated based on the methods described in Chapter 2. The surrounding soil of the drilled shafts included in the databased mainly consisted of sand, clay and IGM. The side and tip resistances of the drilled shafts were estimated based on the soil type. The ultimate resistances were calculated based on the previously obtained side and tip resistances. Utilizing the calculated ultimate resistances of the drilled shafts and the normalized load-settlement curves recommended by Brown et al. (2010), the load-settlement curve was developed for each of the drilled shafts. The load corresponding to the 5% of the diameter of the shaft in the theoretically developed load-settlement curve was taken as the predicted resistance for each of the drilled shafts.

The measured resistances of the drilled shafts were obtained from the load test results. The database considered for the study consists of bidirectional load test and conventional static load test. Conventional static load test results provide a load-settlement curve from which, the measured loads can be achieved. The bidirectional load tests provide top movement curves and bottom movement curves corresponding to the upward displacement and downward displacement of the drilled shafts, respectively. The top movement curves and the bottom movement curves are utilized in order to develop equivalent top-down curves, which are similar to the load-settlement curves achieved from the conventional static load tests. Similar to the predict resistance, the measured resistance was taken from the load-settlement curve or the equivalent top-down curve as the resistance value corresponding to the displace value of 5% of the diameter of the shaft. The

resistance bias values were estimated as the ratio between the measured resistance and the predicted resistance for each drilled shaft. Table 3 – 3 presents the measured resistance, predicted resistance and the calculated resistance bias values for each of the drilled shafts included in the database.

Table 3 - 3 Measured resistance, predicted resistance and bias of the drilled shafts.

Test Shaft	Measured (R_m), tons	Predicted (R_c), tons	Bias, R_m/R_c
LT-8193-1	3133	2023	1.55
LT-8193-2	1569	1820	0.86
LT-8194	2165	902	2.40
LT-8212	3754	1261	2.98
LT-8341	836	624	1.34
LT-8371-1	1551	746	2.08
LT-8371-2	2581	1945	1.33
LT-8373	864	1005	0.86
LT-8461-1	2473	2275	1.09
LT-8461-2	1437	791	1.82
LT-8488-1	1315	389	3.38
LT-8488-2	444	505	0.88
LT-8578	3115	3335	0.93
LT-8618	725	339	2.14
LT-8655	4592	3301	1.39
LT-8745	963	1171	0.82
LT-8786	1296	1229	1.05
LT-8788	213	279	0.76
LT-8800	1340	1683	0.80
LT-8825	1100	1493	0.74
LT-8829-1	1119	1016	1.10
LT-8829-3	501	550	0.91
LT-8905	492	635	0.77
LT-8912-1	2675	1169	2.29
LT-8912-2	3381	1120	3.02
LT-8954-2	1070	1160	0.92
LT-8981	1226	1469	0.83
LT-9147	1350	575	2.35

Test Shaft	Measured (R_m), tons	Predicted (R_c), tons	Bias, R_m/R_c
LT-9191	3424	1825	1.88
LT-9262	4497	1211	3.71
LT-9263	1431	1339	1.07
LT-9280-1	673	674	1.00
LT-9280-2	4303	8023	0.54
LT-9280-3	2641	2187	1.21
LT-9459-2	788	669	1.18
LT-9459-3	380	430	0.89
LT-9459-4	605	750	0.81
LT-9473-1	3008	2203	1.37
LT-9473-2	2282	2996	0.76
LT-9597-1	786	1258	0.62
LT-9597-2	786	1258	0.62
LT-9694-1	1115	1272	0.88
LT-8467	1583	1926	0.82
LT-9694-3	3249	3485	0.93
LT-9694-4	2055	1191	1.73
LT-9934-1	1049	1337	0.78
LT-9934-3	1459	1194	1.22
LT-9934-4	959	881	1.09
LT-9934-5	968	818	1.18
LT-9938-1	552	700	0.79
LT-9938-3	797	893	0.89
LT-9950-1	2692	2126	1.27
LT-9950-2	757	864	0.88
455-08-20, #2	1007	572	1.76
455-08-20, #3	784	444	1.77
LT -8412, #2	343	278	1.23
LT -8470	1560	1630	0.96
LT -8915	1750	1431	1.22
LT -8961, #1	888	706	1.26
LT -8961, #2	599	627	0.96
LT -8412, #1	283	286	0.99
LT -8944	531	571	0.93
455-08-47, 2A	405	351	1.15
455-08-47, 2B	428	498	0.86

Table 3 – 3 (Cont.)

3.3.2. Statistical Parameters for the Calibration

After obtaining the predicted and the measured resistance values for each of the drilled shafts, the resistance bias values were estimated by taking the ratio of measured resistance to the predicted resistance. The bias values were assumed to follow a lognormal distribution. Based on this assumption, the statistical parameters i.e. mean, standard deviation and coefficient of variation were estimated for the bias values included in each of the subcategory of the database mentioned above. The statistical parameters for the load factors were obtained from AASHTO specifications (2010). Table 3 -4 presents the statistical parameters used for the factors of live load and dead load. Figure 3 -1 presents the histograms of the bias distribution along with the probability density function based on the lognormal distribution for the whole database. Figure 3 -2 and 3 – 3 presents the histograms of the bias distribution along with the probability density function based on the lognormal distribution for the Louisiana database and Mississippi Database, respectively. It can be observed from the plots that the bias values closely follow the lognormal distribution.

Table 3 - 4 Statistical parameters for factors of live load and dead load.

Load Factor	Mean	COV
Live Load	1.15	0.18
Dead Load	1.08	0.13

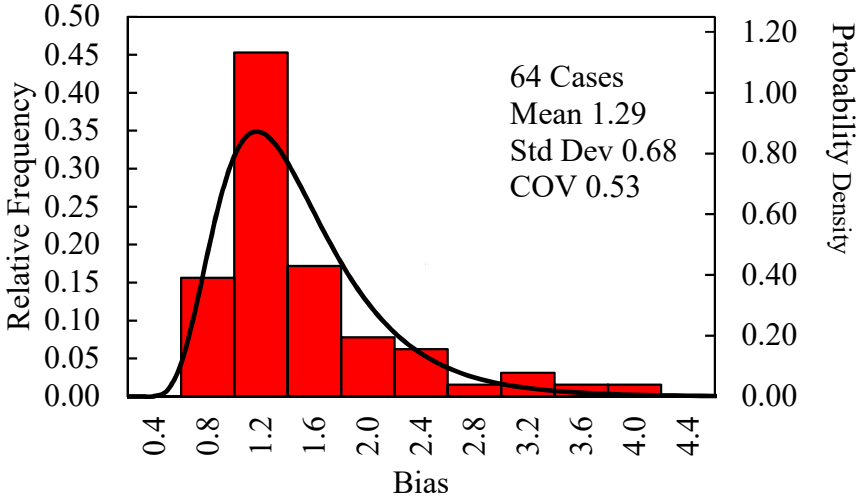

Figure 3 - 1 Histogram of the bias distribution along with probability density function for the whole database.

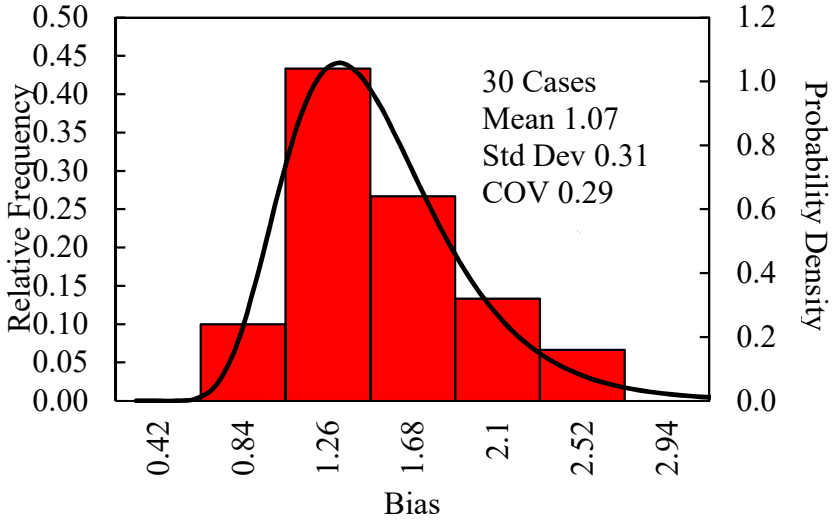

Figure 3 - 2 Histogram of the bias distribution along with probability density function for the Louisiana database.

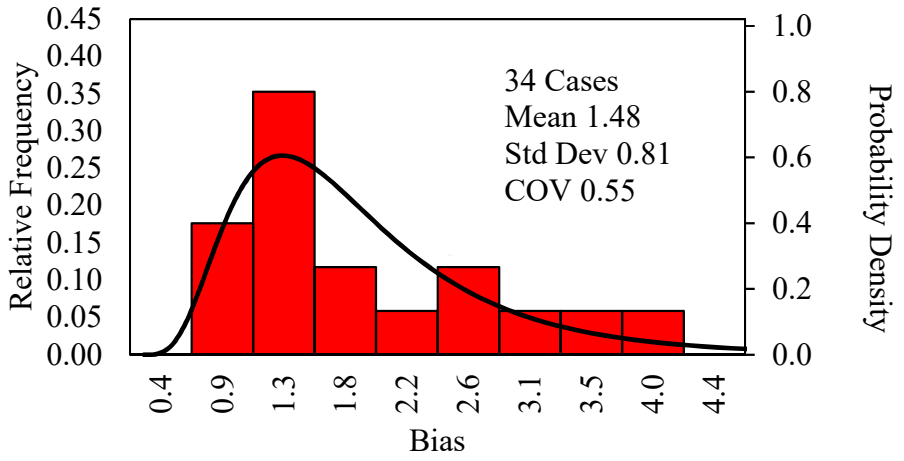

Figure 3 - 3 Histogram of the bias distribution along with probability density function for the Mississippi database.

3.3.3. Monte Carlo Simulation

The Monte Carlo simulation method was utilized to perform the calibration in this study. A MS Excel spreadsheet was prepared for that purpose following Abu-Farsakh et al. (2013). The first step to perform a Monte Carlo simulation was to select a target reliability. Probability of failure can be expressed by the reliability index. For this study, reliability index values of 2.33 and 3.00 were selected based on FHWA specifications. Three sets of random numbers were generated for the bias values of resistance, live load and dead load. Each of the sets contained 50,000 random numbers. As the bias values are assumed to be lognormally distributed, for each lognormal variable, the sample value was estimated by the following equation.

$$x_i^* = \exp\left(\mu_{lnx} + z_i \sigma_{lnx}\right) \tag{3-1}$$

Here, x_i^* is the sample value, μ_{lnx} and σ_{lnx} are the logarithmic mean and standard deviation of the bias values and z_i is the random standard normal variable obtained utilizing the excel

function, z_i = NORMSINV(RAND()). Then the limit state function was defined as (Abu-Farsakh et al. 2013) -

$$g(R,Q) = \left(\frac{\gamma_D + \gamma_L k}{\phi}\right)\lambda_R - (\gamma_D + \gamma_L k) \quad (3\text{-}2)$$

Here, γ_D and γ_L are the dead load factor and live load factor, respectively. k is the ratio between live load and dead load, which was taken as 0.33 according to FHWA specifications. λ_R is the resistance bias and ϕ is the resistance factor. The probability of failure was defined by the following function in the simulation.

$$p_f = \frac{Count(g \leq 0)}{N} \quad (3\text{-}3)$$

Probability of failure is basically the ratio between the number of cases, where limit state function was less than zero and the total number of generated random numbers. The reliability index can be estimated by,

$$\beta = \Phi^{-1}(p_f) \quad (3\text{-}4)$$

To perform the simulation, a resistance factor was assumed and the reliability index (β) was estimated by following the aforementioned steps. This process was repeated until the target reliability index was reached for an assumed resistance factor. Figure 3 -4 presents a flow chart with the steps of the Monte Carlo simulation to calibrate the resistance factors.

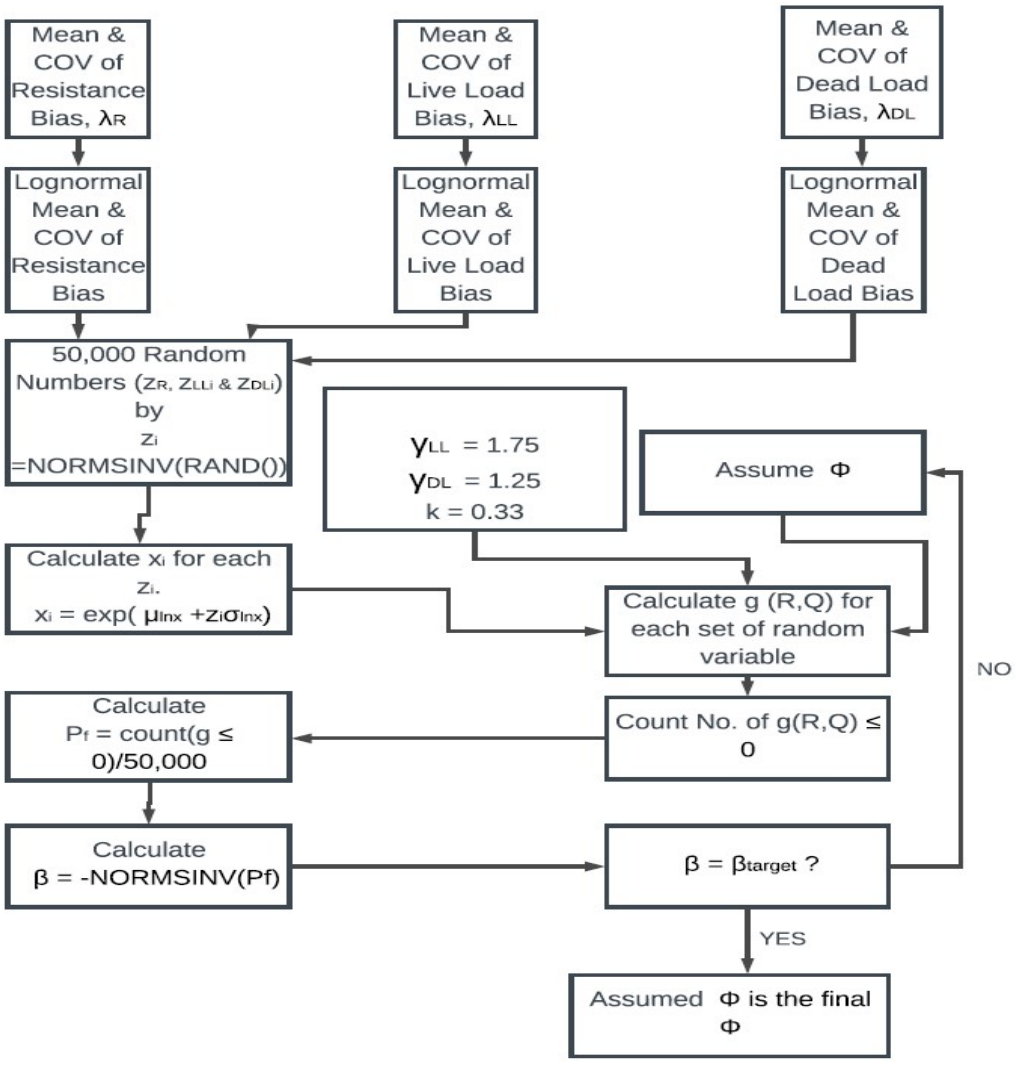

Figure 3 - 4 Flow chart of Monte Carlo simulation.

3.3.4. Calibration Result

The reliability based LRFD calibration was performed for the aforementioned database to estimate the resistance factors. The previously mentioned statistical parameters were utilized to perform a Monte Carlo simulation. The target reliability indices used for the calibration were 2.33 and 3.00. Table 3 – 5 presents the resistance factors achieved by the performed LRFD calibration

based on the accumulated database. Table 3 – 6 presents the calibrated resistance factors for the subcategories of the database.

Table 3 - 5 Statistical parameters and calibrated resistance factors.

Database	Mean	Standard Deviation	Reliability Index	Resistance Factor
Louisiana	1.07	0.31	2.33	0.63
			3.00	0.51
Mississippi	1.48	0.81	2.33	0.48
			3.00	0.33
Louisiana + Mississippi	1.29	0.68	2.33	0.44
			3.00	0.31

It can be observed from 3 - 6 that both cohesionless IGM and cohesive IGM has lower resistance factor values compared to sand and clay. After separating the cohesive and cohesionless IGM, it can be observed that the difference in resistance factor values has been reduced between the two databases. The Mississippi database has about 68% drilled shafts with cohesionless or cohesive IGM. So IGM may cause the lower resistance factor of the Mississippi database. Louisiana database shows higher resistance factor than Mississippi database for cohesionless IGM 1999. Higher average SPT values and low number of drilled shafts in cohesionless IGM may be the probable reasons for this lower resistance factor in LA database. Some of the difference in the resistance factor values may also occur from the error in bias values occurred due extrapolation of the top and bottom movement curves.

Table 3 - 6 Calibrated resistance factors for the subcategories.

Parameters	Subgroups	MS Database		LA Database	
		RI = 2.33	RI = 3.00	RI = 2.33	RI = 3.00
Soil Properties	Sand 2010	0.35	0.23	0.6	0.48
	Clay 2010	0.55	0.38	0.63	0.55
	Sand 1999	0.55	0.42	0.60	0.50
	Clay 1999	0.73	0.52	0.68	0.52
	Cohesionless IGM 1999	0.34	0.22	0.50	0.40
	Cohesive IGM 1999	0.53	0.37	N/A	N/A
	Sand +Clay 1999	0.62	0.44	0.66	0.54
Construction Method	Wet	0.35	0.23	0.65	0.55
	Dry	0.68	0.48	N/A	N/A
	N/A	N/A	N/A	0.75	0.61

Error! Reference source not found. also shows the subgroups based on the construction methods. It can be observed for the wet or slurry method that the Mississippi database has lower resistance factor than the Louisiana database. It's also caused from the presence of IGM. 13 out of 19 drilled shafts has cohesive or cohesionless IGM in the 'Wet' subgroup of the Mississippi database.

3.5. Summary

The database collected for the research on optimization of the reliability based LRFD calibration is described in this chapter. The drilled shaft load test cases included in the database were collected from Louisiana and Mississippi. The database consisted of sixty bidirectional load test cases and four conventional static load test cases. Different types of soils surrounding the

drilled shafts were utilized to separate the database into subcategories. Two subcategories of the database were also based on two different types of construction methods of the drilled shafts. The measured and the predicted resistance for each of the drilled shafts were estimated in order to obtain the resistance bias values. The statistical parameters of the resistance bias and factors of live load and dead load were used to conduct a reliability based LRFD calibration of resistance factors. Monte Carlo simulation was used to perform the LRFD calibration. The calibrated resistance factors for all the subcategories of the database are presented in this chapter.

Chapter 4

EXTRAPOLATION ERROR ANALYSIS

4.1. Introduction

Load and resistance factor design (LRFD) has become increasingly popular over allowable stress design (ASD) for several decades. While the LRFD method considers load factors as well as resistance factors to be applied to the limit state inequalities, the ASD method combines both of the factors into one single factor of safety. Consideration of two separate factors for load and resistance has made the LRFD method more consistent than the ASD method (Abu Farsakh et al. 2010). After the publication of the first edition of AASHTO LRFD Bridge Design Specifications, the major challenge was to make the transition from ASD to LRFD. To begin the transition from ASD to LRFD, the Federal Highway Administration (FHWA) released a policy in 2000 that required all new federally-funded bridges to be designed using the AASHTO LRFD specifications by October 2007 (Fortier, 2016). Despite this steady progression into LRFD, however, deep foundation design still does not take full advantage of the probabilistic framework in many parts of the United States due to a lack of area-specific calibrated resistance factors. Instead, many regions rely on values provided in specifications from AASHTO (2012), which were developed by fitting to the allowable state design (ASD) safety factors (Stanton et al. 2017). Studies like Abu-Farsakh et al. (2012), Long et al. (2009), Roling et al. (2011); Garder et al. (2012), Rahman et al. (2002), and McVay et al. (2005) were performed with an objective of calibrating region wise load and resistance factors for foundation design. To carry out the calibration of resistance factors, each of the studies collected a data base of load tests performed on drilled shafts. The databases were

developed based on area specific soil condition, type of load tests, availability of adequate information and failure criteria. The load tests included in the databases consisted of conventional static load test, bidirectional load test and statnamic test. The results from the abovementioned studies were compared to the resistance factors recommended by AASHTO specifications. It was observed from the perusal of the studies that the calibrated resistance factors were much lower than the recommendation by AASHTO specifications. The decrease in the resistance factor values may occur from the difference in subsurface condition, location of the drilled shafts, and difference in the type of load tests or inconsistencies in the calibration approach.

Many of the studies mentioned above have included databases of drilled shafts from different states. One of the major components of these databases was the measured resistance of the drilled shafts that were accumulated from different types of load tests performed on the drilled shafts. Load test is essential to estimate the resistance of drilled shafts and driven piles. Osterberg load cell test is one of the widely used load tests for both construction and research purposes. A jack like loading device is installed in the shaft to conduct the load test. It can be installed either at the toe or near the toe of the drilled shaft or the driven pile. A bi-directional load is applied by the loading device to mobilize both side and tip displacement (Osterberg, 1998). A top-down load-settlement curve can be constructed from the acquired top and bottom load-displacement curves. The load leading to the failure of the shaft can be estimated from the constructed top-down load-settlement curve. The measured data of the Osterberg cell load test provides a top movement curve and a bottom movement curve from which a top-down load-settlement curve is constructed (Loadtest, 2001). If the top or bottom movement curves does not reach the displacement corresponding to the failure criteria, it is required to extrapolate the curve up to the failure displacement to estimate the failure load. As extrapolation is prone to errors, the reconstructed top-

down curve from the Osterberg cell test data is not accurate. As a result, the resistance factors required for LRFD design of drilled shafts and driven piles are also affected by the errors that occurred from the extrapolation of the top and bottom movement curves.

Extrapolation is a method to estimate values beyond the observed range by following the trend of the acquired test data. This method is often used to interpret measured load test data, it is criticized for the unknown uncertainties and may result in meaningless estimation. In the case of the O-cell test approach, extrapolation can result in an erroneous equivalent top-down curve due to insufficient displacement, inaccurate data, and various other reasons. Paikowsky and Tolsoko (1999) performed an analysis on non-failed load test. The procedure was based on a database of 63 driven piles tested to failure. Loading was assumed to be known up to 25%, 33%, 50%, 75%, and 100% of the entire load settlement data points. It was observed during the study that the extrapolated capacity with 25% and 33% data was 1.5 times to 2.3 times the actual capacity in some cases. This procedure of truncating load test data can be fit to analyze the effect of extrapolation error on the equivalent top-down curve. Ooi' et al. (2004) also performed a similar analysis by incrementally truncating data from load vs. settlement curve. The study compared the extrapolated measured capacities to the predicted capacities in order to point out some conditions where extrapolations can result in reasonable values in capacity. Kam Ng et al. (2013) proposed a procedure to construct an equivalent top-down curve from load test data. The study was performed on drilled shafts located in rock material. They categorized the typical shaft response under bidirectional load into three categories as case A, Case B and case C. In case A, the side resistance reaches the ultimate value before the tip resistance. In case B, the tip resistance reaches the ultimate value before the side resistance. In case C, neither the side resistance nor the tip resistance reaches ultimate value. According to Kam Ng et al. (2013), if the side resistance does not reach the ultimate

value, the maximum applied upward load is compared to the predicted resistance estimated by following O'Neil and Reese (1999) and the larger value is chosen as the primary ultimate side resistance. Then, the primary ultimate side resistance is compared to the structural side resistance estimated by following AASHTO specifications (AASHTO, 2012) and the smaller value is selected as the final ultimate side resistance. If the selected ultimate side resistance is larger than the maximum applied load, the upward movement curve is extrapolated up to the selected ultimate side resistance by following conventional extrapolation method described in a later section.

The objective of this research is to develop a procedure to minimize the effect of errors due to extrapolation on the resistance factors. Two databases of Osterberg cell load test data on drilled shafts were accumulated for this purpose. One of the databases was collected from Mississippi and the other one was collected from Louisiana. Eight drilled shafts were selected from the two databases based on failure criterion in order to analyze errors occurring from extrapolation. A regression analysis was performed on the load test data of the selected eight shafts in order to develop a relationship to estimate errors due to extrapolation. Following the validation of the regression analysis, the equation developed from the analysis was applied to both of the databases from Mississippi and Louisiana to estimate the bias error in each of the load test cases. Finally, calibration of the resistance factor was performed for both of the databases to check the effect of the correction of the bias on the resistance factor values.

4.2. Construction of Equivalent Top-Down Curve

O-cell is a hydraulic jack that is installed at or near the bottom of the drilled shaft to conduct the O-cell test. Fluid pressure can be applied to the cell through a pipe fixed at the top of the center of the cell. A bi-directional force can be applied to the shaft through the O-cell which causes both

upward and downward movement to the shaft. Tell-tale pipes are used to measure the upward and downward movements. A top movement curve is plotted from the upward movement data, and a bottom movement curve is plotted from the downward movement data. In turn, the top and the bottom movement curves are utilized to reconstruct the top-down curve. It was assumed that the pile body is rigid in Osterberg (1998) to construct an equivalent top-down curve from top and bottom movement curves. Later, this method was improved by taking pile elastic compression in consideration by Loadtest (2001), Kwon et al. (2007) and Lee and Park (2008). Kim and Chung (2012) reviewed and compared the existing methods of construction of equivalent top-down curve.

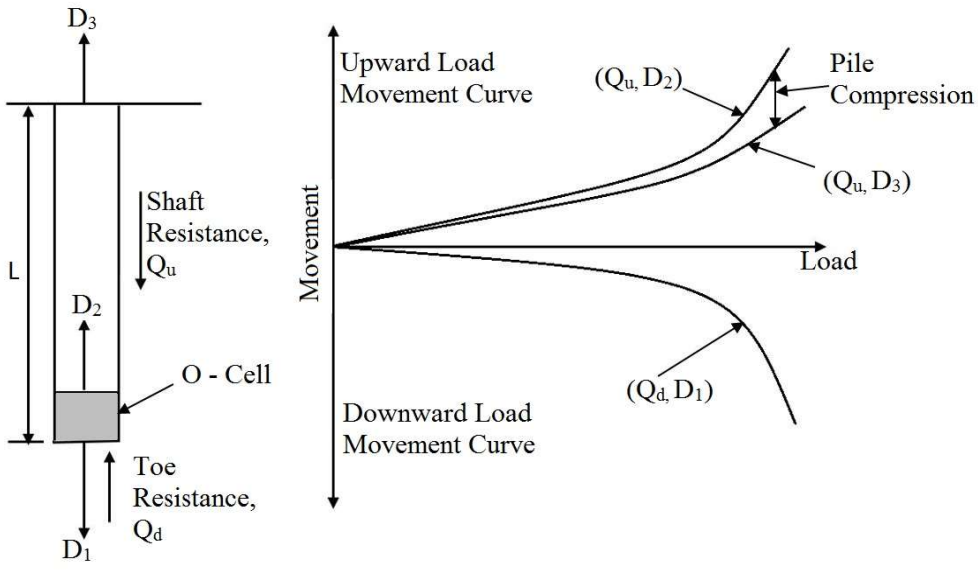

Figure 4 - 1 Load Movement Curves from O-cell Test (Kim and Chung, 2012).

Figure 4 - 1 shows load-displacement curves in an O-cell test: toe resistance (Q_d) vs. shaft tip displacement (D_1), shaft resistance (Q_u) vs. upward shaft tip displacement (D_2), and shaft resistance (Q_u) vs. upward shaft head movement (D_3). Assuming the shaft as a rigid body as considered in Osterberg (1998), the head and bottom of the shaft have the same deflections.

Construction of an equivalent top-down load-displacement curve starts by selecting a random displacement value, and its corresponding resistance values from the top and bottom movement curves, i.e., (Q_d, D_1) and (Q_u, D_2) curves as shown in Figure 4 - 1. Summation of the two resistance values and the displacement is a single point in the displacement vs. total resistance curve without considering elastic compression. The displacement vs. total resistance curve can be plotted following this procedure for different values of displacement. However, the maximum total resistance determined from the above procedure is usually less than the failure load or even less than the proof load, i.e., two times of the design load. Chin's hyperbolic extrapolation method (Ng et al. (2013) described by equation (4-1) is usually used for extrapolation (Ooi et al. 2004).

$$\frac{\rho}{Q} = C_1\rho + C_2 \tag{4-1}$$

Here, ρ is the top or bottom O-cell movement, C_1 and C_2 are the slope and y-intercept, and Q is the drilled shaft load capacity. The displacement determined from the above procedure is for the load applied at the toe. For the top-down load, the load is applied downward at the pile top and cause additional elastic compression of the pile due to the inversed loading direction. Loadtest (2001) prescribed a method to determine the elastic compression by equation (4-2).

$$\Delta = \Delta_d + \Delta_{head} - \Delta_{toe} \tag{4-2}$$

Where,

Δ = Additional pile displacement due to elastic compression,

Δ_d = Pile elastic comprssion due to equivalent top-down load of Q_d,

Δ_{head}= Pile elastic compression due to equivalent top-down load of Q_u,

Δ_{toe}= Pile elastic compression due to upward toe load of Q_u.

4.3. Types of Top and Bottom Movement Curves

Extrapolation of top or bottom movement curves depends on the shape of the curve. After analyzing the top and bottom movement curves from both Mississippi and Louisiana databases, three major types of top and bottom movement shapes were discerned. Figure 4 – 2 presents the types of the top and bottom movement curve shapes.

Type (a) represents the top and bottom movement curves when the upward movement is very small compared to the downward movement. The bottom movement curve may or may not reach the failure load but it has a well-developed shape contrary to the shape of the top movement curve. Type (b) is the exact opposite of type (b). In this case, the top movement has a well-developed shape. The downward displacement is very small compared to the upward displacement. In type (c), both top and bottom movement curves have well-developed shapes. Both of the curves may or may not reach the failure load.

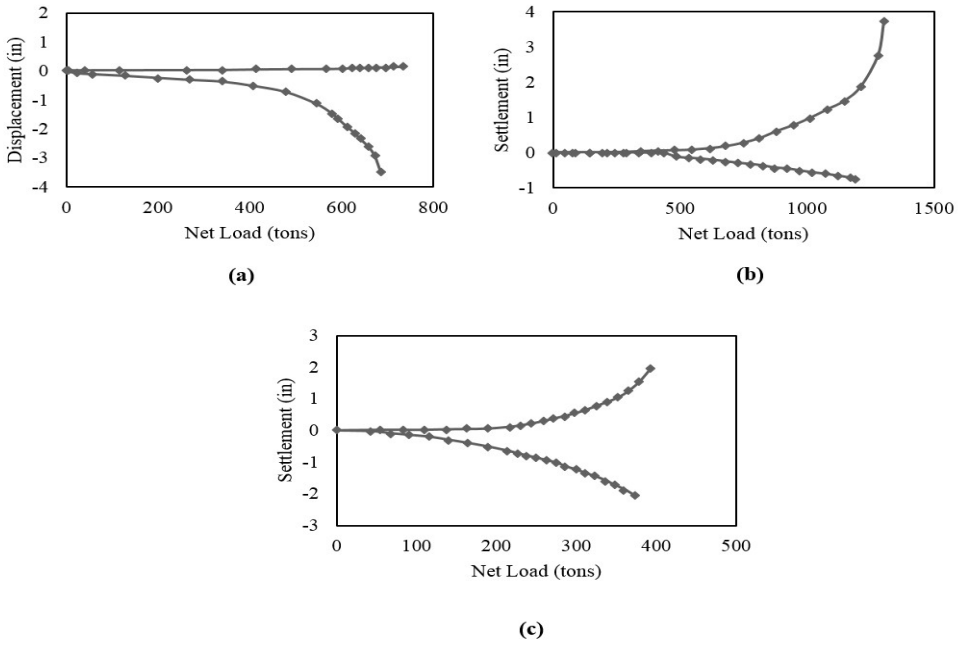

Figure 4 - 2 Types of Top and Bottom Movement shapes.

If the curves don't have well-developed shapes, errors from the extrapolation of the curves are prone to have larger magnitudes. Type (a) and type (b) has underdeveloped top or bottom movement curves, whereas both top and bottom movement curves has well-developed shapes in type (c). So type (c) of the top and bottom movement curves' shapes have smaller errors due to extrapolation. 38% of the Mississippi database and 19% of the Louisiana database have the type (c) top and bottom movement shape. So it can be stated that the Mississippi database will have less extrapolations error than the Louisiana database.

4.4. Bidirectional Load Test Database for Extrapolation Error Analyses

Load tests with measured either tip or side resistance close to failure were selected for extrapolation error analyses. Among the 64 cases, seven drilled shafts from Louisiana and one drilled shaft from Mississippi were identified with the defined failure loads. Table 4 – 1 presents the details of the eight drilled shafts under consideration. For all the eight shafts, the top or bottom movement curves or both of the curves reached 5% B failure. The top and bottom movement curves were extrapolated if the curves did not reach the 5% B failure load. Equivalent top-down curves were constructed from the top and bottom movement curves. From the equivalent top-down curve, the loads corresponding to the 5% B displacement were recorded as the measured resistance in Table 4 - 1. Predicted resistances were attained following the procedure in Brown et al. (2010). In the calculation of nominal resistance, soil properties, including unit weight, water table, internal friction angle for sand, and undrained shear strength for clay, are obtained from the attached soil boring logs. Bias is the ratio of the measured resistance and the predicted resistance.

Table 4 - 1 Summary of the Bi-Directional Database for Extrapolation Error Analyses.

Test Shaft ID	Diameter, D (ft)	Length, L (ft)	5% B Failure Criteria			Extrapolated Curve (Top/Bottom)	Extrapolation Percentage
			Measured Resistance, (tons)	Predicted Resistance, (tons)	Bias, R_m/R_c		
LT-8800-1	4.0	92.5	1673	1836	0.91	Bottom	110%
LT-8412, #1	2.5	49.9	288	286	1.01	Top	270%
LT-8412, #2	3.0	54.1	338	278	1.22	Top	235%
LT-8470	5.5	76.1	1567	1630	0.96	Top	130%
LT-8915	6.0	86.9	1656	1431	1.16	Top	215%
LT-8961, #1	2.5	77.4	931	706	1.32	Top	155%
LT-8961, #2	2.5	65.0	672	627	1.07	Bottom	140%
LT-8944	5.5	40.7	730	571	1.28	Top	113%

4.5. Analyses of Bias Error due to Extrapolation

4.5.1. Extrapolation Analyses

The eight load tests of drilled shaft were used to perform extrapolation analyses to quantify the extrapolation error and its effect on calibration of resistance factors. A database was fabricated based on the selected eight cases by truncating the measured data points in order to perform an analysis on the bias error occurring due to extrapolation (Hasan et al. 2018). Data points acquired from the O-cell test were truncated from the end of the top and bottom movement curves to perform the analysis. The remaining top and bottom movement curves were extrapolated in order to construct the equivalent top-down curves. Analysis procedure for one of the drilled shafts is shown as an example. Figure 4 - 3 shows the extrapolation of top and bottom movement curves.

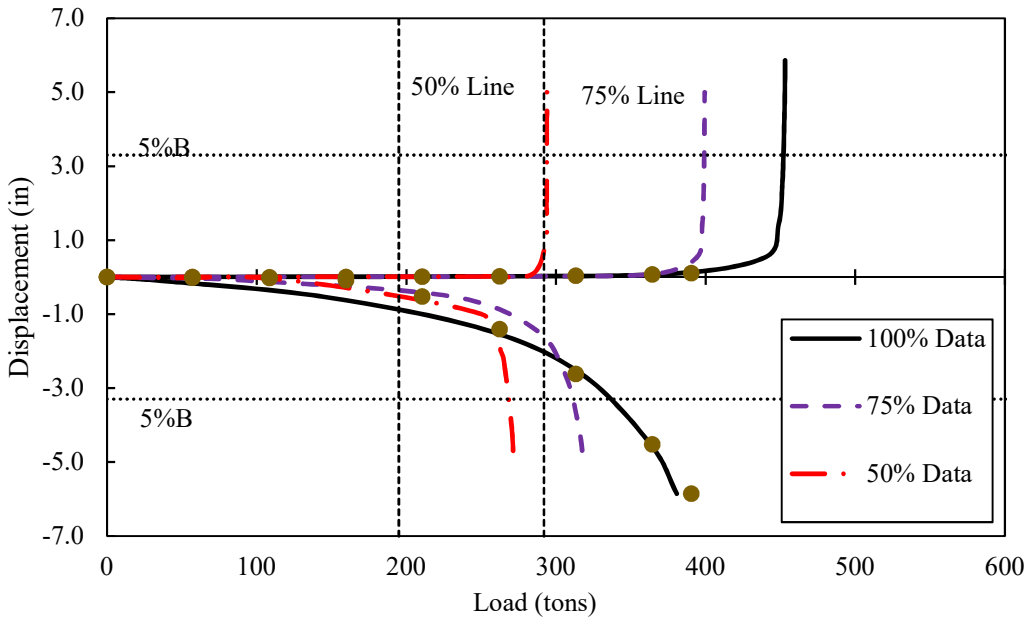

Figure 4 - 3 Extrapolation of top and bottom movement curves based on remaining data points at 100%, 75% and 50% of maximum load.

As shown in Figure 4 - 3, the curves '100% Data' correspond to the extrapolated upward and downward movement curves based on all the measured data points. As all of the eight cases are very close to 5% B failure criterion, little or no extrapolation is required for '100% Data'. These curves are referred as the base upward and downward movement curves. After getting the base upward and downward movement curves, both upward and downward measured data points were truncated by one data point for a new extrapolation. Each extrapolation case was performed on the remaining measured data points. For example, '75% Line' in Figure 4 – 3 corresponds to 75% of the maximum Bi-Directional load in the dataset. '75% Data' corresponds to the curve extrapolated with the data points located only on the left side of the '75% Line'. Data points on the right side of the '75% Line' was truncated. So, 133% extrapolation is required for '75% Data' based on loads. Similarly, '50% Line' in Figure 4 – 3 corresponds to 50% of the maximum load in the dataset. '50% Data' corresponds to the curve extrapolated with the data points located only

on the left side of the '50% Line'. 200% extrapolation is required for '50% Data' based on loads. As a result of the extrapolation analyses, a total of 10 extrapolations excluding the baseline case were obtained for each load test.

Figure 4 - 4 shows the reconstructed top-down settlement curves from the extrapolated top and bottom movement curves. '100% Data' in Figure 4 - 4 corresponds to the reconstructed top-down load settlement curve from the base upward and downward movement curves, i.e. no truncated data. '75% Data' and '50% Data' are the reconstructed top-down settlement curves plotted from the upward and downward movement curves extrapolated from truncated data. The predicted movement was calculated based on FHWA 2010 method (Brown et al. 2010).

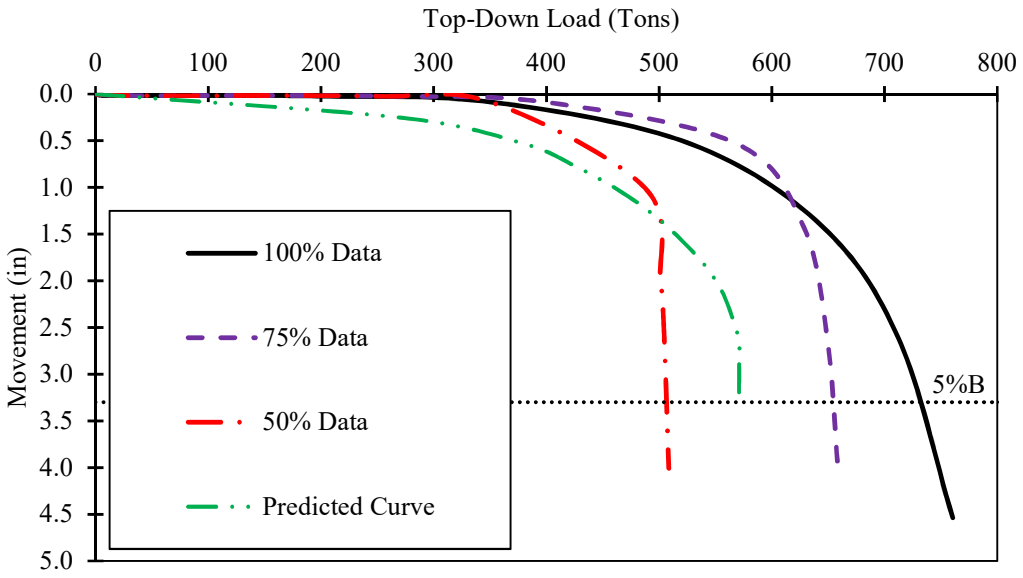

Figure 4 - 4 Reconstructed top-down curve from 100%, 75% and 50% measured data and the predicted movement curve using FHWA 2010 design method.

5% B failure criteria was applied to get the failure loads of the drilled shafts. According to the 5% B criteria, the displacement value equivalent to 5% of the diameter of the shaft is selected

in the plot. The top-down load corresponding to the 5%B displacement is taken as the failure load of the shaft. The procedure of obtaining measured load based on truncated data points was performed for truncation of every 5% of the data points until 50% of the data remained intact. There were ten stages of truncation in total. Here, bias values are compared for only the three stages described previously to present the effect of the extrapolation. As bias is the ratio of the measured resistance to the predicted resistance, it changes with the change in the measured resistance due to extrapolation with truncated data. Statistics parameters, such as mean and standard deviation of the bias values at the three different stages of the truncation of data points were used to perform Monte Carlo simulation in order to estimate the resistance factors.

Table 4 - 1 has the measured resistances and bias values for the whole data set from each of the 8 load tests for 5% B failure criteria. Table 4 – 2 presents the bias values before and after the truncation of the data points. Table 4 – 2 also contains the errors due to extrapolation obtained after the truncation of the data points. Error is the difference between the bias values before and after the truncation.

Estimated resistance factors for 5% B failure criteria are provided in Table 4 - 3. The resistance factors were determined following Monte Carlo simulation utilizing the statistical parameters presented in Table 4 - 3. It can be observed from Table 4 – 3 that the resistance factors decrease with the truncation of data. This decrease in resistance factor values is resulted from the error caused by extrapolation.

Figure 4 - 5 shows the histograms of bias values after truncation of data. For each drilled shaft, 10 extrapolation analyses were performed by truncating data point by 5% of the data and a total 80 extrapolation was obtained excluding the 8 cases without any truncation. Bias errors due

to extrapolation are defined as the difference between the base bias (no-truncation of data) and the bias for each extrapolation case based truncated data.

Table 4 - 2 Bias and error values with 75% and 50% remaining data for 5% B failure criteria.

Shaft ID	Bias (100% Data)	Bias (75% Data)	Error (75% Data)	Bias (50% Data)	Error (50% Data)
LT-8800-1	0.91	0.90	0.01	0.83	0.08
LT-8412, #1	1.01	0.99	0.02	0.92	0.08
LT-8412, #2	1.22	1.21	1.00	1.19	0.03
LT-8470	0.96	0.92	0.04	0.86	0.10
LT-8915	1.16	1.11	0.05	1.01	0.15
LT-8961, #1	1.32	1.34	-0.02	0.63	0.69
LT-8961, #2	1.07	1.04	0.03	0.93	0.14
LT-8944	1.28	1.15	0.13	0.81	0.47

Table 4 - 3 Statistical Parameters and Resistance Factors for 5% B Failure Criteria.

Dataset	Mean	Standard Deviation	Resistance Factor (β =2.33)	Resistance Factor (β =3.00)
100%	1.12	0.15	0.93	0.83
75%	1.09	0.17	0.87	0.77
50%	0.91	0.16	0.69	0.60

Figure 4 - 5 also shows the probability density function for lognormal distribution over the histograms of bias. It can be observed from Figure 4 - 5 that the bias values follow lognormal distribution pretty well. Figure 4 - 6 shows the histograms for the extrapolation errors estimated from the bias values after truncation of data points. Most of the error values are close to 0 (-0.02 to 0.22) which is an indication of good extrapolation. By examining the extrapolated curves, these good extrapolations correspond to Bi-Directional load tests with larger movement (close to failure) and closer fitting of hyperbola function. The larger bias errors correspond to Bi-Directional load

tests with less movement (usually less than 0.1 inches) or sudden jump of measured settlement curves.

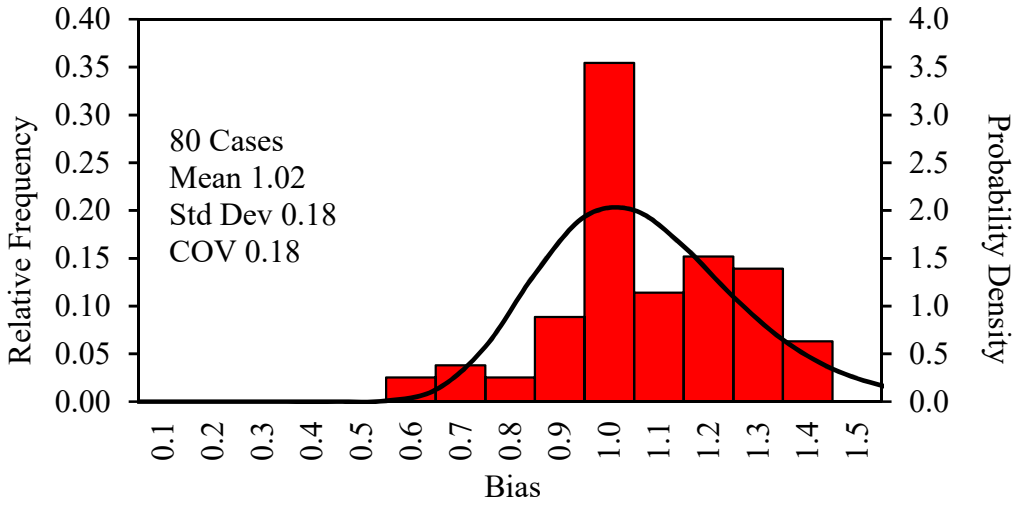

Figure 4 - 5 Bias values at 5% B failure criteria after truncation of data.

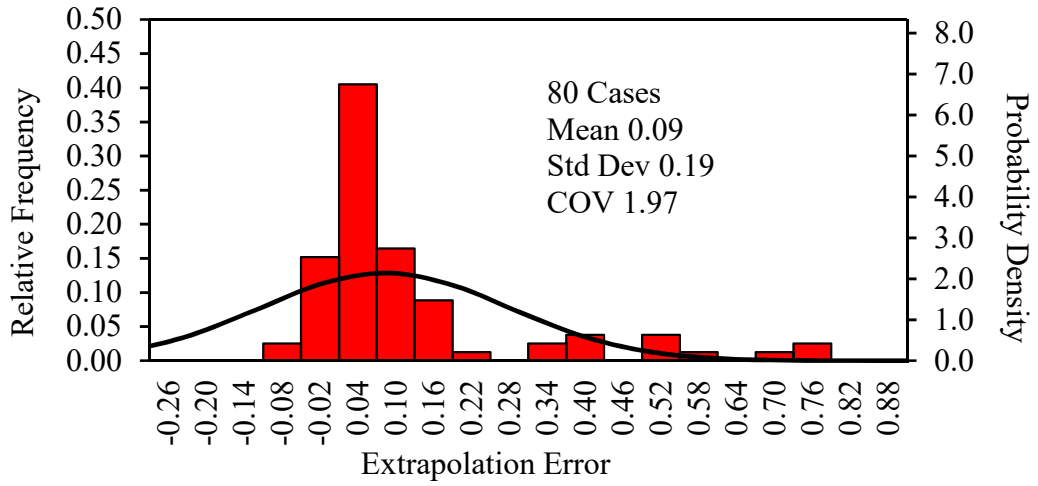

Figure 4 - 6 Errors in bias values at 5% B failure criteria after truncation of data.

4.5.2. Regression Model

Regression analysis can be performed to generate a relationship between the errors and other parameters of the drilled shafts. This relationship will make it possible to estimate the error due to extrapolation for a drilled with O-cell test of less mobilized resistance. The regression analysis was executed based on the general multiple linear regression analysis model from Neter (1983) and Neter et al. (1996). The model is,

$$Y_i = \beta_0 + \beta_1 X_{i1} + \beta_2 X_{i2} + \cdots + \beta_n X_{in} + \varepsilon_i \quad (4\text{-}3)$$

Here, Y_i is the response variable in the i^{th} trial. $X_{i1}, X_{i2}, \ldots X_{in}$ are the independent predictor variables in the i^{th} trial. $\beta_0, \beta_1, \beta_2, \ldots \beta_n$ are the parameters of the model. ε_i is the error at the i^{th} trial. The regression model must follow five conditions to be considered validated. The conditions are linearity of the function, constant variance of the error terms, normal distribution of the error terms, independency of the predictor variables, and absence of outliers with significant effect on the model (Neter, 1983).

4.5.2.1. Regression Variables

As estimating the errors in bias due to extrapolation is the major concern of the analysis under consideration, the bias errors were selected as the response variable i.e. Y_i in the regression model. The predictor variables were selected from the available parameters of the drilled shaft and the O-cell load test results. Primarily, the selected parameters considered for the regression analysis were bias, measured and predicted resistance corresponding to the failure criterion (5% B), maximum applied load, maximum top and bottom displacements, failure displacement (5%

B), diameter of the shaft and length of the shaft. Here, maximum top and bottom displacement values are taken from the top and bottom movement curves after the truncation of data points. Measured resistances are the resistance values corresponding to 5% B, obtained from the equivalent top down curve reconstructed from extrapolated top and bottom movement curves after truncation. Predicted resistances were estimated following the FHWA 2010 drilled shaft design methods (Brown et al. 2010). Maximum applied loads are the maximum bidirectional loads after the truncation of data points. Bias values were also calculated using the truncated data of the load tests. Regression analysis was performed on all the available parameters at the beginning to get a preliminary regression model. The preliminary model was validated against the conditions mentioned above. As it did not conform to all the assumptions, unnecessary variables were removed and the remaining predictor variables were transformed to meet the assumptions. The predictor variables in the final regression model were maximum top displacement, maximum bottom movement, measured load corresponding to the failure criterion, bias values and the 5% of the diameter of the shaft. All the variables including the response variable were transformed to conform to the assumptions. The final regression model that was successfully validated against all the five conditions is shown below.

$$\log(\text{Error} + 0.20) = -1.37 - 0.15\log\left(\frac{\text{Max.Top Movement,in}}{\text{5\% B,in}}\right) - 0.10\log\left(\frac{\text{Max.Bottom Movement,in}}{\text{5\% B,in}}\right) - 0.19\log\left(\frac{\text{Measured Resistance,tons}}{\text{Max.Applied Load,tons}}\right) + \frac{0.60}{\text{Bias}} \quad (4\text{-}4)$$

4.5.2.2. Validation of the Regression Model

To finalize the regression model, some analyses were required to be performed in order to check if the models meet the required conditions. As discussed before, the conditions to be met by a regression model are linearity, constant variance, independency among the predictor variables,

normality and outlier check. The linearity and the constant variance of the model can be checked by performing a residual analysis. Residual values are plotted against each of the predictor variables to check the linearity and constant variance of the model. A correlation analysis can be conducted to check the dependency of the predictor variables on each other. For this, correlation coefficient between all the predictor variables are estimated. Normal probability plot can be prepared to perform a normality check on the regression model to ensure the model follows normal distribution. A cook's distance analysis can be performed to check the effect of the outliers on the model (Neter et al 1996).

Residual analysis was performed to check the linearity and the constant variance of the model. Residual is the difference between the observed response variable and the fitted response variable for i^{th} trial. In order to perform the analysis, the residuals are plotted against the predictor variables as well as the fitted values. Fitted values are the response variables estimated based on the regression model. Figure 4 – 7 shows the residual values against the fitted values estimated from the proposed model. If a curvature or linear trend is found in a residual plots, it can be concluded that the model is not linear. If the data points of a residual plot exhibits a funnel shape, it can be deduced that the error variance is not constant (Neter, 1983). Linearity and Constant variance were achieved by the transformation of the predictor variables as well as the response variables. Residual values were plotted against all the respond variables as well as the fitted values. All the residual plots (not provided due to limited space) exhibited random relationships between the residuals and the respond variables. The fitted values also did not show any linear, curvature or funnel shape against the residuals. It indicates that there is no nonlinearity between the error and respond variables. It also indicates that the residuals have constant variance.

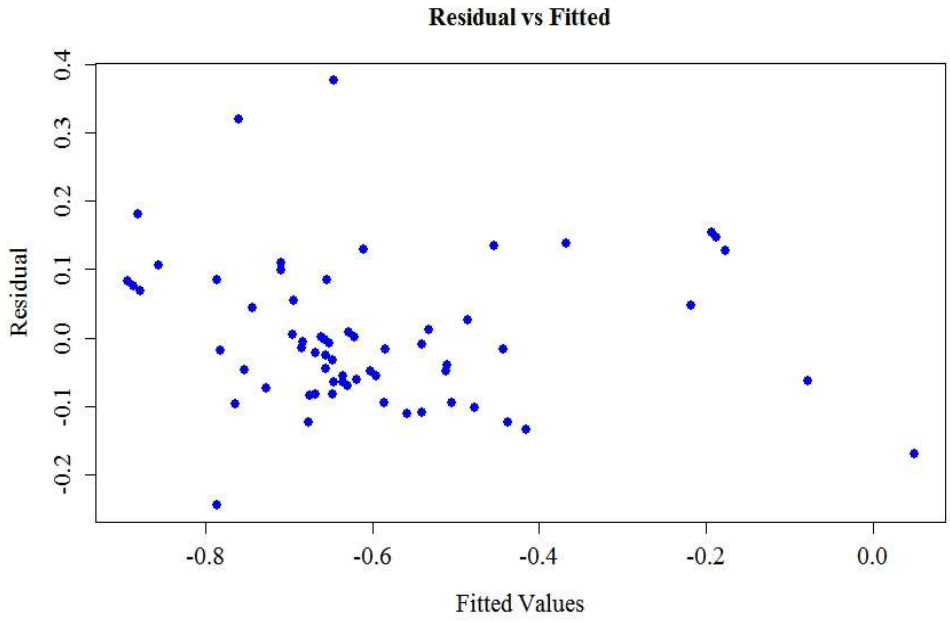

Figure 4 - 7 Residual vs fitted values for the proposed regression model.

It was mentioned earlier that the residuals of a regression model should closely follow normal distribution. To examine the normality of the residuals, a normal probability plot was prepared which presented a fairly linear trend with a few outliers. Figure 4 – 8 presents the normal probability plot. If the normal probability plot follows a linear trend, then the residuals follow normal distribution. On the other hand, if the plot deviates substantially from linearity, then the residuals deviate from normal distribution. If the outliers do not have a significant effect on the regression model, it can be concluded that the residuals follow normal distribution fairly well.

Correlation analysis was performed to estimate the correlation between two variables. If the coefficient of correlation is more than 0.7 between two variables, it can be concluded that there is high correlation between those variables (Neter, 1983). After performing the correlation analysis, coefficient of correlation was found to be less than 0.50 between all the predictor variables. As the model under consideration does not have high coefficient of correlation among

the predictor variables, there is less possibility of multicollinearity. Still it was necessary to ensure that there is no multicollinearity among the predictor variables. Variance Inflation analysis was applied to examine the multicollinearity and it was found that no serious multicollinearity is present among the variables.

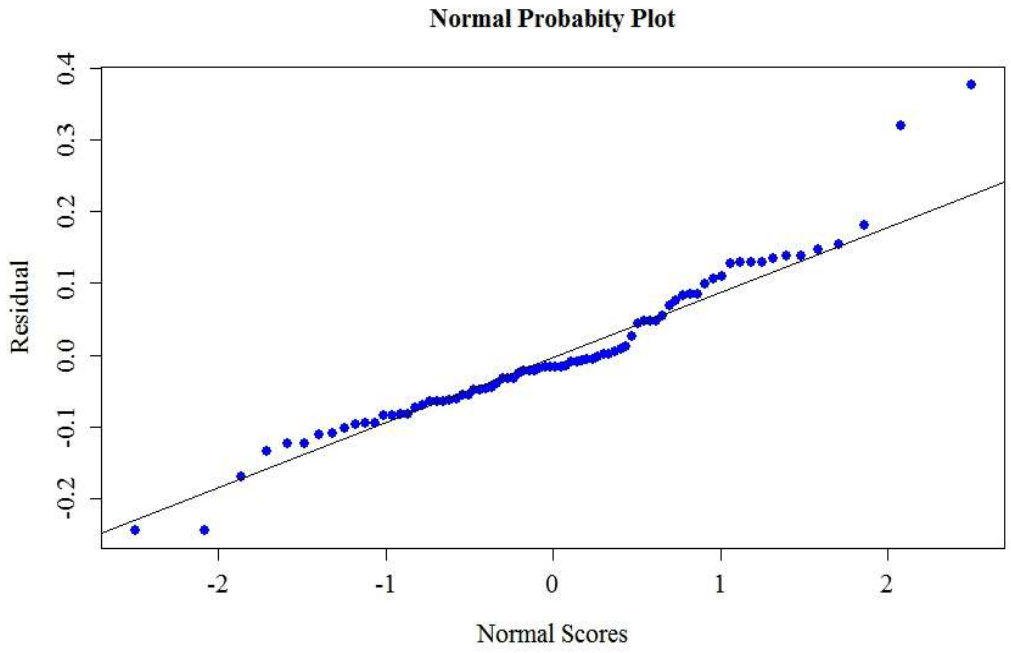

Figure 4 - 8 Normal probability plot for the proposed regression model.

Cook's distance measure was utilized to estimate the presence of outliers and the effect of the outliers on the fitted values. Cook's distance is denoted by D_i, i being the index number of the observation under consideration. Average of cook's distance measures for all the observations was taken. The observations that have cook's distance measures of more than four times of the average cook's distance are considered as outliers. F- Test was used to find out the influence of an outlier on the model. If corresponding percentile value of F (p, n-p) and D_i for an outlier is less than 20 percent, then the outlier under consideration does not have a significant effect on the fitted values. Here, p is the number of regression coefficients and n is the number of observations utilized for

the regression analysis (Neter et al. 1996). The cook's distance measures were estimated for all the fitted values. Figure 4 – 9 presents the Cook's distance values for the 80 cases included in the regression analysis. The maximum cook's distance measure was found to be 0.20. Relating this cook's distance measure to F (5, 75) distribution, the corresponding percentile value was found to be about 4%. So it was concluded that the farthest outlier does not have any significant influence on the regression model.

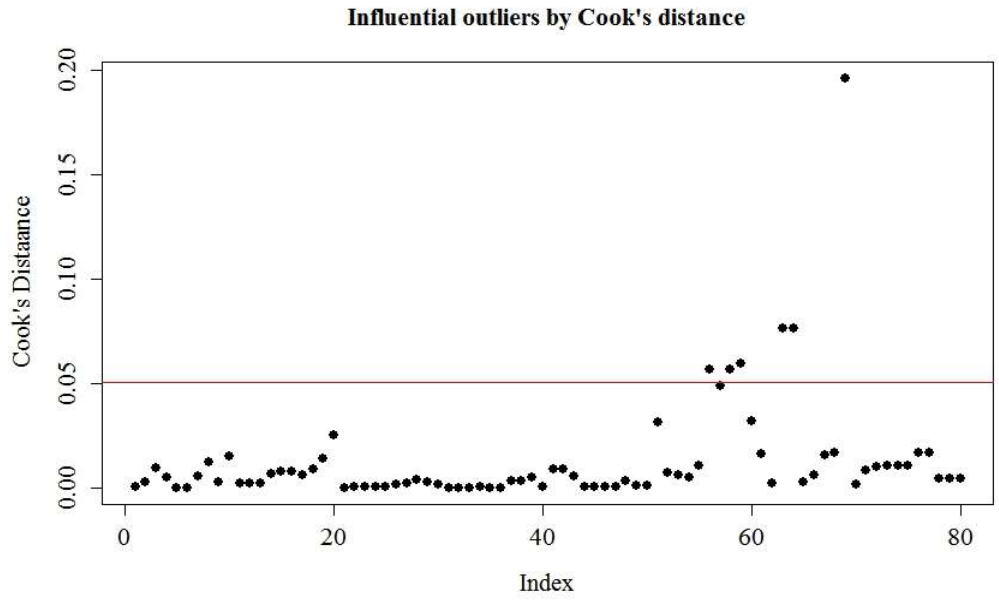

Figure 4 - 9 Check for the influential outliers by Cook's distance.

4.6. Application of the Regression Model

The final regression model was applied on the truncated top and bottom movement curves to estimate the error in the bias values. The estimated error was utilized to calculate the corrected bias which was in turn used to reach the corrected resistance factor values for reliability index values of 2.33 and 3.00. The equation to calculate the corrected bias was,

$$\text{Corrected Bias} = \text{Bias} + \text{Error} \quad (4\text{-}5)$$

Error! Reference source not found.4 - 4 and **Error! Reference source not found.**4 - 5 show the estimation of the error values and the corrected bias values by utilizing the final regression equation. The tables include all the parameters necessary for the regression equation. In these tables, the measured resistances are estimated from the reconstructed top-down curves for each of the drilled shaft load tests. The top and bottom movement curves with truncated data were utilized to reconstruct the equivalent top-down curves and the resistance values corresponding to the 5% B displacement were taken as the measured resistance. The bias values are the ratio of the measured resistance from extrapolated data to the predicted resistance values. The maximum top movement is the maximum displacement value taken from the truncated top movement curve without extrapolation. Similarly, the maximum bottom movement is the maximum displacement value taken from the truncated bottom movement curve without extrapolation. 5% B denotes to the displacements equal to the 5% of the diameter of the shaft. Error in bias values were calculated based on equation 10. Corrected bias values were estimated using equation 4 - 5.

Table 4 - 4 Estimation of error and corrected bias for 25% truncated top and bottom movement curves.

Shaft ID	Measured Resistance (tons)	Bias	Max. Applied Load (tons)	Max. Top Movement (in)	Max. Bottom Movement (in)	5%B (in)	Error in Bias	Corrected Bias
LT-8800-1	1661	0.90	675	0.340	1.51	2.4	0.006	0.91
LT-8412, #1	284	0.99	65	0.050	1.08	1.5	0.074	1.07
LT-8412, #2	337	1.21	86	0.026	1.57	1.8	0.024	1.24
LT-8470	1503	0.92	677	0.100	3.81	3.3	0.035	0.96
LT-8915	1583	1.04	413	0.013	1.19	3.6	0.081	1.12
LT-8961, #1	947	1.34	254	0.110	0.79	1.5	-0.063	1.28
LT-8961, #2	654	1.04	143	0.220	0.50	1.5	0.001	1.04
LT-8944	654	1.15	294	0.040	2.62	3.3	0.043	1.19

Table 4 - 5 Estimation of error and corrected bias for 50% truncated top and bottom movement curves.

Shaft ID	Measured Resistance (tons)	Bias	Max. Applied Load	Max. Top Movement (in)	Max. Bottom Movement (in)	5% B (in)	Error in Bias	Corrected Bias
LT-8800-1	1530	0.83	450	0.100	0.780	2.4	0.090	0.92
LT-8412, #1	264	0.92	43	0.030	0.270	1.5	0.184	1.11
LT-8412, #2	331	1.19	57	0.020	0.980	1.8	0.049	1.24
LT-8470	1398	0.86	451	0.070	2.700	3.3	0.090	0.95
LT-8915	1445	1.01	275	0.007	0.440	3.6	0.157	1.17
LT-8961, #1	445	0.63	169	0.040	0.270	1.5	0.469	1.10
LT-8961, #2	582	0.93	95	0.100	0.070	1.5	0.132	1.06
LT-8944	462	0.81	196	0.010	0.529	3.3	0.403	1.21

Figure 4 - 10 compares the bias values with complete dataset to the bias values with 75% and 50% data as well as the bias values after correction of the bias errors to extrapolation. Figure 4 - 10 shows a band that encompass 5% of the actual bias values at both sides of the line connecting the actual bias values. It can be observed that the corrected bias values fall between the bands except one single case. LT-8961#1 has a large difference between the corrected and the actual bias values because this case has a sudden shift in the top and bottom movement curves. It can be concluded from the aforementioned results of the extrapolation error analysis that the regression model can reasonably estimate the bias errors due to extrapolation unless there is any unusual shapes in the load test results.

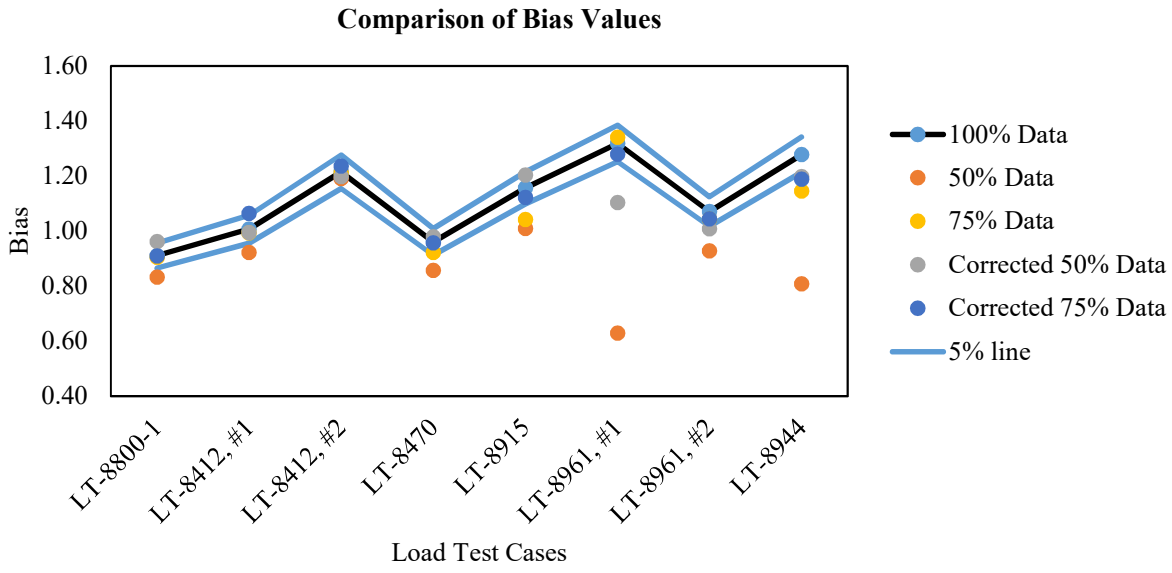

Figure 4 - 10 Comparison of bias values at different phases of the analysis.

Table 4 - 6 presents the comparison between the resistance factors before and after the truncation of top and bottom movement curves. It can be observed from **Error! Reference source not found.** 4 - 6 that the truncation of top and bottom movement curves causes the resistance factors to decrease due to the extrapolation errors. If the regression equation is applied on the

truncated data, the resistance factors increases very close to their original values. To get the resistance factor values, mean and standard deviation of the bias values were calculated for each step of the truncation. The estimated mean and standard deviation were used to perform a Monte Carlo simulation as previously described which provided the resistance factor values for all the steps of truncation of data points.

Table 4 - 6 Comparison of resistance factors before and after correction.

Truncation	Reliability Index	Resistance Factor	Corrected Resistance Factor
0%	2.33	0.93	-
	3.00	0.83	-
25%	2.33	0.87	0.93
	3.00	0.77	0.84
50%	2.33	0.69	0.94
	3.00	0.60	0.85

So, it can be declared that the regression equation can be utilized to reduce the errors due to extrapolation in resistance factors. To check the effect of the equation on the Mississippi and the Louisiana database, the regression equation was applied on both of the databases. **Error! Reference source not found.** 4 - 7 and **Error! Reference source not found.** 4 - 8 present the effect of the regression equation on both of the databases.

It can be observed from **Error! Reference source not found.** 4 - 7 and **Error! Reference source not found.** 4 - 8 that the regression equation increases the resistance factors of both the databases by reducing the errors due to extrapolation. To check the extrapolation level in both Mississippi and Louisiana databases, an analysis was performed by estimating the ratio of the displacement value corresponding to 5% B to the maximum displacement occurred due to applied

bidirectional load. The ratio was estimated for both top and bottom movement of the shaft due to load test.

Table 4 - 7 Effect of regression equation on the resistance factors of the Mississippi database.

Soil Properties	MS Database				
	Cases	RI = 2.33		RI = 3.00	
		Resistance Factor	Corrected Resistance Factor	Resistance Factor	Corrected Resistance Factor
Sand 2010	17	0.35	0.44	0.23	0.31
Clay 2010	14	0.55	0.63	0.38	0.45
Sand 1999	5	0.55	0.70	0.42	0.55
Clay 1999	5	0.73	0.83	0.52	0.63
Sand IGM 1999	14	0.34	0.43	0.22	0.32
Clay IGM 1999	9	0.53	0.61	0.37	0.43
Sand +Clay 1999	9	0.62	0.72	0.44	0.53
Whole	34	0.48	0.56	0.33	0.41

Table 4 - 8 Effect of regression equation on the resistance factors of the Louisiana database.

Soil Properties	LA Database				
	Cases	RI = 2.33		RI = 3.00	
		Resistance Factor	Corrected Resistance Factor	Resistance Factor	Corrected Resistance Factors
Sand 2010	18	0.60	0.79	0.48	0.68
Clay 2010	12	0.63	0.75	0.55	0.66
Sand 1999	15	0.60	0.78	0.50	0.68
Clay 1999	13	0.68	0.77	0.52	0.63
Sand IGM 1999	5	0.50	0.72	0.4	0.63

Clay IGM 1999	1	-	-	-	-
Sand +Clay 1999	25	0.66	0.75	0.54	0.65
Whole	30	0.63	0.77	0.51	0.66

It was observed from the analysis, both of the databases needed about 1700% of extrapolation of the top movement curves in average to reach the failure criteria. Also, both of the databases needed about 300% of extrapolation of the bottom movement curves in average. So, both of the databases needed similar level of extrapolation. After the correction in the bias values for the error occurring from the extrapolation, the amount of improvement in the resistance factors for both of the databases were found to be similar.

It can be observed in Table 4 -7 and 4 – 8 that the resistance factors are similar for Sand 1999, Clay 1999 and Sand + Clay 1999. Sand IGM and Clay IGM have less resistance factors in Mississippi database which is decreasing the resistance factors for the Mississippi database.

It can be concluded after scrutinizing the effect of the regression equation to estimate bias error on the Mississippi and Louisiana database that a regression analysis can be a good way to improve the resistance factor values for calibration of LRFD design of drilled shafts. The recommended regression equation can be used for a calibration approach for resistance factors if the collected database has bidirectional load test data performed on drilled shafts and the subsurface condition is similar to the databases mentioned in this study.

4.7. Summary

The objective of this research was to look for a way to minimize the effect of errors due to extrapolation on the calibration of resistance factors. Eight drilled shaft load test cases were selected for this study from out of 64 cases collected in Mississippi and Louisiana. The data points

in the top and bottom movement curves of the selected eight cases were truncated systematically in order to carry out a statistical analysis. Equivalent top-down curves were reconstructed for each of the steps of the truncation of the data points. There were 80 truncated equivalent top-down curves fabricated from the truncated top and bottom movement curves of the selected eight cases. It was found that the increase in the amount of extrapolation decreased the resistance factors by up to 0.22. These eighty fabricated cases by truncation were used to perform a regression analysis and finally, a regression equation was proposed with the ability to estimate the bias error occurring from the extrapolation of top and bottom movement curves. The proposed regression equation was validated statistically. The usability of the equation was also checked against the eight cases with truncated data and it was found that the equation was able to estimate the actual resistance factors of the eight cases before truncation. The proposed regression was also used to estimate the corrected bias values for all the cases included in the databases from Mississippi and Louisiana. It was found that the corrected bias values of both of the databases resulted in improved LRFD calibration of resistance factors through a decrease in standard deviation of the bias values. So, it can be concluded after the analysis that it is possible to minimize the effect of the errors by constructing regression relationships. The suggested regression equation can be utilized to estimate the errors occurred from extrapolation of the top and the bottom movement curves. The error values can be applied to calculate the corrected bias values and in turn, calibrated to estimate corrected resistance factors.

The general subsurface condition of the database collected for this study mainly consisted of sand and clay. It did not include any rock. As the load-settlement behavior of drilled shaft in rock will be different from in sand or clay, the proposed regression will not work accurately for drilled shafts in rock. If a database includes O-cell load tests on drilled shafts located in rock, a

regression analysis can be performed including the behavior of the rock in the database to get better relationships to estimate the error occurring from extrapolation. It was also observed in the analysis that IGM soils can result in lower resistance factors. Further analysis on load tests performed on drilled shafts located in IGM may improve some uncertainties in the LRFD calibration of resistance factor of drilled shafts in IGM soils.

Chapter 5

FINITE ELEMENT MODELING

5.1. Introduction

Load and resistance factor design (LRFD) has become increasingly popular over allowable stress design (ASD) for several decades. While the LRFD method considers load factors as well as resistance factors to be applied to the limit state inequalities, the ASD method combines both of the factors into one single factor of safety. Consideration of two separate factors for load and resistance has made the LRFD method more consistent than the ASD method (Abu Farsakh et al. 2010). After the publication of the first edition of AASHTO LRFD Bridge Design Specifications, the major challenge was to make the transition from ASD to LRFD. To begin the transition from ASD to LRFD, the Federal Highway Administration (FHWA) released a policy in 2000 that required all new federally-funded bridges to be designed using the AASHTO LRFD specifications by October 2007 (Fortier, 2016). Despite this steady progression into LRFD, however, deep foundation design still does not take full advantage of the probabilistic framework in many parts of the United States due to a lack of area-specific resistance factors derived using reliability theory–based calibrations. Instead, many regions rely on values given in specifications from AASHTO (2014) which were developed by fitting to allowable state design (ASD) safety factors (Stanton et al. 2017). Studies like Abu-Farsakh et al. (2012), Long et al. (2009), Roling et al. (2011), Garder et al. (2012), Rahman et al. (2002), and McVay et al. (2005) were performed with an objective of calibrating region wise load and resistance factors for foundation design.

The results from the studies performed for region based LRFD calibration of resistance factors varied from the resistance factors recommended by AASHTO (2012) in most cases. In order to find out the reasons behind the difference between the resistance factors among different studies, several new studies were performed on the possible sources of uncertainties in the LRFD calibration procedure. The major sources of uncertainties affecting the LRFD calibration of resistance factors are foundation types, subsurface condition, type of load test, interpretation of load test result, effect of outlier load test cases etc. To observe the effect of subsurface condition, LRFD calibration can be performed separately for different types of soils. Outlier load test cases basically depend on the collected database in order to perform the calibration analysis. Interpretation of load test results depend on the type of load test performed on the deep foundation. The scope of this study includes uncertainties occurring form the interpretation of load test data for bidirectional load tests performed on drilled shafts.

For bidirectional load test, a jack like device, often termed as Osterberg cell or O-cell, is installed at or near the bottom of a drilled shaft. A bidirectional load is applied on the drilled shaft from the jack like device, which causes the mobilization of side resistance and tip resistance of the drilled shaft. From the result of the load test, an upward movement curve representing the side resistance and the corresponding displacement as well as a downward movement curve representing the tip resistance and the corresponding displacement can be obtained. The upward and downward movement curves are also termed as top and bottom movement curves, respectively. An equivalent top-down curve is developed from the top and the bottom movement curves, which is equivalent to the load-settlement curve obtained from a conventional static load test. The top and bottom movement curves obtained from a bidirectional load test does not always reach the failure load. In order to develop the equivalent top-down curve, it is necessary to

extrapolate the top and the bottom movement curves to ensure that the curves reach the failure load. As the method of extrapolation is prone to developing errors, extrapolation of the top and the bottom movement curves can result in some level of erroneous estimation of the failure load of the drilled shafts, which in turn, will also affect the LRFD calibration of resistance factors for drilled shafts. Several studies were performed to investigate the errors occurring from the extrapolation of the top and the bottom movement curves.

Paikowsky and Tolosko (1999) conducted a study on the extrapolation of non-failed load tests performed on driven piles. A non-failed load test is a type of load test in which, a load equivalent to a given factor times the design load is applied on the pile. In case of a non-failed load test, extrapolation is required to be performed in order to estimate the measured load beyond the applied load in the load test. Paikowsky and Tolosko (1999) recommended a procedure to practically estimate the measured resistance based on extrapolated load-settlement curves. They compared the proposed method with two other possible methods i.e. Chin's method (Chin, 1971) and Brinch-Hansen method (Brinch-Hansen, 1963). To carry out the study, they collected database of 63 driven piles with conventional static load test data performed to the failure point. In the study, it was assumed that the data points of the load tests were known up to 25%, 33%, 50%, 75% and 100% of the bearing capacity as well as the maximum applied load. The assumed known data was extrapolated based on the three methods and the results were compared to the actual capacity of the driven piles. Statistical analysis was performed on the results to estimate the reliability of the proposed methods. It was noticed from the study that Chin's method significantly over predicts the failure load even when 100% data is used to estimate the failure load. Brinch-Hansen method can close estimate the failure load when requirement for extrapolation is very little. On the other hand, this method over predicts the failure load by about two times the actual load when the amount

of extrapolation is significant. Also, the extrapolation method proposed by Paikowsky and Tolosko (1999) underestimates the extrapolated failure load compared to the actual failure load.

Ooi et al (2004) conducted a study for the extrapolation of non-failed test performed on drilled shafts. They used a load test data for drilled located in the island of Oahu in Hawaii supporting the H-3 freeway viaduct. Truncation of the data points collected from the load test data was performed and six different extrapolation techniques were utilized to estimate the failure loads. More reliable of the six different techniques were recommended by Ooi et al (2004). They also discussed about the limitations of the techniques to extrapolate the load-settlement curves achieved from the load tests. The objective of the study was to improve the confidence in using the extrapolation methods to estimate measured loads from non-failed tests. The six methods considered for the extrapolation in this study are, A) Chin's method, B) Brinch-Hansen 80% criterion, C) Brinch-Hansen's polynomial method, D) Chin's/Davisson's method, E) Brinch-Hansen 80% criterion/Davisson's method and F) Brinch-Hansen's polynomial/Davisson's method. In the first three methods, the failure loads are estimated based on the equations for Chin's method, Brinch-Hansen method and Brinch-Hansen's polynomial method. For the last three methods, the failure loads are estimated from the intersection points of the extrapolated load-settlement curves based on the corresponding methods and the offset line of the Davisson's criterion. To perform the study, the data points were truncated consecutively in between the elastic line and the offset line from Davisson's criteria. The analysis was conducted for 100%, 75%, 50% and 25% data coverage. The data coverage was estimated by $\frac{\delta_{max}-\delta_{ec}}{\delta_0-\delta_{ec}}$, where, δ_{max} is the maximum displacement value in the load-settlement curve, δ_{ec} is the displacement value at the intersection of the load-settlement curve and the elastic line and δ_0 is the displacement value at the intersection of the load-settlement curve and the offset line. The failure loads were estimated from

the extrapolated load-settlement curve for each of the steps of the truncation using all six aforementioned methods. The estimated failure loads from extrapolated load-settlement curves were compared to the actual failure load by estimating the capacity ratio between the extrapolated failure load and the actual failure load. It was observed from the study that methods D, E and F estimated the failure loads in a narrower range compared to method A, B and C. Methods E and F over predicted the failure loads of the drilled shafts by about 36% of the actual loads. Method D over predicted the failure load by about 17%. Also, method D has smaller standard deviation value than method E and F.

Ng et al. (2013) proposed an improved procedure to develop the equivalent top-down curve from the top and the bottom movement curves achieved from bidirectional load tests performed on drilled shafts. They performed the study on the database mentioned in Garder et al. (2012). The database consisted of 41 drilled shaft load test cases collected from 11 states, 28 of which were usable for the study. The study used the approach recommended by Loadtest Inc (2006) to develop the equivalent top-down curves from the top and the bottom movement curves. They proposed a method for the top and the bottom movement curves to reach the failure load. Based on the proposed procedure, the study estimated the measured loads and the predicted loads and finally, performed LRFD calibration of the resistance factors. Ng et al. (2013) recommended an improved procedure to develop the equivalent top-down curve based on three different load-settlement behavior scenarios. Case A was defined as the scenario, when the side resistance reaches the failure load before the tip resistance and Case B occurs when tip resistance reaches the failure load before the side resistance. Case C occurs, when neither side resistance nor tip resistance reaches the failure load. For the estimation of ultimate side resistance according to Ng et al. (2013), if there's excessive upward movement with little increase in the load value, the side resistance value is

limited to the maximum upward applied load. Then it's compared to the structural capacity, which is estimated based on AASHTO Specifications (2012). The smaller value between the O-cell load and the structural capacity is selected as the ultimate side resistance. For case A, tip resistance does not reach the ultimate value. If the tip is not located in rock, the maximum downward applied load is compared to the ultimate tip resistance estimated based on static analysis methods (O'Neil and Reese, 1999) and the larger value is selected. The selected tip resistance is then compared to the structural capacity. If the selected tip resistance is smaller than the structural capacity, the bottom movement curve is extended to the larger value between the estimated tip displacement and the extrapolated displacement. The estimated tip displacement can be obtained by Vesic (1977) for all soils, O'Neill and Reese (1999) for cohesive IGM, Mayne et al. (1993) for cohesionless IGM and Kulhawy et al. (1992) for rock. If the structural capacity is smaller than the selected tip resistance, then the bottom movement curve is extended to the structural capacity. If the side resistance does not reach the ultimate value, the top movement curve can be extended in a similar procedure. The measured resistance values for each of the drilled shafts were estimated by following the aforementioned procedure. Ng et al. (2013) also conducted a LRFD calibration of resistance factors for drilled shafts. The modified FOSM method of calibration was utilized for the estimation of the resistance factors. The Anderson-Darling (1952) method was used to find out the type of distribution of the bias values obtained from the collected load tests. The statistical parameters for the load factors were collected from AASHTO (2010). The dead load live load ratio was assumed to be 2.0. A range of target reliability index values were selected including 2.00, 2.33, 2.50, 3.00 and 3.50.

In chapter 4, a study was performed to investigate the error in estimating the failure load occurring from the extrapolation of the top and the bottom movement curves. For the investigation,

a load test database on drilled shafts was accumulated from Louisiana and Mississippi. Out of 64 drilled shaft cases in the database, 8 cases were selected for the study. For each of the eight cases, the top and the bottom movement curves were truncated systematically. The truncation was performed 10 times on each of the drilled shaft cases. At each step of truncation, data points for 5% of the total applied load were removed. Also, the equivalent top-down curve was developed for each step of truncation for all the eight drilled shaft cases included in the study. The equivalent curves developed from the truncated top and bottom movement curves were compared to the equivalent curves developed from the original top and bottom movement curves in order to estimate the errors occurring from the extrapolation of the top and the bottom movement curves. The errors were estimated in terms of the resistance bias values. Bias is the ratio between the measured load and the predicted load for a particular drilled shaft case. Measured load is the failure load obtained from the equivalent top-down curve corresponding to a failure criteria. Hasan et al. (2018) utilized the 5%B failure criteria, which is the load corresponding to a displacement value of 5% of the diameter of the shaft. Predicted resistances were estimated based on the methods described in Brown et al. (2010). The errors in the bias values were estimated for 80 truncation cases. The statistical parameters for the estimated errors were calculated. In Chapter 4, a regression analysis was performed on the truncated database of 80 cases and proposed an empirical relationship to estimate the error in the bias values occurring from extrapolation of the top and the bottom movement curves. The empirical relationship was consisted of maximum top displacement, maximum bottom displacement, measured load, maximum applied load, 5% of the diameter of the shaft and the bias values as the predictor variables. Based on the proposed regression equation, it is possible to approximate the error in resistance bias values and estimate the corrected bias values. A study was also performed a LRFD calibration of the resistance factors based on the corrected

resistance bias values of the drilled shafts included in the database collected from Louisiana and Mississippi. It was observed from the calibration result that the resistance factors increased significantly after the consideration of the corrected resistance bias values in the Calibration procedure.

Though very studies were performed on numerical simulation of a whole database, several studies were performed for a single or more cases of numerical simulations of load tests performed on drilled shafts. Viktor Limas and Rahardjo (2015) performed a study, in which, numerical simulations were performed for both bidirectional load test and conventional static load test conducted on a bored pile in order to compare the results. The bored pile under consideration was 1500 mm in diameter and 50 m in length. PLAXIS 2D was utilized to perform the simulations. The simulation was based on an axisymmetric model. The soil materials were developed based on Mohr-Coulomb model with 15-nodes elements. Properties of the soil materials were selected from laboratory tests. Then a back analysis was performed by changing the values of stiffness and interface to match the simulated top and bottom movement curves with the top and bottom movement curves obtained from field results. After the completion of the simulation, it was observed that the simulated equivalent top-down curve was very close to the top-down curve obtained from the field load test.

El-Mossallamy (2016) also performed a numerical simulation of a bidirectional load test on a bored pile in order to compare the results to the field conventional static load test results. PLAXIS 2D was also utilized in this case for the simulation. Axisymmetric model was used to develop the simulation. Mohr-Coulomb model was used to simulate the soils and linear elastic model was utilized to simulate the drilled shaft material. To simulate the soil to pile material, an interface element was introduced along the length of the pile. The interface element was extended

beyond the tip of the pile by 0.5 m in order to avoid high stress and strain arising from the corner of the pile. The O-cell, which is the jack used to apply the bidirectional load, was simulated by solid element of 10 cm thickness. When the O-cell was inactive, it was assigned the same properties as the pile material. On the other hand, when the O-cell was active, it was kept as a void. A horizontal fixity was introduced to avoid lateral displacement at the location of the void. In this case also, back analysis was implemented to obtain the top and the bottom movement curves. The study resulted in a close match between the simulated equivalent top-down curve and the top-down curve obtained from field load test.

Bui et al. (2005) also performed a back analysis of bidirectional load test by finite element method using PLAXIS 2D. In this case also, the O-cell was simulated by a 10 cm thick element, which was assigned to have the same material as the pile while inactive. When active, the 10 cm O-cell material was assigned a very low stiffness value compared to the stiffness of the pile material, in order to ensure the upward and downward displacement of the pile. Four levels of loading the O-cell was performed in the simulation instead of the 34 levels of loading performed in field load test. The simulated top and bottom movement curves were matched with the curves obtained from the field load test and extrapolation of the top and bottom movement curves were executed to develop the equivalent top-down curve.

The objective of this study is to investigate the effect of numerical simulation of the bidirectional load tests to minimize the effect of errors occurring from the extrapolation of top and bottom movement curves. The databased utilized by Hasan et al. (2018) is also used for this study. Out of 64 drilled shaft cases included in the database, bidirectional load test was performed on 60 of the cases. Numerical simulation of these sixty bidirectional load tests is performed by PLAXIS 2D. In each of the simulated bidirectional load tests, load is applied on the drilled shafts until the

top and the bottom movement curves reach the failure load corresponding to 5% of the drilled shaft diameter (B). The measured load is obtained for each of the drilled shafts from the equivalent top-down curve developed from the simulated top and bottom movement curves. A LRFD calibration of resistance factors is performed based on the simulated database. Finally, the results are compared to the resistance factors achieved in Chapter 4.

5.2. Finite Element Modelling Using PLAXIS 2D

PLAXIS 2D is a tool to perform deformation and stability analysis of various types of geotechnical structures by finite element modelling. The soil layers and geotechnical structures can be graphically inserted in the model to perform a finite element modelling. The properties of different types of soils can be easily assigned to the soil layers. Defining various construction stages and assigning loads and boundary conditions in the model allows a detailed analysis of a wide range of geotechnical problems.

In PLAXIS 2D, two types of finite element models can be developed, i.e. plain strain model and axisymmetric model. Plain strain model is usually utilized for geotechnical structures with uniform linear cross-section and the presence of corresponding stress state and loading condition situated over a certain length perpendicular to the uniform cross-section. Axisymmetric model can be utilized for a structure with uniform radial cross section. The loading scheme is supposed to be situated around the central axis of the cross section. Any displacement and stress state are presumed to be similar at any radial direction. The finite element modelling of a pile should be developed based on an axisymmetric model (Li Yi, 2004).

To develop the model for deformations and stresses occurred in soil, quadratic 6-node triangular element and 4th order 15-node triangular element can be obtained in PLAXIS 2D. A

second-order interpolation is yielded by the 6-node triangular element and a fourth-order interpolation is yielded by the 15-node triangular element. If there is an interaction between two types of materials in the model, an interface is required to be assigned along the length of the interaction between the two materials. For example, an interface is needed to be assigned along the length of the drilled shaft, where the shaft material interacts with the soil. For 6-node triangular elements of soil, three pairs of nodes are used to define the interface elements. In case of 15-node triangular elements of soil, five pairs of nodes define the interface elements. The basic properties of interface elements correspond with the properties of the soil and the interacting material. The interface strength depends on the surface friction of the structure and adhesion.

There are several models available in PLAXIS 2D to define the soil and other material properties present in a finite element model. Some of the models are linear elastic model, Mohr-Coulomb model, Hoek-Brown model, hardening soil model. For this study, Mohr-Coulomb model will be mostly used to define the soil properties. Also, linear elastic model is going to be utilized to define the drilled shaft materials. Utilizing the Mohr-Coulomb model requires five parameters of soil, which are cohesion, internal friction angle, dilatancy angle, Young's modulus and Poisson's ratio. Dilatancy angle will be ignored in this study to define the soil properties. Linear elastic model basically requires the Young's modulus and Poisson's ratio to define the drilled shaft material.

The generation of finite element mesh can be achieved in a completely automated way. Unstructured meshes are generated based on a triangulation method. The generated mesh can be 'very coarse', 'coarse', 'medium', 'fine' or 'very fine' based on the average element size. For this study, the generated meshes will be ranging from medium to very fine.

It is possible to change the geometrical arrangements by activating or deactivating clusters assigned as soil layers or structural components in PLAXIS 2D. This feature allows the performance of the simulation of the installation of a drilled shaft in the necessary location by changing the soil material into drilled shaft material. The material properties and pore pressure distribution can also be changed at each stage. The program also ensures an accurate and realistic simulation of the actual construction stages such as the loading stages by increasing or decreasing the applied load from the O-cell.

5.3. Database

A database consisting of 64 load tests on drilled shafts was accumulated from Abu Farsakh et al. (2013) and Fortier (2016). Out of the 64 shafts, 30 drilled shafts are located in Louisiana and 34 shafts are located in Mississippi. O-cell load test was performed on 60 of the drilled shafts in the collected database. Conventional static load test was performed on only 4 of the drilled shafts. Almost all of the drilled shafts with O-cell load test needed extrapolation of the top or bottom movement curves in order to get the top-down curve. All of the drilled shafts in the collected database are part of bridge foundations. Some of the shafts are located under water. According to the soil classification of Brown et al. (2010), the database have 35 drilled shafts with a majority of the surrounding soil being sand. Rest of the 29 shafts have clay as the dominating soil material to affect the shaft resistance. Based on the soil classification from O'Neil and Reese (1999), there are 29 drilled shafts located in cohesive and cohesionless IGM, 23 of which are in the database from Mississippi. The drilled shafts in the database were constructed by dry or wet method. Out of 64, 34 of the shafts were constructed by wet method and 15 were constructed by dry method. Constructed method of 15 of the shafts were not available. To calibrate the resistance factors, bias

values were obtained for each of the drilled shaft load tests. As it was mentioned before, bias is the ratio of the measured resistance and the predicted resistance. Measured resistances were obtained from the load test results for each case. Predicted values were estimated based on Brown et al. (2010). A Monte Carlo Simulation spreadsheet was prepared following the steps in Abu-Farsakh et al. (2012) to estimate the resistance factors. 50,000 random numbers were generated for each of the live load, dead load and resistance bias values. The random numbers were generated based on the mean and coefficient of variance of each of the bias values. The mean and coefficient of variance for the live load and dead load were collected from AASHTO specifications (2012). The mean, standard deviation and coefficient of variance were estimated for bias values of the 64 drilled shafts included in the database. The generated 50,000 random number make estimating resistance factor (ϕ) possible where otherwise limited quantity of data has restricted the reliable estimate of the resistance factors. Resistance factors were obtained by Monte Carlo Simulation for reliability index values of 2.33 and 3.00. The database was discussed in detail in Chapter 3.

5.4. Simulation of Load Tests to Failure

The 60 bidirectional load test cases, included in the accumulated database, are going to be simulated to failure using PLAXIS 2D for this study. An axisymmetric model is going to be utilized to develop the finite element model for the drilled shafts. An analysis was performed to observe the effect of the width and height of the finite element model on the result and based on the analysis, the width of the model was kept at more than 0.75 times the length of the drilled shaft and the height of the model was kept more than 1.5 times the length of the shaft. Figure 5 - 1 shows a sample finite element model of an O-cell load test. Figure 5 - 2 presents the flow chart for the steps to develop the finite element model of the bidirectional load test. To simulate the load test,

the required soil properties and the drilled shaft material properties were acquired from the geotechnical investigation report and load test report. The soil parameters collected from the geotechnical investigation reports were cohesion (c), friction angle (φ), dry unit weight (γd) and saturated unit weight (γs). For the material properties of the drilled shafts, young's modulus values were obtained from the load test reports. A Poisson's ratio of 0.3 was assumed for all the drilled shafts. The Young's modulus and the Poisson's ratio of the soil parameters are assumed based on the type of soil. After obtaining all the required parameters for the soil layers and the drilled shaft material, the material for the soil and the drilled shaft are defined in the PLAXIS 2D in the 'Soil' interface of the program. The geometry of the soil profile and the location of the drilled shaft and the O-cell are developed on the 'Structures' interface of the program. The O-cell is defined by a 10 cm thick block. At this stage, the previously defined soil properties are assigned to the developed geometry for the soil profiles. The location of the drilled shaft is also assigned by the corresponding soil properties at this point. An interface element is also introduced along the length of the drilled shaft extended beyond the tip by 0.5 m. The interface can be automatically generated in PLAXIS 2D.

When the geometry of the finite element model is complete with all the soil layers, the mesh is generated. The generated mesh size varies from very fine to medium. If a water table is present at the location of the drilled shaft, it can be inserted in the model after the generation of the mesh in the 'Flow conditions' interface of the program. Then the construction stages of the load test are defined. The first stage is basically the soil profile at rest condition. The drilled shaft is installed in the second stage. To install the drilled shaft, the material properties at the location of the drilled shaft is simply changed from the soil properties to the drilled shaft properties. At this stage, the O-cell is inactive, so, the 10-cm thick location fixed for the O-cell is assigned by the

material properties of the drilled shaft. The O-cell is activated in the next stage by applying loads in the O-cell location, in which, the loading of the drilled shaft begins. At this stage, the material properties of the O-cell are changed for a fictitious material with very little stiffness compared to the stiffness of the drilled shaft. The loading of the drilled shaft from the O-cell is performed in several stages up to the maximum load, which was applied on the field load test. When all the stages are set up, the simulation run is performed. The drainage type of soil can be fixed while the soil materials are defined in the 'Soils' interface of the program. Undrained drainage type is used based on the reported soil parameters.

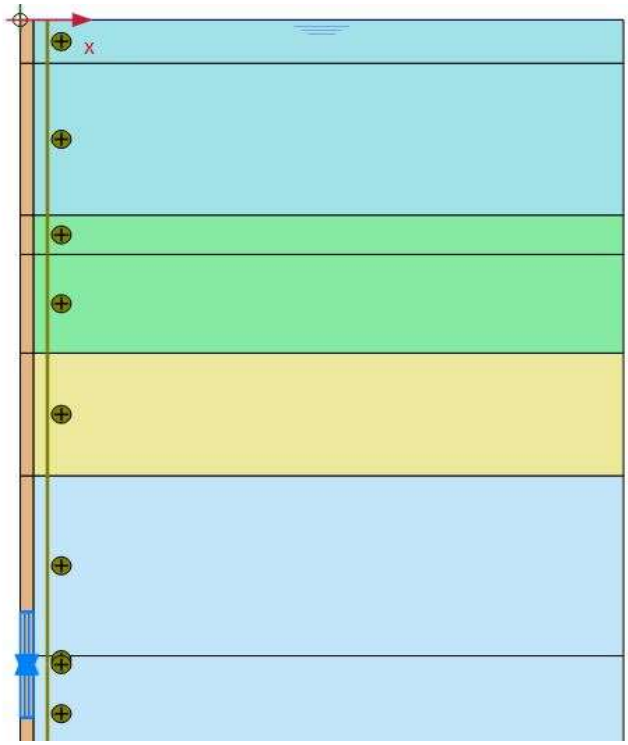

Figure 5 - 1 Sample PLAXIS 2D model of O-Cell load test.

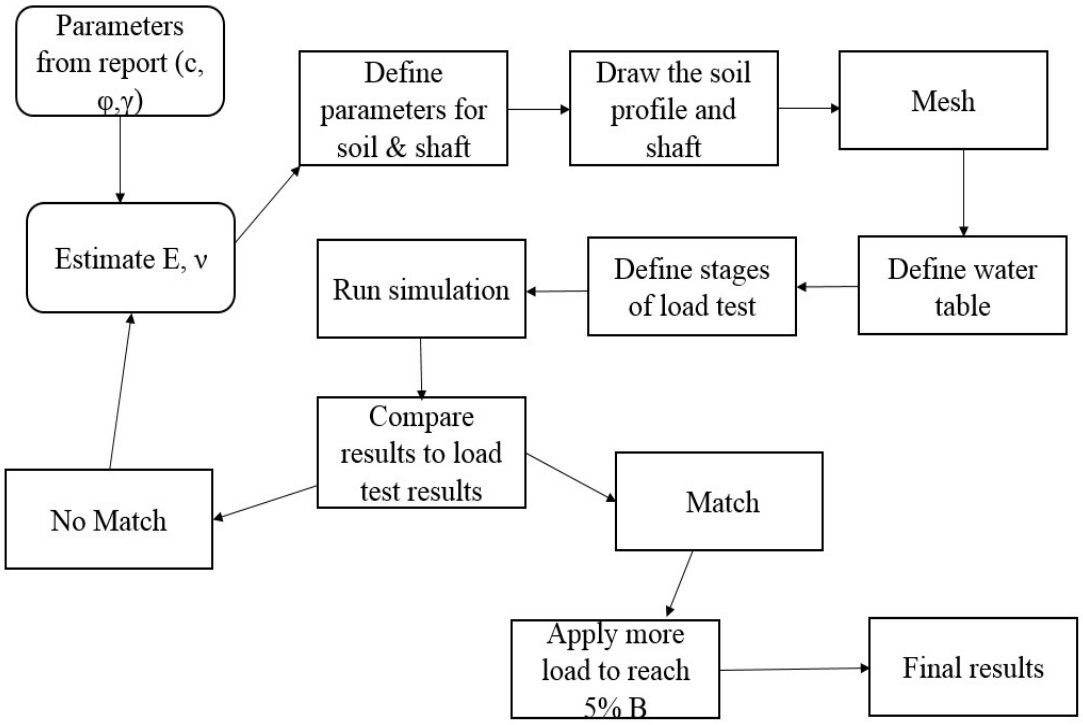

Figure 5 - 2 Flow chart for the finite element modelling of the bidirectional load tests to failure.

From the result of the simulation, the upward and the bottomward displacements of the drilled shaft are recorded for different stages of the loading. The top and bottom movement curves can be developed from the data recorded from the simulation result. The simulated top and bottom movement curves are compared with the top and bottom movement curves achieved from the field load test data. If the simulated result does not match with the field result, the assumed values of the Young's modulus and Poisson's ration are changed, and the procedure is repeated. This procedure of back analysis is continued until the results from the simulated load test matches with the field load test. Figure 5 - 3 shows an example of the comparison between the top and bottom movement curves achieved from field and simulated load tests.

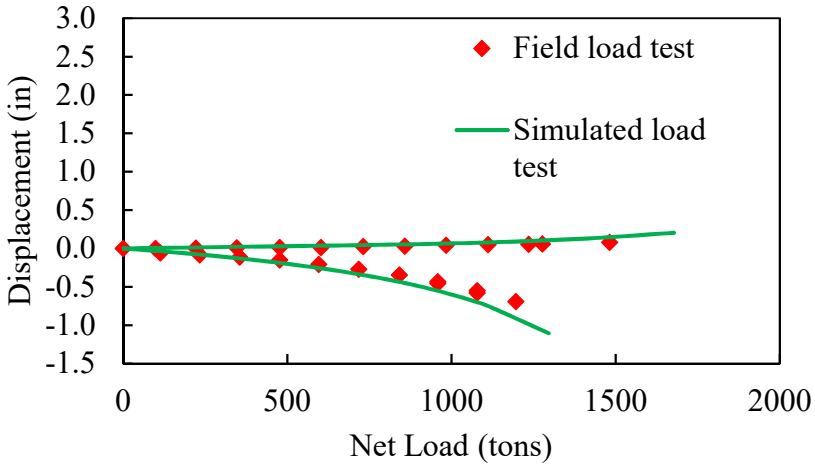

Figure 5 - 3 Comparison between field and simulated top and bottom movement curves.

Once the simulated top and bottom movement curves are close enough to the field top and bottom movement curves, the applied bidirectional load is increased until failure occurs to the top and the bottom movement curves. Finally, the simulated top and bottom movement curves are utilized to develop the equivalent top-down curve. Figure 5 - 4 presents the comparison between the extrapolated and the simulated top and bottom movement curves up to the failure points.

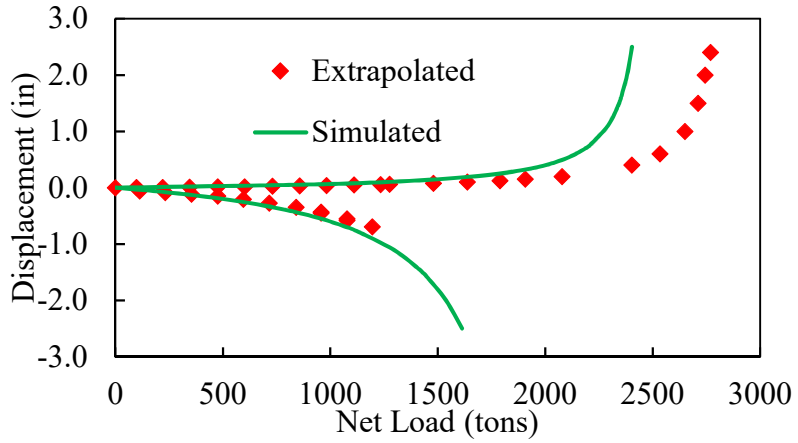

Figure 5 - 4 Comparison between extrapolated and simulated top and bottom movement curves.

5.5. Reconstruction of Equivalent Top-Down Curve

The simulated top and bottom movement curves were utilized to reconstruct the equivalent top-down curve. The reconstruction of equivalent top-down curve from the simulated top and bottom movement curves was performed based on Osterberg (1996). Figure 5 - 5 presents the process of obtaining the equivalent top-down curve from the top and the bottom movement curves.

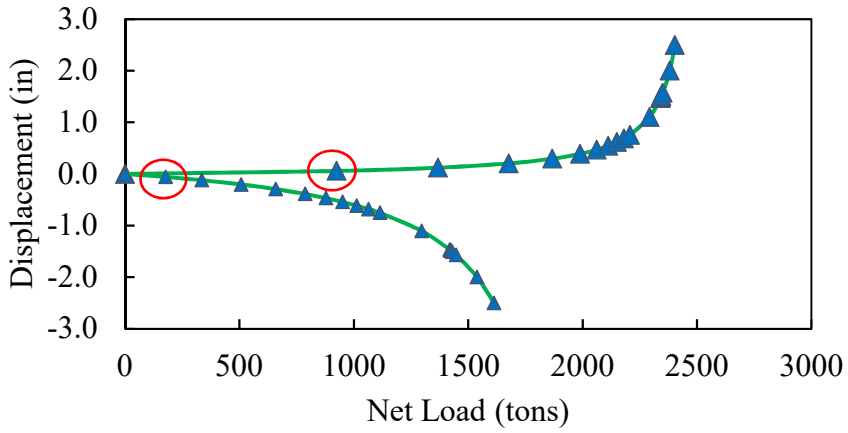

Figure 5 - 5 Procedure to obtain equivalent top down curve from the top and the bottom movement curves.

In Figure 5 - 4, the green line represents top and the bottom movement curves, obtained from the simulated bidirectional load test result. To get a data point for the equivalent top-down curve, two data points corresponding to the same displacement value are selected from the top and the bottom movement curves. The loads corresponding to the selected displacement value are summed up and the buoyant weight is subtracted from the summation. The resulting load and the selected displacement develop a data point in the equivalent top-down curve. The red marked data points in Figure 5 - 4 represents the loads corresponding to a displacement value of 0.06 in. The corresponding loads are 925 tons and 178 tons from the top and the bottom movement curves, respectively. Adding the loads and subtracting the buoyant weight of 21 tons, the first data point

in the equivalent top-curve can be found as 1082 tons corresponding to 0.06 in displacement. This process is repeated to obtain the equivalent top-down curve. Figure 5 - 5 shows the reconstructed top-down curve from the simulated top and bottom movement curves. An elastic compression correction is performed based on Loadtest International Pte. Ltd. (2013). The reconstructed top-down curve considering the elastic compression, which is the final reconstructed top-down curve, is also presented in Figure 5 - 6. The top-down curve obtained from the finite element model is compared to the top-down curve achieved from the field load test. The top-down load corresponding to a displacement value of 5% of the diameter of the shaft (B) is taken as the measured load, which is required for the LRFD calibration of resistance factors.

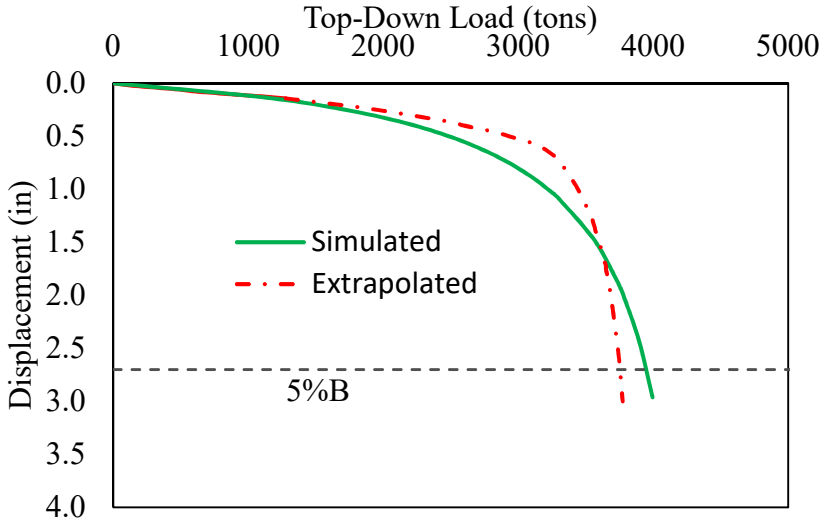

Figure 5 - 6 Comparison of top-down curves.

5.6. Calibration Based on Simulated Database

Both the measured resistance and the predicted resistance of the drilled shafts included in the database were needed to perform the LRFD calibration considering the simulated bidirectional load tests of the drilled shafts. The measured resistance values are taken from the simulated equivalent top-down curves corresponding to 5% of the diameter of the shaft. The predicted

resistance values were estimated based on the methods described in Brown et al. (2010). To obtain the predicted resistance maintaining the failure criteria, resistance corresponding to the 5% of the diameter of the shaft (B) was taken from the predicted load-settlement curves developed based on the normalized load-settlement curves recommended by Brown et al. (2010). Resistance bias values are estimated by calculating the ratio of the measured resistance to the predicted resistance for each of the drilled shafts. The mean, standard deviation and coefficient of variation of the resistance bias values were estimated for all the subcategories mentioned before. The statistical parameters for the load factors were obtained from AASHTO specifications (2012). Table 5 - 1 shows the mean resistance bias values estimated based on the field load tests as well as the simulated bidirectional load tests for all the previously mentioned subcategories. The corrected bias values based on the regression model recommended in Chapter 4 is also presented in Table 5 - 1. The conventional bias values are estimated based on the field measured resistance obtained by the extrapolation of the top and the bottom movement curves. The simulated bias values are based on the simulated bidirectional load tests. The corrected bias values are obtained based on the regression equation recommended in Chapter 4. It can be observed from the comparison that the simulated load tests have higher measured load compared to the extrapolated measured load obtained from the field load tests.

The statistical parameters for the resistance and load factors were utilized to perform a LRFD calibration of resistance factors for drilled shafts. The LRFD calibration was performed by Monte Carlo Simulation method. 50,000 random numbers were generated for each of the live load factor, the dead load factor and the resistance factor in MS Excel to perform the calibration.

Table 5 - 1 Mean resistance bias values for the subcategories.

Parameters	Subgroups	MS Database Bias		LA Database Bias	
		Conventional	Simulated	Conventional	Simulated
Soil Properties	Sand 2010	1.27	1.63	1.01	1.21
	Clay 2010	1.64	1.75	1.16	1.19
	Sand 1999	1.18	1.35	1.02	1.17
	Clay 1999	1.92	1.74	1.13	1.26
	Cohesionless IGM 1999	1.32	1.66	0.91	1.18
	Cohesive IGM 1999	1.65	1.84	N/A	N/A
	Sand +Clay 1999	1.59	1.55	1.10	1.21
Construction Method	Wet	1.26	1.67	0.94	1.16
	Dry	1.80	1.87	1.06	1.18

The limit state function recommended by Abu Farsakh et al. (2013) was used to in the Monte Carlo simulation to estimate the resistance factors for the previously obtained statistical parameters of the load and resistance bias values. The LRFD calibration was performed for target reliability indices of 2.33 and 3.00. Table 5 - 2 presents the resistance factors for target reliability index of 2.33 and Table 5 - 3 presents resistance factors for the target reliability index of 3.00. As the probability of failure is higher for reliability index of 2.33 than 3.00, resistance factors are also higher for reliability index of 2.33.

The corrected resistance factors based on the corrected bias values are based on a regression equation, which minimizes the effect of extrapolation error on the bias values. It can be observed from Table 5 - 2 and Table 5 - 3 that the resistance factors for the corrected bias and the resistance factors for the simulated load tests are very close in most of the subcategories. It proves that the finite element modelling of the bidirectional load tests to ensure the top and the bottom movement

curves to reach the failure criteria can be useful to minimize the effect of errors due to the extrapolation of top and the bottom movement curves.

Table 5 - 2 Comparison of the resistance factors for reliability index of 2.33.

Parameters	Subgroups	MS Database		LA Database	
		Conventional	Simulated	Conventional	Simulated
Soil Properties	Sand 2010	0.35	0.46	0.60	0.74
	Clay 2010	0.55	0.64	0.63	0.75
	Sand 1999	0.55	0.77	0.60	0.73
	Clay 1999	0.73	0.82	0.68	0.76
	Cohesionless IGM 1999	0.34	0.42	0.50	0.59
	Cohesive IGM 1999	0.53	0.62	N/A	N/A
	Sand +Clay 1999	0.62	0.77	0.66	0.76
Construction Method	Wet	0.35	0.45	0.65	0.71
	Dry	0.68	0.75	N/A	N/A

Table 5 - 3 Comparison of the resistance factors for reliability index of 3.00.

Parameters	Subgroups	MS Database		LA Database	
		Conventional	Simulated	Conventional	Simulated
Soil Properties	Sand 2010	0.23	0.31	0.48	0.60
	Clay 2010	0.38	0.46	0.55	0.61
	Sand 1999	0.42	0.61	0.50	0.60
	Clay 1999	0.52	0.62	0.52	0.61
	Cohesionless IGM 1999	0.22	0.28	0.40	0.47
	Cohesive IGM 1999	0.37	0.43	N/A	N/A
	Sand +Clay 1999	0.44	0.55	0.54	0.63
Construction Method	Wet	0.23	0.32	0.55	0.59
	Dry	0.48	0.55	N/A	N/A

Also, the consideration of minimizing the extrapolation error increases the resistance factors for all the subcategories. So, it can be stated that the errors initiating from the extrapolation of the top and the bottom movement curves obtained from bidirectional load tests affects the LRFD calibration of resistance factors negatively. Minimizing the errors can result in more realistic and economical design of drilled shafts.

The measured resistances obtained from the finite element models were compared to the measured resistances obtained from the field load tests. It was observed from the comparison that 21 of the simulated load tests had measured resistances within a range of 10% of the measured resistances estimated from the field load tests. The top and the bottom movement curves of these 21 cases were extrapolated by an average of 175%. The percentage of the extrapolation was estimated based on the applied load during the load test. Also, 13 of the simulated load test cases had measured resistances, which differed by more than 30% compared to the field measured resistances. These 13 cases needed average 210% of extrapolation of the top and the bottom movement curves. So, it can be stated that the estimation of measured load is significantly affected by the amount of extrapolation of the top and the bottom movement curves. If the amount of extrapolation of the movement curves is more than 175%, the measured load may vary widely compared to the actual measured load. If the extrapolation cannot be avoided, correction for the extrapolation should be performed. Finite element modeling of the bidirectional load test can also be useful to speculate the possible change in the equivalent top-down curve due to extrapolation.

5.7. Summary

The objective of this study was to minimize the effect of errors occurring from extrapolation of the top and the bottom movement curves on the LRFD calibration approach by

means of finite element modelling. A database of load test database was collected from Louisiana and Mississippi. The database consisted of 60 bidirectional load tests and 4 conventional static load test. Finite element modelling of the bidirectional load tests were performed in order to conduct a LRFD calibration of resistance factors based on the simulated load tests. Plaxis 2D was utilized to develop the finite element models. In case of the bidirectional load test, extrapolation of the top and the bottom movement curves are required in order to construct an equivalent top-down curve. The top and the bottom movement curves are extrapolated to reach the failure load of the drilled shafts. In this study, 5% B failure criteria was used, which, is the load corresponding to a displacement of 5% of the diameter of the shaft in the equivalent top-down curve. As extrapolation method is prone to make errors, it affects the LRFD calibration of the resistance factors for drilled shafts. In order to minimize the effect of the extrapolation errors, the finite element modelling was performed until the top and the bottom movement curves met the failure criteria of 5% B. The preparation of the finite element models of the bidirectional load test required details information about the subsurface condition of the surrounding soil for each of the drilled shafts. Equivalent top-down curve was prepared from the top and the bottom movement curves obtained from the finite element models. Utilizing the measured loads obtained from the simulated equivalent top-down curves, LRFD calibration of the resistance factors was performed for reliability index values of 2.33 and 3.00. The obtained resistance factors were compared to the resistance factors estimated by conventional method. It was observed from the comparison that the resistance factors increased significantly, providing a more realistic and economical design method for drilled shafts. The obtained resistance factors from the simulated database of bidirectional load tests were also compared to the resistance factors estimated based on the corrected bias values recommended in Chapter 4. A method was also proposed to estimate the errors in bias values

occurring from extrapolation of the top and the bottom movement curves. The comparison showed that the resistance factor values from the simulated database were similar to the ones obtained from the corrected bias values. So, it can be stated that the finite element modelling of bidirectional load tests can result in more realistic resistance factors by minimizing the effects of the errors occurring from the extrapolation of the top and the bottom movement curves.

Chapter 6

LOWER BOUND OF RESISTANCE

6.1. Introduction

Deep foundations are referred to structural components that carry the load from the superstructure to soil layers in extensive depth compared to shallow foundations. Driven piles, drilled shafts, micropiles can be mentioned as examples of deep foundations. Initially, allowable stress design (ASD) method was followed to design the components of deep foundation of bridges. On the other hand, load factor design (LFD) method was followed to design the superstructures. While the LRFD method considers load factors as well as resistance factors to be applied to the limit state inequalities, the ASD method combines both of the factors into a single factor of safety. Consideration of two separate factors for load and resistance has made the LRFD method more consistent than the ASD method (Abu Farsakh et al., 2010). After the publication of the first edition of AASHTO LRFD Bridge Design Specifications, the major challenge was to make the transition from ASD to LRFD. To begin the transition from ASD to LRFD, the Federal Highway Administration (FHWA) released a policy in 2000 that required all new federally-funded bridges to be designed using the AASHTO LRFD specifications by October 2007 (Fortier, 2016). Despite this steady progression into LRFD, however, deep foundation design still does not take full advantage of the probabilistic framework in many parts of the United States due to a lack of area-specific resistance factors derived using reliability theory–based calibrations. Instead, many regions rely on values given in specifications from AASHTO (2010) which were developed by fitting to allowable state design (ASD) safety factors (Stanton et al. 2017). Studies like Abu-

Farsakh et al. (2012), Long et al. (2009), Roling et al. (2011); Garder et al. (2012), Rahman et al. (2002), and McVay et al. (2005) were performed with an objective of calibrating region wise load and resistance factors for foundation design. Perusing all the studies, it was observed that the resistance factors did not improve with the consideration of region-based soil properties, in fact, they decreased in some cases. The low resistance factor values may occur from different uncertainties like inaccuracy in load test data, inaccurate soil test data, effect of outlier cases etc.

The calibration procedure of resistance factors include estimation of the measured and predicted resistance for drilled shafts. The predicted resistance factors are estimated by following various analytical methods like O'Neil and Reese (1999) and Brown et al (2010). The measured resistance factors are obtained from the results of load tests performed on drilled shafts. For the probabilistic reliability analyses, the statistical parameters (mean, standard deviation and coefficient of variation) for resistance bias and load bias values are utilized while it is assumed that the resistance bias values follow a lognormal distribution. The statistical parameters for the load factors can be obtained from AASHTO Specifications (2010). The resistance bias is the ratio of the measured resistance to the predicted resistance of drilled shaft. Several studies performed with an objective of calibration of resistance factors for drilled shafts included some kind of analysis on the resistance bias values in order to achieve more reliable resistance factor values. Oregon Department of Transportation performed a study to calibrate resistance factors for driven piles in 2011 (Smith et al. 2011). The study included an analysis to remove the bias values outside the range of +/- 2 times of the standard deviation from the mean bias value in order to optimize the calibration of resistance factors. Though in the final calibration approach, they did not apply this method due to lack of justification in removing the extreme data points. Iowa Department of Transportation performed a study on the calibration of resistance factors for drilled shafts based

on database developed by Garder et al. (2012). A data quality check was conducted based on type of load tests, accuracy of load test result and availability of information on subsurface condition in order to perform an accurate calibration. Nevada Department of Transportation also performed a study on calibration of resistance factors, in which, they developed a scoring system of the drilled shaft cases included in the database to separate the cases with better data quality and more accurate load test results (Motamed et al. 2016). New Mexico Department of Transportation (Ng and Fazia, 2012) performed a study on calibration with the assumption of the resistance values following a polynomial distribution, in addition to the calibration with lognormality of the bias values. After the completion of the study, the calibration approach with the polynomial function of the bias values yielded higher resistance factor values compared to the calibration approach with the lognormal function of the bias values. They concluded that the polynomial distributions are more rational. Bathurst et al. (2008) recommended a process to recognize the extreme load test cases by plotting the bias values against the predicted resistances. The data points in the developed plots should be randomly distributed. The study recommended to separate the extreme data points in the bias vs predicted resistance plot as the outlier cases. Kim et al. (2016) performed a calibration study by introducing lower bound capacity to the calibration procedure. They estimated the lower bounds of the side as well as tip ultimate resistances and considered the lower bounds for the calibration procedure. The consideration of lower bounds for the calibration resulted in the increase of the side resistance factors by up to 8%. The tip resistance factors also increased by up to 13% due to the involvement of the lower bounds in the calibration approach.

Najjar and Gilbert (2009) also recommended consideration of lower bound capacities for the calibration of resistance factors. They performed a study, in which, the effect of lower bounds was investigated for driven piles in cohesive and cohesionless soil. The study utilized a database

of driven piles presented by Olson and Dennis (1982). Methods proposed by Najjar (2005) were used to obtain the lower bound capacities for the driven piles in cohesive and cohesionless soil. Najjar and Gilbert (2009) concluded with the proof of the presence of lower bounds in the capacity distribution and they suggested to incorporate lower bound capacity in the LRFD calibration of resistance factors.

According to Najjar and Gilbert (2009), the assumed distributions of the load and resistance values does not express a realistic scenario. It was observed in all the studies related to calibration of resistance factors that the bias or the capacities are usually assumed to have a lognormal distribution. A lognormal distribution of the bias values starting from zero does not reflect the realistic scenario of the bias values to have lower bound. Figure 1 shows the distribution of load and capacity for drilled shafts. Since the capacity of the drilled shaft has to be larger than the applied load to avoid failure, it can be observed from Figure 1 that the probability of failure depends on the lower tail of the assumed distribution of the capacity. So, including the lower bound of the capacity or resistance of the drilled shaft in the calibration approach can result in more accurate resistance factor values.

The objective of this study is to observe the effects of incorporating lower bound of the resistances in the calibration of resistance factors for drilled shafts. A database was accumulated on the load test performed on drilled shafts in order to perform the study. The database included load test data collected from Louisiana and Mississippi. Load tests performed on drilled shafts placed in both cohesive and cohesionless soil were included in the database. In order to discern the effect of lower bound of the resistance of drilled shafts on the calibration approach, the lower bound of the resistance values were calculated for the drilled shafts included in the collected database. From the calculated lower bound resistance values, a lower bound resistance bias was

estimated for each of the drilled shafts. The lower bound resistance bias was incorporated in the calibration approach for estimating the resistance factors for drilled shafts. In this paper, the current practice of calibration of resistance factors will be discussed along with the process of estimating the lower bound of the resistance values for the drilled shafts located in both cohesive and cohesionless soil. The approach to incorporating the lower bound in the calibration process will also be discussed in this paper. Finally, the effect of the lower bounds will be presented by comparing the original resistance factor values achieved from the collected database to the resistance factor values achieved by incorporating the lower bound resistance bias values in the calibration approach.

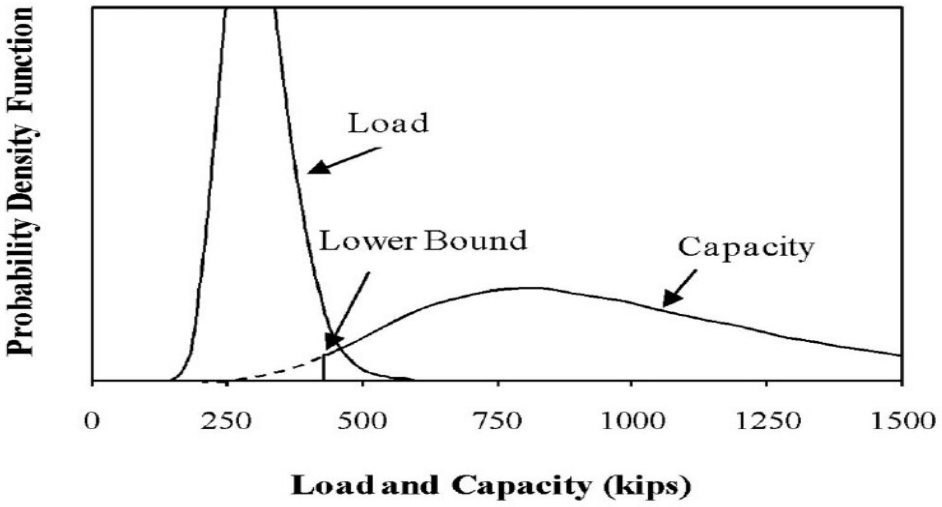

Figure 6 - 1 Distribution of load and capacity for conventional practice as well as with a lower bound (Najjar and Gilbert, 2009).

6.2. Estimation of Lower Bounds

Najjar (2005) proposed a hypothesis of the presence of a lower bound resistance in the capacity of piles. The hypothesis was developed based on the principle that even a considerably disturbed soil sample has an undrained shear strength value of more than zero. Though Najjar

(2005) performed the study on driven piles, it can also be utilized for drilled shafts. Based on the aforementioned principle, the procedure for estimating lower bound capacity or resistance of drilled shafts is discussed in this section. After estimating the lower bound resistance values for each of the drilled shafts, the lower bound of the resistance bias values were estimated by taking the ratio of the lower bound resistance to the predicted resistance.

6.2.1. Lower Bound Resistance in Cohesive Soil

For drilled shafts located in a cohesive soil, the lower bound of the resistance of the shafts can be obtained by utilizing the residual shear strength. Residual shear strength is basically obtained from lab tests but because of the lack of tests for residual shear strength, it was obtained based on empirical relationships for this study. Residual shear strength can resemble remolded shear strength, which is the undrained shear strength of cohesive soil resulting from the effect of a long-term large strain. Residual shear strength can also be calculated from the drained residual friction angle between soil and the shaft material.

Previous studies showed a relationship between remolded shear strength and the liquidity index of cohesive soil. The remolded shear strength decreases with the increase of the liquidity index of soil. Several studies were performed to establish an empirical relationship between the remolded strength and the liquidity index of soil. For this study, the relationship recommended by Wroth and Wood (1978) will be utilized. According to Wroth and Wood (1978), the undrained shear strength (S_{ur}) can be estimated by the following equation.

$$S_{ur} = 3550\mathrm{e}^{-4.6(\mathrm{LI})}\ psf \qquad (6\text{-}1)$$

The aforementioned relationship applies for normally consolidated soil to slightly overconsolidated soil. To verify the relationship between undrained shear strength and liquidity index of cohesive soil, Najjar (2005) compared the liquidity indices and the corresponding undrained shear strength for normally consolidated soil provided by Dutt et al. (1995) to the model proposed by Wroth and Wood (1978). Figure 6 - 2 presents the comparison between the actual data and the proposed model by Wroth and Wood (1978). This model will be used in this study to estimate the undrained residual strength based on the liquidity index of cohesive soil.

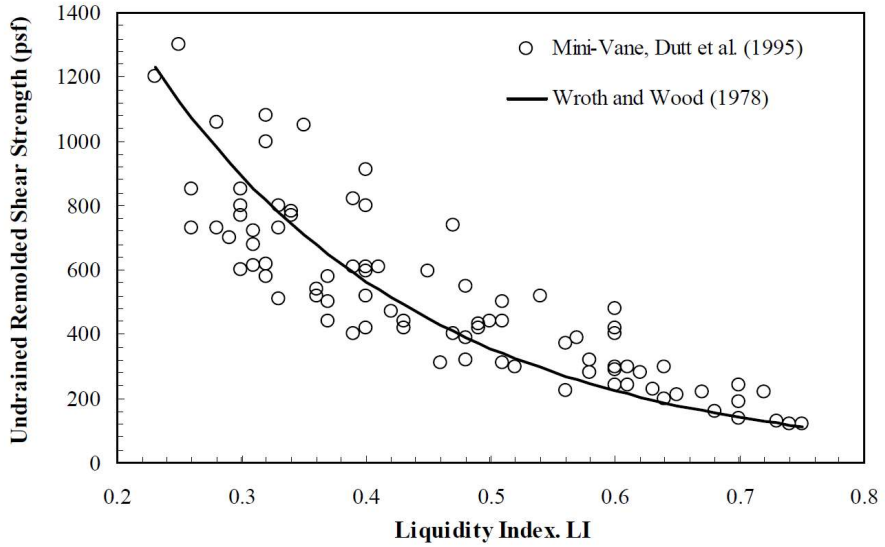

Figure 6 - 2 Effectiveness of the undrained remolded shear strength and liquidity index (Najjar, 2005).

To estimate the lower bound for the side and tip resistance of drilled shaft in cohesive soil, the undrained shear strength can be replaced by the undrained residual shear strength. So, the lower bound for the unit side and tip resistance can be estimated by the following equation.

$$q_{s(LB)} = \alpha S_{ur} \quad (6\text{-}2)$$

$$q_{p(LB)} = 9 S_{ur} \quad (6\text{-}3)$$

6.2.2. Lower Bound Resistance in Cohesionless Soil

The side and tip resistance of drilled shafts in cohesionless soil is estimated based on number of SPT blows per feet in the soil layer under consideration. The density of the cohesionless soil can be determined from the SPT blow counts. Table 6 - 1 shows the SPT blow counts corresponding to the relative density of cohesionless soil. Najjar (2005) recommended a method to estimate the lower bound resistance in cohesionless soil by modifying the API method of estimating driven piles resistance. The lower bounds of the side and tip resistance for drilled shafts in cohesionless soil can be obtained by decreasing the SPT blow count value of the soil layer to a value with one category less in density.

Table 6 - 1 Relative density of cohesionless soil based on SPT blow counts (Terzaghi et al. 1996).

Relative Density	No. of Blow Counts, N_{60}
Very Loose	0 – 4
Loose	4 – 10
Medium	10 – 30
Dense	30 – 50
Very Dense	>50

6.3. Bounded Probability Distribution

The lower bound bias values can be incorporated into the reliability-based calibration procedure by utilizing a bounded probability distribution of the resistance bias values. Najjar (2005) checked the effect of different types of bounded distribution of the pile capacity on the reliability index. The study described in Najjar (2005) applied truncated normal and lognormal

distribution, beta distribution, uniform distribution and mixed lognormal distribution for the reliability analysis. Figure 6 - 3 shows a comparison of the effects of different types of bounded distributions.

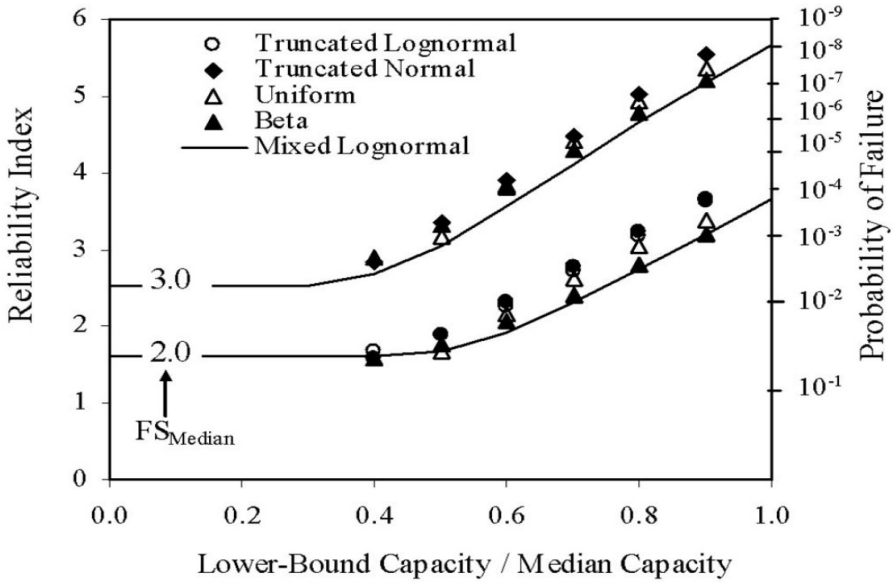

Figure 6 - 3 Effect of different types of bounded distribution of the capacity on the reliability analysis (Najjar and Gilbert, 2009).

For this comparison, the applied load was assumed to be lognormally distributed for all types of bounded distribution of capacity. It can be observed from Figure 6 that the reliability index values are not significantly affected by the type of the distribution. Rather, the ratio between the lower bound capacity and the median capacity impacts the reliability index significantly. After a threshold, the reliability index increases linearly with the increase of the lower bound capacity. Also, the threshold decreases with the increase of factor of safety value. It can be said from this analysis that the reliability index will increase with the increase of the lower bound bias values in the case of the current study.

As the load and resistance are taken as lognormally distributed in most of the calibration related studies, Najjar (2005) recommended the mixed lognormal distribution for the incorporation

of the lower bounds into the resistance values. For the resistance values greater than the lower bounds, resistance follows a lognormal distribution in the mixed lognormal distribution. For the resistance values at the lower bound, a finite probability value is assigned as the probability of the resistance being equal to or less than the lower bound value. For this study, mixed lognormal distribution of the resistance bias values was utilized for the calibration of the resistance factors. Figure 6 - 4 presents the mixed lognormal distribution of the resistance as shown in Najjar and Gilbert (2009).

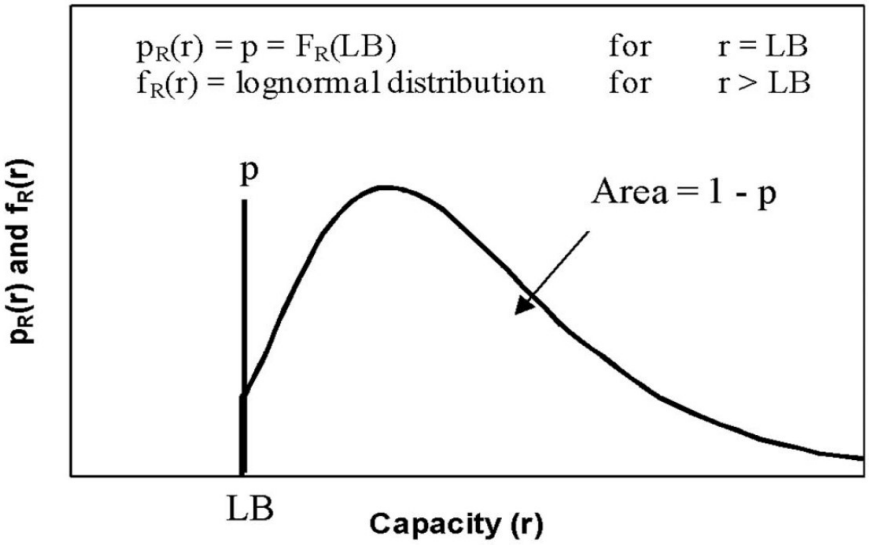

Figure 6 - 4 Mixed lognormal distribution of the resistance values (Najjar and Gilbert, 2009).

6.4. Incorporation of Lower Bound Bias in LRFD Calibration

In practical cases, the lower bound of the resistances will have some level of uncertainties. Najjar (2005) performed a study on the effect of the uncertainties of the lower bound of the resistance values. The study showed that the presence of lower bound with uncertainties increases the reliability. The study also showed that the reliability increases with the increase of the lower bound value. Also, the uncertainties in the lower bounds are usually very small as the lower bounds

estimated based on the shear strength of soil are less susceptible to be affected by in situ subsurface condition, soil test methods etc. The small level of uncertainty in the lower bounds will not significantly impact the reliability, if the lower bound is incorporated in the calibration procedure.

To incorporate the lower bounds in the LRFD calibration, the conventional LRFD design check equation can be replaced by the following equation.

$$\sum \eta_i \gamma_i Q_i \leq \sum \varphi_{i(LB)} R_i \tag{6-4}$$

Here, η_i is a load modifier which accounts for ductility, redundancy and operational importance of the structure. γ_i is the load factor. Q_i is the load applied on the shaft. $\varphi_{i(LB)}$ is the resistance factor incorporating the lower bounds and R_i is the resistance of the shaft. $\varphi_{i(LB)}$ can be estimated by the following equation (Najjar, 2005).

$$\varphi_{(LB)} = \frac{e^{\beta\sqrt{\ln(1+COV_L^2)(1+COV_R^2)}}}{e^{\beta\sqrt{\ln(1+COV_L^2)(1+COV_{LB}^2)}}}\varphi \tag{6-5}$$

Here, β is the target reliability index. COV_L, COV_R and COV_{LB} are the coefficient of variations of the bias values for load, resistance and lower bounds. COV values are estimated based on the mean and the standard deviation of the applied load, resistance and lower bound resistance.

6.5. Calibration of Resistance Factors

Based on the previously discussed methods, the lower bounds of the resistance values were estimated for all the drilled shafts included in the collected database. The lower bound bias was estimated by taking the ratio of the lower bound resistance to the predicted resistance. The

estimated lower bound bias had a coefficient of variation value of 0.15. The statistical parameters for the lower bound bias were utilized to estimate the resistance factors incorporating the lower bound resistance. Table 6 - 2 presents the comparison between the calibrated resistance factors without the lower bounds and the resistance factors with the lower bounds. The calibrated resistance factors are presented for a target reliability index of 3.00.

Table 6 - 2 Effect of lower bound bias on the calibrated resistance factors.

Soil Properties	MS Database			LA Database		
	Cases	W/O Bound	Bounded RF	Cases	Without Bound	Bounded RF
Sand 2010	17	0.23	0.62	18	0.48	0.58
Clay 2010	14	0.38	0.57	12	0.55	0.62
Sand 1999	4	0.42	0.60	15	0.50	0.58
Clay 1999	5	0.52	0.68	13	0.52	0.60
Sand IGM 1999	14	0.22	0.61	5	0.40	0.55
Clay IGM 1999	9	0.37	0.57	1	NA	NA
Sand +Clay 1999	9	0.44	0.62	25	0.54	0.68
Whole	34	0.33	0.65	30	0.51	0.58

It can be observed from Table 6 - 2 that the incorporation of the lower bounds in the LRFD calibration significantly increased the resistance factors. The increase in the resistance factor values implies that the incorporation of lower bound of resistances of drilled shafts in the LRFD calibration of resistance factors can result in the realistic and economical design of drilled shafts. So, the resistance factors calibrated incorporating the lower bound resistances can be considered along with the conventionally calibrated resistance factors for the design of drilled shafts.

The calibrated resistance factors are affected by the variability in the soil properties which was not considered in the calibration procedure for this study. Though, an analysis for the

variability in soil properties was performed. A statistical analysis was performed on the undrained shear strength and friction angle of soil. Figure 5 – 7 shows the variability in undrained shear strength and figure 5 – 8 shows the variability in friction angle of soil. The undrained shear strength and the friction angle values were collected from the geotechnical reports of the aforementioned load test database. It can be observed that the undrained shear strength has COV of 0.89, on the other hand, friction angle has a COV of 0.14. It means that the undrained shear strength values of cohesive soil vary more widely compared to the friction angles of cohesionless soil. Consideration of the variability in soil properties in the calibration process will increase the accuracy and reliability of the calibrated resistance factors.

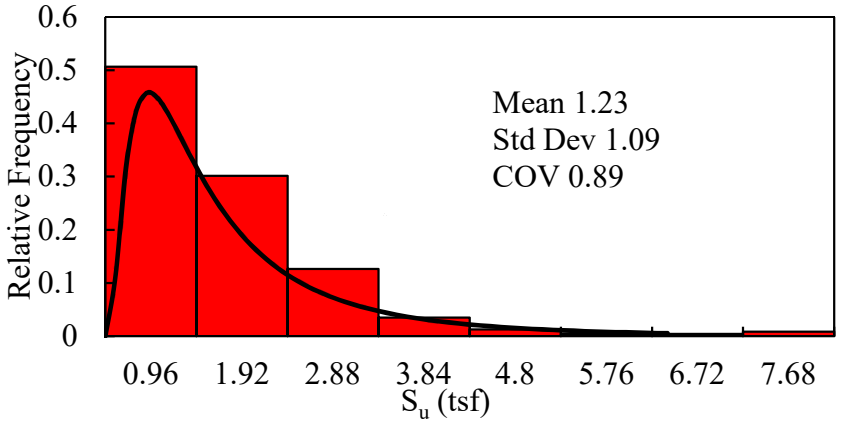

Figure 6 - 5 Variability in undrained shear strength of cohesive soil.

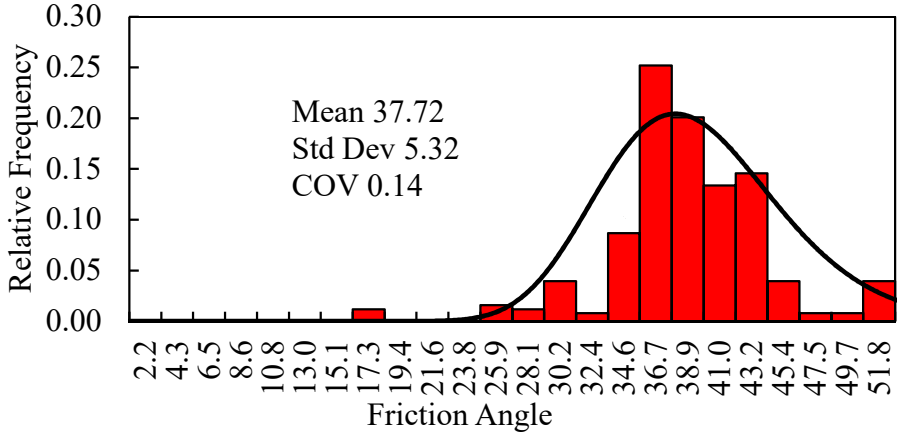

Figure 6 - 6 Variability in friction angle of cohesionless soil.

6.6. Summary

The objective of this study was to develop a more realistic and economical design method for drilled shafts by utilizing the presence of a physical lower bound of the resistance values in the LRFD calibration of resistance factors. Since the probability of failure depends on the lower tail of the distribution of the resistance of drilled shafts, introducing a lower bound, which is more than zero, will result in a more realistic calibration of resistance factors for drilled shafts. With that in mind, a load test database was collected, which included only drilled shaft cases. Based on the load test database, a LRFD calibration was performed following conventional procedure to estimate the total resistance factors for the drilled shafts. Lower bounds of the resistances of the drilled shafts were estimated for both cohesive and cohesionless soil. Since the current practice of LRFD calibration is based on the resistance bias values, a lower bound bias was estimated for each of the drilled shafts. With consideration of the presence of the lower bound bias, the resistance bias values were assumed to have a mixed lognormal distribution. The calibration of the resistance factors were performed again incorporating the lower bound bias in the procedure. When the results were compared the resistance factors calibrated by conventional method, it was observed that the consideration of the lower bounds resulted in higher resistance factors with the same level of reliability, which will make it possible to perform more realistic and economical design of drilled shafts.

The lower bound of the resistances of drilled shafts located in cohesive soil was estimated based on undrained residual shear strength of soil. Undrained residual shear strength can be obtained from lab tests on the soil samples. As the load test database of the drilled shafts did not include information on undrained residual shear strength, an empirical relationship developed by Wroth and Wood (1978) was utilized to estimate the undrained shear strength values. Future work

can be performed based on undrained shear strength values obtained from laboratory tests, which may increase the accuracy of the LRFD calibration of resistance factors.

Chapter 7

FINDINGS AND FUTURE RECOMMENDATIONS

7.1. Introduction

In the transition of the drilled shaft design from allowable stress design (ASD) method to load and resistance factor design (LRFD) method, the major challenge was to calibrate reliable and realistic resistance factors for the LRFD method. At the preliminary stage, the resistance factors were calibrated based on the fitting of the global safety factors of the ASD method. The drawback of designing with resistance factors achieved by fitting to ASD safety factors is that the resistance factors does not consider the difference in subsurface conditions in different regions. Several Departments of Transportation (DOTs) organized some studies in order to calibrate area specific resistance factors for LRFD design of drilled shafts. The calibrated resistance factors achieved from region specific studies varied from the resistance factors recommended by AASHTO specifications. Also, few studies were performed to investigate the possible sources of uncertainties in the LRFD calibration procedure. The possible sources of uncertainties in the LRFD calibration procedure includes subsurface condition, interpretation of different types of load test data, presence of outliers in the load test database, distribution of load and resistance etc. Uncertainties occurring from subsurface condition can be considered by conducting separate LRFD calibration for different types of soil. Uncertainties from different types of load tests can occur because of the difference in the interpretation of different load test results. For example, load is applied from the top of the test shaft in case of conventional static load test, which, provides a load-settlement curve. The failure load can be obtained from the load-settlement curve. On the

other hand, a jack or O-cell is used to apply bidirectional load in case of a bidirectional load test. The jack is installed either at the bottom or in the middle of the shaft. The load test provides an upward and a downward movement curve. The upward movement curve corresponds to the side resistance of the shaft and the downward movement curve corresponds to the tip resistance of the shaft. An equivalent top-down curve is developed from the upward and the downward movement curves. The failure load can be obtained from the equivalent top-down curve, which is similar to the load settlement curve obtained from conventional static load test. The development of the equivalent top-down curve requires extrapolation of the upward or the bottomward movement curves in order to ensure that the curves reach the failure criteria. The extrapolation of the upward and the downward movement curves cause uncertainties in the LRFD calibration of drilled shafts. To minimize the effect of outlier load test cases, several ways are usually followed in the studies on LRFD calibration. For example, plotting the predicted resistance against the measured resistance and removing any load test data recognized as outlier in the plot. Also, some studies recommend removing load test cases with bias value falling outside the range of two or three times of the standard deviation of the bias from the mean bias. The drawback of removing a data is that it can affect the distribution of the bias and as a result, the distribution may not be realistic. Since failure occurs when the resistance of a shaft is smaller than the applied load, the probability of failure depends on the lower tail of the assumed distribution of the resistance. Load and resistances are usually assumed to be lognormally distributed. As the drilled shafts has a physical lower limit of resistances, introducing a lower limit to the distribution of the resistance can result in more realistic LRFD calibration.

The main objective of this study was to optimize the LRFD calibration procedure for drilled shafts. A drilled shaft database was accumulated for the sake of the study. The database consisted

of 64 load test data performed on drilled shafts. 60 of the load test cases were bidirectional load tests and the rest were conventional static load test. Three major tasks were performed in order to achieve the objective. The first task was to minimize the error in bias occurring from the extrapolation of upward and the downward movement curves obtained from bidirectional load tests. Eight load test cases were selected from the accumulated database to investigate the errors developed from the extrapolation. The data points were systematically truncated from the upward and the downward movement curves of the selected eight cases. The equivalent top-down curve was produced for each of the truncation of the data points. The resistance bias values were calculated based on the measured resistances obtained from the equivalent top-down curves developed with truncated data. The errors occurring in the bias values due to extrapolation were also estimated. In total, 80 truncation cases were produced from the selected eight cases. A regression analysis was performed on these 80 cases, which produced a regression equation. The regression equation was statistically validated. The developed regression equation was used to estimate the corrected bias values, which were, in turn, used to perform a LRFD calibration based on the accumulated database. In the second task, finite element model was developed for the bidirectional load tests included in the database in order to investigate the ability of finite element method to minimize the errors occurring from the extrapolation of the upward and the bottomward movement curves. PLAXIS 2D was utilized to develop the finite element models. The soil parameters for the location of the drilled shafts were collected from the corresponding load test reports. The models were developed based on axisymmetric principles. Soils were defined by Mohr-Coulomb model and the drilled shaft material was defined by elastic plastic model. The jack or O-cell used to apply the bidirectional loads were simulated by 10 cm thick blocks. The application of the loads were performed in several stages in the models. The maximum apply loads

in the finite element models of the load tests were similar to the maximum applied load in the field load tests. Then, a back analysis was performed to match the upward and the bottomward movement curves achieved from the models to the curves obtained from the field load tests. When the upward and the bottomward curves were matching between the finite element models and the field load tests, the applied load in the models were increased until the upward and bottomward curves reached the failure points. The upward and bottomward curves constructed from the finite element models of the bidirectional load tests were used to develop equivalent top-down curves. Again, the resistance bias values were estimated from the simulated equivalent top-down curves and a LRFD calibration was performed based on the finite element models of the bidirectional load tests. In the third task of the study, lower bound of the resistance of the drilled shafts were incorporated in the LRFD calibration procedure. The procedure for the estimation of the lower bounds of the resistance of the drilled shafts in different types of soils were discussed in the corresponding chapter of this study. Based on the discussed procedure, the lower bounds of the resistances were estimated for the drilled shafts included in the database collected for this study. The lower bounds of the resistance values were obtained utilizing the estimated lower bound resistances. The distribution of the bias values was assumed to follow a mixed lognormal distribution with a finite probability of the bias values to be less the lower bounds. LRFD calibration was performed based on the lower bound bias values in order to investigate the effect of considering the lower bounds on the resistance factors.

7.2. Findings

The major findings based on the results of the aforementioned studies are summarized here.

1. From the analysis on the errors developed from the extrapolation of the upward and the bottomward curves, it was observed that the amount of required extrapolation significantly affects the developed error in resistance bias. The truncation of the data points on the previously mentioned eight cases was performed until 50% of the data remained. The percentage is based on the applied load. The error was increased up to a value of 0.7 with the increase of the amount of the extrapolation.

2. The amount of extrapolation also affects the calibrated resistance factors. It was observed that the increase of the amount of extrapolation decreases the resistance factor values. The resistance factor values decreased by an amount of 0.22 with the maximum truncation of 50% of the data points.

3. It was observed from the developed regression equation that the error in bias can be estimated from the amount of extrapolation. In the regression equation, the amount of extrapolation was defined by the maximum upward and the maximum bottomward displacement normalized by 5% of the dimeter of the shaft as well as the ratio of the measured resistance and the maximum applied load in the load test data.

4. The regression model to estimate bias error was validated statistically. Validation of the regression model was also performed by applying it on the truncated cases used for the analysis. Use of the regression model enabled the calibration of the resistance factors based on the truncated database within a range of 0.01 of the original calibration.

5. The regression model was applied in the calibration of the database of load tests collected from Louisiana and Mississippi to estimate the error in bias values and corrected bias values were obtained using the errors for each of the bidirectional load tests. This procedure increased the resistance factor values by 0.06 to 0.20.

6. The calibration of the resistance factors based on the simulated load tests resulted in increased resistance factors by 0.06 to 0.19 compared to the conventional calibration based on the field load test database. The resistance factors based on the simulated database were close to the resistance factors based on the corrected bias for extrapolation errors.

7. It was observed in the simulated load test database that the simulated measured resistances were within a range of less than 10% of the field measured resistance for 21 load test cases. Out of the 21 cases, 11 cases were dominated by clay, 7 cases were dominated by sand and 3 cases were dominated by IGM. For 13 cases, the simulated resistances varied from the field measured resistances by more than 30% of field the measured resistances. 7 of the 13 cases were located in IGM. Overall, the difference between the simulated and the measured resistance was higher in IGMs. It can be stated that the simulated load tests are closer to the actual measured loads compared to the field measured resistance, since the field measured resistances were obtained from the extrapolation of the upward and the bottomward movement curves and the hyperbolic extrapolation method does not take the type of soil into consideration.

8. It was observed from the study that the incorporation of lower bound resistances can increase the resistance factors. The incorporation of lower bounds in the calibration procedure increased the resistance factors by 0.10 to 0.39.

7.3. Future Recommendations

The effect of the error occurring from the extrapolation of the upward and the downward movement curves on the calibration of the resistance factors are investigated in this research. The effect of incorporation of lower bound resistance of the drilled shafts in the calibration procedure

was also observed here. A few recommendations for future studies on LRFD calibration of resistance factors are listed here.

1. The subsurface properties in the load test data included in the database collected for this study mostly consisted of sand and clay. A study on the extrapolation error in the equivalent top-down curve can be performed with database including rock materials.

2. For this study, the lower bound resistance of drilled shafts located in cohesive soil was estimated based on undrained remolded strength. The undrained remolded shear strength of soil was estimated based on an empirical formula. A study based on undrained remolded shear strength obtained from lab tests can improve the accuracy of the calibrated resistance factors incorporating the lower bound resistance.

3. In this study, the predicted resistances were estimated based on FHWA 2010 method of drilled shaft design (Brown et al. 2010). A LRFD calibration can be performed based on the newly published FHWA 2018 method of drilled shaft design (Brown et al. 2018).

4. The effect of expansive soil is not considered in the procedure of LRFD calibration, which can result in over prediction of the predicted side resistances of drilled shafts. A study can be performed on the effect of expansive soil on the LRFD calibration of resistance factors.

5. Variability in the soil properties were not considered in the LRFD calibration procedure study. Considering the variability in soil properties for different types of soils in the LRFD calibration will improve the reliability of the calibration.

6. Lateral loading and group effect of drilled shafts were not included in this study. Studies can be conducted for the effect of lateral loading and group on the LRFD calibration of drilled shafts.

REFERENCES

AASHTO (2007), AASHTO LRFD Bridge Design Specifications, Customary U.S. Units, 4th Ed., 1510 p.

AASHTO (2012). "AASHTO LRFD Bridge Design Specifications: Sixth Edition. Parts I and II." American Association of State Highway and Transportation Officials, Washington, DC.

AASHTO (2017), U.S. Customary Units, 8th Edition, Washington, D.C.

Abu-Farsakh, M. Y., Yu, X., Yoon, S., & Tsai, C. (2010). "Calibration of resistance factors needed in the LRFD design of drilled shafts." (No. FHWA/LA. 10/470) Louisiana Transportation Research Center.

Abu-Farsakh, M., Yu, X., & Zhang, Z. (2012). "Calibration of side, tip, and total resistance factors for load and resistance factor design of drilled shafts." *Transportation Research Record: Journal of the Transportation Research Board*, (2310), 38-48.

Abu-Farsakh, M. Y., Chen, Q., & Haque, N. (2013). "Calibration of resistance factors for drilled shafts for the new FHWA design method" (No. FHWA/LA. 12/495). Louisiana Transportation Research Center.

Allen, T. M., (2005). "Development of Geotechnical Resistance Factors and Downdrag Load Factors for LRFD Foundation Strength Limit State Design," Publication No. FHWA-NHI-05-052, Federal Highway Administration, Washington, DC, 41 p.

Allen, T. M., Nowak, A. S., & Bathurst, R. J. (2005). "Calibration to determine load and resistance factors for geotechnical and structural design." *Transportation Research Circular, (E-C079).*

Amir J.M. (1981). “Experience with rock piles in Israel.” *Seminar on Engineering Geology of Dolomite Areas, Pretoria, pp. 381-383.*

Anderson, T. W., & Darling, D. A. (1952).” Asymptotic theory of certain" goodness of fit" criteria based on stochastic processes.” *The annals of mathematical statistics, 23(2), 193-212.*

ASTM D1143-81 (1989), Standard method of testing piles under static axial compressive load. Vol. 04.08, Philadelphia, pp. 179-189.

ASTM. (2000). ASTM D 2488, Standard Practice for Description and Identification of Soil (Visual-Manual Procedure) (Tech. Rep.). ASTM, West Conshohocken.

Barker, R.M., Duncan, J.M., Rojiani, K.B., Ooi, P.S.K., Tan, C.K., and Kim, S.G. (1991). “Manuals for the Design of Bridge Foundations.” NCHRP Report 343*, Transportation Research Board, National Research Council, Washington, DC, 308 p.*

Bathurst, R. J., Allen, T. M., & Nowak, A. S. (2008). “Calibration concepts for load and resistance factor design (LRFD) of reinforced soil walls.” *Canadian Geotechnical Journal, 45(10), 1377-1392.*

Brinch Hansen, J. (1963). Discussion of Hyperbolic Stress-Strain Response: Cohesive Soil. by Robert L. Kondner. J. Soil Mech., Found. Div., *ASCE, 89(4), 241-242.*

Brown, D. A., Turner, J. P., and Castelli, R. J. (2010). Drilled shaft: construction procedures and LRFD design methods. Publication No. FHWA NHI-1-016, Washington, DC, Federal Highway Administration.

Brown, D. A., Turner, J. P., Castelli, R. J., and Loehr, E.J. (2018). Drilled shaft: construction procedures and LRFD design methods. Publication No. FHWA NHI-18-024, Washington, DC, Federal Highway Administration.

Bui, T. Y., Li, Y., Tan, S. A., & Leung, C. F. (2005). "Back analysis of O-cell pile load test using FEM." *In Proceedings of the International Conference on Soil Mechanics and Geotechnical Engineering (Vol. 16, No. 4, p. 1959).* Aa Balkema Publishers.

Butler, H. D., & Hoy, H. E. (1976). User's manual for the Texas quick-load method for foundation load testing (No. FHWA-IP-77-8). United States. Federal Highway Administration. Office of Research and Development.

Canadian Geotechnical Society (1995), "Canadian Foundation Engineering Manual", 2nd Edition, Ottowa, 456 p.

Carter, J.P. and F.H. Kulhawy. (1988). "Analysis and Design of Drilled Shaft Foundations Socketed into Rock". Report EL-5918, Electric Power Research Institute, Palo Alto, CA, 188 p.

Chin, F. K. (1970). "Estimation of the ultimate load of piles from tests not carried to failure." In Proc. *2nd Southeast Asian Conference on Soil Engineering, Singapore, 1970.*

Chin, F. K. (1971). "Discussion of pile test: Arkansas River Project." *ASCE Journal for Soil Mechanics and Foundation Engineering, 97, 930-932.*

Chen, Y-J, and Kulhawy, F.H. (2002), "Evaluation of Drained Axial Capacity for Drilled Shafts," Geotechnical Special Publication No. 116, Deep Foundations 2002, M.W. O'Neill and F.C. Townsend, Editors, ASCE, Reston, VA, pp. 1200-1214.

Davisson, M. T. (1972). High capacity piles. Proc. Innovations in Found. Const., 52.

Decourt, L. (1999). "Behavior of foundations under working load conditions." *Proc. of 11th Pan-American Conference on Soil Mechanics and Geotechnical Engineering*, Foz DoIguassu, Brazil, August 1999, Vol. 4, pp. 453-488.

Décourt, L. (2008). "Loading tests: interpretation and prediction of their results." In From Research to Practice in Geotechnical Engineering (pp. 452-470).

Dutt R.N., Doyle E.H., Collins J.T., and Ganguly P. (1995) "A Simple Model to Predict Soil Resistance to Driving for Long Piles in Deepwater Normally Consolidated Clays" *Proceedings, 27th Offshore Technology Conference, OTC 7668.*

El-Mossallamy, Y., Abdelmalak, R., & Riad, B.(2016). "Finite element modelling of Osterberg cell pile load test. Case history: St. Croix river crossing bridge, USA."

England, M. (2008). "Review of methods of analysis of test results from bi-directional static load tests." *Deep Foundations on Bored and Auger Piles, BAP V, Ghent, 235-239.*

Fellenius, B.H., (2015). "Analysis of results of an instrumented bidirectional-cell test." *Geotechnical Engineering Journal of the SEAGS & AGSSEA*, 46(2) 64-67.

Fortier, A. R. (2016). "Calibration of Resistance Factors Needed in the LRFD Design of Drilled Shafts."

Fuller, F. M., & Hoy, H. E. (1970). "Pile load tests including quick-load test method, conventional methods, and interpretations." Highway Research Record, (333).

Garder, J. A., Ng, K. W., Sritharan, S., and Roling, M. J. (2012). “Development of a database for drilled SHAft foundation testing (DSHAFT).” Rep. No. In Trans 10-366, Institute for Transportation, Iowa State Univ., Ames, IA.

Gibbs, H. J. (1957). “Research on determining the density of sands by spoon penetration testing.” *Proceedings 4th International Conference on Soil Mechanics and Foundation Engineering*, 1957, pp. 35-39.

Gibson, G.L. and Devenny, D.W. (1973). “Concrete to bedrock testing by jacking from the bottom of a borehole.” *Canadian Geotechnical Journal*, 10(2) 304-306.

Gunaratne, M. (2006). The foundation engineering handbook. CRC Press.

Hasan, Md Rakib, Xinbao Yu, and Murad Abu-Farsakh. (2018) "Extrapolation Error Analysis of Bi-Directional Load-Settlement Curves for LRFD Calibration of Drilled Shafts." *IFCEE 2018. 331-340.*

Hunley, A. (1915). Concrete Pile Standards. Published by Hunley Abbott, New York, 59p.

Kim, S. R., and Chung, S. G. (2012). “Equivalent head-down load vs. Movement relationships evaluated from bi-directional pile load tests.” *KSCE Journal of Civil Engineering, 16(7), 1170-1177.*

Kim, S. J., Park, J. H., & Kim, M. M. (2016). “Calibration of resistance factors for drilled shafts considering lower-bound resistance.” *Japanese Geotechnical Society Special Publication, 2(76), 2627-2632.*

Kondner, R. L. (1963). “Hyperbolic stress-strain response: Cohesive soil.” *Journal of Soil Mechanics and Foundation Engineering Division*, ASCE, 189(SM1), 1 15 - 143.

Kwon, O., Choi, Y., Kwon, O., and Kim, M. (2005). "Comparison of the bidirectional load test with the top-down load test." *Transportation Research Record: Journal of the Transportation Research Board, (1936), 108-116.*

Kulhawy, F. H. (1991). Drilled shaft foundations. In Foundation engineering handbook (pp. 537-552). Springer, Boston, MA.

Kulhawy, F.H. and J.P. Carter. (1992). "Settlement and Bearing Capacity of Foundations on Rock Masses". In Engineering in Rock Masses, F.G. Bell, Ed., Butterworth–Heinemann, Oxford, England, pp. 231–245.

Lee, J. S. and Park, Y. H. (2008). "Equivalent pile load-head settlement curve using a bi-directional pile load test." *Computers and Geotechnics, Vol. 35, No. 2, pp. 124-133*.

Limas, V. V., & Rahardjo, P. P. (2015). "Comparative study of large diameter bored pile under conventional static load test and bi-directional load test." *Malaysian Journal of Civil Engineering, 27.*

Loadtest (2001). Construction of the equivalent top-loaded load settlement curve from the results of an O-cell test, Loadtest Appendix to Reports.

Loadtest International Pte. Ltd. (2013). Reports on Barrette Pile Testing, Exim Bank Tower, HCMC, Vietnam, 13813I-1, 178 p.

Long, J., Hendrix, J., and Baratta, A. (2009). "Evaluation/modification of IDOT foundation piling design and construction policy." Rep. No. ICT-09-037, Illinois Center for Transportation, Rantoul, IL.

Mayne, P.W., and Harris, D.E. (1993). "Axial Load Displacement Behavior of Drilled Shaft Foundations in Piedmont Residuum". FHWA No. 41-30-2175, Georgia Tech Research Corporation, Geotechnical Engineering Division, Georgia Institute of Technology, School of Civil Engineering, Atlanta, GA.

Mayne, P.W. (2007). NCHRP Synthesis 368: "Cone Penetration Testing", Transportation Research Board, National Research Council, Washington, D.C., 117 p.

Mazurkiewicz, B. K. (1972). "Test Loading of Piles According to Polish Regulations." *Royal Swedish Academy of Engineering Sciences Commission on Pile Research*. Report No. 35, Stockholm, 20p.

McVay, M. C., Kuo, C. L., & Singletary, W. A. (1998). Calibrating resistance factors in the load and resistance factor design for Florida foundations (No. WPI 0510772,).

McVay, M., Kuo, C. L., & Guisinger, A. L. (2003). "Calibrating resistance factors for load and resistance factor design for statnamic load testing."

McVay, M., Hoit, M., Hughes, E., Nguyen, T., and Lai, P. (2005). "Development of a web based design, and construction bridge substructure database." *Transportation Research Board 84th Annual Meeting,* Transportation Research Board, Washington, DC, 9–13.

Motamed, R., Elfass, S., & Stanton, K. (2016). "LRFD resistance factor calibration for axially loaded drilled shafts in the Las Vegas valley". No. Report No. 515-13-803. Nevada. Dept. of Transportation.

Mullins, G. (2002). Innovative Load Testing Systems, Sub-Group Statnamic Testing, Critical Evaluation of Statnamic Test Data. *National Cooperative Highway Research Program, Washington, DC*.

Najjar, S. S. (2005). The importance of lower-bound capacities in geotechnical reliability assessments (Doctoral dissertation).

Najjar, S. S., & Gilbert, R. B. (2009).” Importance of lower-bound capacities in the design of deep foundations.” *Journal of Geotechnical and Geoenvironmental Engineering, 135(7), 890-900.*

Neter, J. (1983). Applied linear regression models (No. 04; QA278. 2, N4.).

Neter, J., Kutner, M. H., Nachtsheim, C. J., & Wasserman, W. (1996). Applied linear statistical models (Vol. 4). Chicago: Irwin.

Ng, T. T., & Faiza, S. (2012). “Development and validation of a unified equation for drilled shaft foundation design in New Mexico.” NMDOT Research Bureau.

Ng, K., Garder, J., Sritharan, S., & Ashlock, J. (2013). “An investigation of load and resistance factor design of drilled shafts using historical field test data.”

Ng, K. W., Sritharan, S., & Ashlock, J. C. (2014).” Development of preliminary load and resistance factor design of drilled shafts in Iowa.”

Nguyen, H. M. (2017). “Development of Cone Testing Device for Improved Deep Foundation Design Protocols.” Doctoral dissertation.

Olson, R. E., and Dennis, N. D. (1982). “Review & compilation of pile test results, axial pile capacity.” PRAC Project 81-29, American Petroleum Institute, Dallas.

O'Neill, M. W., & Reese, L. C. (1999). "Drilled shafts: Construction procedures and design methods." No. FHWA-IF-99-025.

Ooi, P. S., Chang, B. K., & Seki, G. Y. (2004). "Examination of proof test extrapolation for drilled shafts." *Geotechnical Testing Journal, 27(2), 123-133.*

Osterberg, J.O. (1986). "Device for testing the load-bearing capacity of concrete-filled earthen shafts." Patent US4614110 A, September 30, 13p.

Osterberg, J.O. (1996). "Method and apparatus for subterranean load-cell testing." Patent US 5576494 A, November 19, 7p.

Osterberg, J.O. (1998). "The Osterberg load test method for drilled shaft and driven piles. The first ten years." Deep Foundation Institute, *Seventh International Conference and Exhibition on Piling and Deep Foundations*, Vienna, Austria, June 15 - 17, 1998, 17 p.

Paikowsky, S. G., & Tolosko, T. A. (1999). Extrapolation of pile capacity from non-failed load tests (No. FHWA-RD-99-170,).

Paikowsky, S. G., Birgisson, B., McVay, M., Nguyen, T., Kuo, C., Baecher, G., ... & O'neill, M. (2004). "Load and resistance factor design (LRFD) for deep foundations", NCHRP Report 507. *Transportation Research Board*, Washington, DC, 76.

Prakash, S., & Sharma, H. D. (1990). Pile foundations in engineering practice. John Wiley & Sons.

Rackwitz, R., and Fiessler, B. (1978). "Structural Reliability Under Combined Random Load Sequences," *Computers and Structures, Vol. 9, pp. 489-494.*

Rahman, M. S., Gabr, M., Sarica, R., and Hossain, M. (2002). “Load and resistance factor design (LRFD) for analysis/design of piles axial capacity.” Rep. No. FHWA/NC/2005- 08, North Carolina State Univ., Raleigh, NC.

Roling, M. J., Sritharan, S., and Suleiman, M. T. (2011). “Introduction to PILOT database and establishment of LRFD resistance factors for the construction control of driven steel H-piles.” J. Bridge Eng., 10.1061/(ASCE)BE.1943-5592.0000247, 728–738.

Romeu, J. L. (2003). “Anderson-Darling: a goodness of fit test for small samples assumptions.” .START 2003-5, Vol. 10, Number 5, Reliability Analysis Center, Rome, 2010.

Rosenblueth, E., & Esteva, L. (1972). Reliability basis for some Mexican codes. Special Publication, 31, 1-42.

Rowe, R.K. and H.H. Armitage. (1987). “A Design Method for Drilled Piers in Soft Rock”. *Canadian Geotechnical Journal, Vol. 24, pp. 126–142.*

Smith, T., Banas, A., Gummer, M., & Jin, J. (2011). “Recalibration of the GRLWEAP LRFD resistance factor for Oregon DOT”. No. FHWA-OR-RD-11-08. Oregon. Dept. of Transportation. Research Section.

Stanton, K., Motamed, R., & Elfass, S. (2017). “Robust LRFD resistance factor calibration for axially loaded drilled shafts in Las Vegas.” *Journal of Geotechnical and Geoenvironmental Engineering*, 143(6), 06017004.

Navy, U. S. (1971). Soil Mechanics, Foundations, and Earth Structures, NAVFAC Design Manual DM-7. Washington, DC.

Vesic, A.S. (1977). “Design of Pile Foundations”. *NCHRP Synthesis 42, Transportation Research Board, National Research Council, Washington, D.C., 68 p.*

Withiam, J.L., Voytko, E.P., Barker, R.M., Duncan, J.M., Kelly, B.C., Musser, S.C., and Elias, V. (1998). “Load and Resistance Factor Design (LRFD) for Highway Bridge Substructures,” Publication No. FHWA HI-98-032, Federal Highway Administration, Washington, DC.

Wroth C.P. and Wood D.M. (1978) “The Correlation of Index Properties with Some Basic Engineering Properties of Soils”, *Canadian Geotechnical Journal, Vol. 15, No. 2, pp. 137-145.*

Yi, L. (2005). Finite element study on static pile load testing (Doctoral dissertation).

Yu, X., Abu-Farsakh, M. Y., Yoon, S., Tsai, C., & Zhang, Z. (2011). “Implementation of LRFD of drilled shafts in Louisiana.” *Journal of Infrastructure Systems, 18(2), 103-112.*